FINAL SCIENTIFIC/TECHNICAL REPORT

Project Title:	Advanced High Energy Li-ion Cell for PHEV and EV Applications
Federal Agency:	Department of Energy
Grant Period:	October 1, 2013 to March 31, 2016
Date of Report:	June 29th, 2016
Recipient:	3M Company
DUNS number:	00-617-3082
Award Number:	DE-EE0006448
Working Partners:	GM, Umicore, Iontensity, LBNL, ARL
Cost-Sharing Partners:	GM, Umicore, Iontensity

Principal Investigator Jagat D. Singh
Phone: 651-575-1230
Fax: 651-736-7478
Email: jdsingh@mmm.com

Business Contact: Steven Kays
Phone: 651-737-0853
Fax: 651-736-0047
Email: slkays@mmm.com

DOE Project Team: DOE Program Manager - John G. Tabacchi
Address: 3610 Collins Ferry Road P.O. Box 880
Morgantown, WV 26507-0880

Executive Summary

Lithium Ion Battery (LIB) technology's potential to enable a commercially viable high energy density is the key to a lower $/Wh, thereby a low cost battery. The design of a LIB with high energy, high power, safety and long life is a challenge that requires cell design from the ground up and synergy between all components. 3M Company (3M), the Recipient, led by its Principal Investigator, Jagat Singh, pursued this challenging task of a LIB by 'teaming' key commercial businesses [General Motors (GM), Umicore and Iontensity] and labs [Army Research Laboratory (ARL) and Lawrence Berkley National Laboratory (LBNL)]. The technology from each team member was complimentary and a close working relationship spanning the value chain drove productivity.

With this team approach, we successfully demonstrated an Advanced High Energy Li-Ion Cell with improved performance over the baseline design. The specific deliverables met were:

- Successfully leveraged the learnings and developed chemistry under 3M's contract number DE-EE0005499 titled, "High Energy Novel Cathode / Alloy Automotive Cell" to establish a baseline cell >2.Ah. These cells used a Si anode and high voltage cathode.
- Developed an advanced cell > 2Ah with advanced chemistry
    - Met wet laminate target of 600W/L (volumetric energy density), 800W/kg (gravimetric power density) and temperature range between -30°C and 65°C
    - Well exceeded wet laminate target of 1200W/L(volumetric discharge power density), 400W/kg (gravimetric regen power density) and 600W/L (volumetric regen power density)
    - Significant improvements were made towards increasing wet laminate gravimetric energy and cycle life performance in full cells >2.0 Ah.
- Demonstrated commercial scale manufacturing feasibility of both Si alloy anode and high energy (>4.5V) NMC cathode.

The completion of this project is a significant step towards more energy efficient and environmentally friendly vehicles, making America less dependent on imported oil.

Project Goals and Objectives Accomplished

The deliverables of this program included integrating high-performance, commercially feasible materials, thereby allowing a transformative step change in energy density and cost reduction of LIB for automotive applications. Below are the results and accomplishments:

Goal & Objectives	Results and Accomplishment
Develop high capacity cathode performance	- Developed multiple advanced NMC based cathode candidates (core shell structure and particle coated structure). - Demonstrated Lithiation capacity up to 250 mAh/g and >95% capacity retention in half coin cells after 50 cycles at >4.5V vs Li. - Down selected final advanced cathode (particle coated structure) based on 1st cycle efficiency, energy, cycle life in full cells, lower gas generation and better rate capability.
Develop high capacity Si alloy anode performance	- Developed multiple advanced Si alloy anode candidates with different formulations, surface treatments and particle morphology. - Demonstrated capacity of >1100 mAh/g of base Si Alloy anode material and > 95% capacity retention in half coin cells after 50 cycles.
Develop binder for high capacity Si anode performance	- Developed multiple candidates of binder for advanced Si anode. - Evaluated performance of binder in full cells - Improved the electrode areal capacity (3mAh/cm2)
Advanced electrolyte performance	- Investigated multiple formulations to evaluate synergistic performance with a >4.5V cathode and Si/graphite anode - Down selected final electrolyte formulation for 18650 cells sampling to GM and ANL
Demonstrate advanced material synthesis for large cell testing and commercial feasibility	- Successfully optimized materials synthesis parameters for both advanced anode and advanced cathode to establish a commercially scalable and viable process. - Successfully scaled up advanced anode (Si alloy type) in >100 kg quantities. Manufacturing scale up plan based on customer demand. - Successfully scaled up advanced cathode in >30 kg quantity. Manufacturing scale up plan based on customer demand.
Demonstrate advanced materials performance in >2.0Ah cells	- Demonstrated advanced chemistry in an 18650 cell, >2.0Ah, with energy improvement, rate capability at different temperatures, pulse characterization and life performance. - Also demonstrated advanced chemistry in a pouch cells.
Ship baseline cells for testing	Successfully delivered 12, >2.0 Ah, 18650 cells to Argonne National Laboratory.
Ship advanced cells for testing	Successfully delivered 12, >2.0 Ah, 18650 cells to Argonne National Laboratory.

Project Activity Summary

Project activity was completed by a synergistic team effort in a two phases. The focus of work in phase I was advanced materials development and baseline validation. In phase II, the work was an iterative integration of advanced materials and testing in 18650 and Pouch cells. The work sites and their respective key roles were:

- St. Paul, MN (3M): Develop advanced cathode, anode and electrolyte; Sample 18650's;
- Fremont, CA (Iontensity): Design, test, diagnose and sample Pouch cells;
- Adelphi MD; (ARL): Develop advanced electrolyte and additives;
- Berkeley, CA; (LBNL): Develop advanced Si alloy specific binder;
- Warren, MI (GM): Evaluate 18650/Pouch cells; Gap analysis versus vehicle requirements;
- Belgium and South Korea (Umicore): Cathode synthesis and pilot scale manufacturing

Activity Summary and Accomplishments by 3M Company

3M's contribution to this project was the materials development of anode and cathode powders. 3M also showed the commercial scale manufacturing feasibility of Si alloy anode powder. The cathode powder was scaled to multiple kg levels for making 18650 cells and transferring the cathode synthesis know how to Umicore. Below are the key accomplishments from the 3M team.

The 3M Anode team made significant progress in improving the performance of Si alloy anode with improvement in the alloy microstructure. The change was achieved by improving the alloy manufacturing process and changes to the composition.

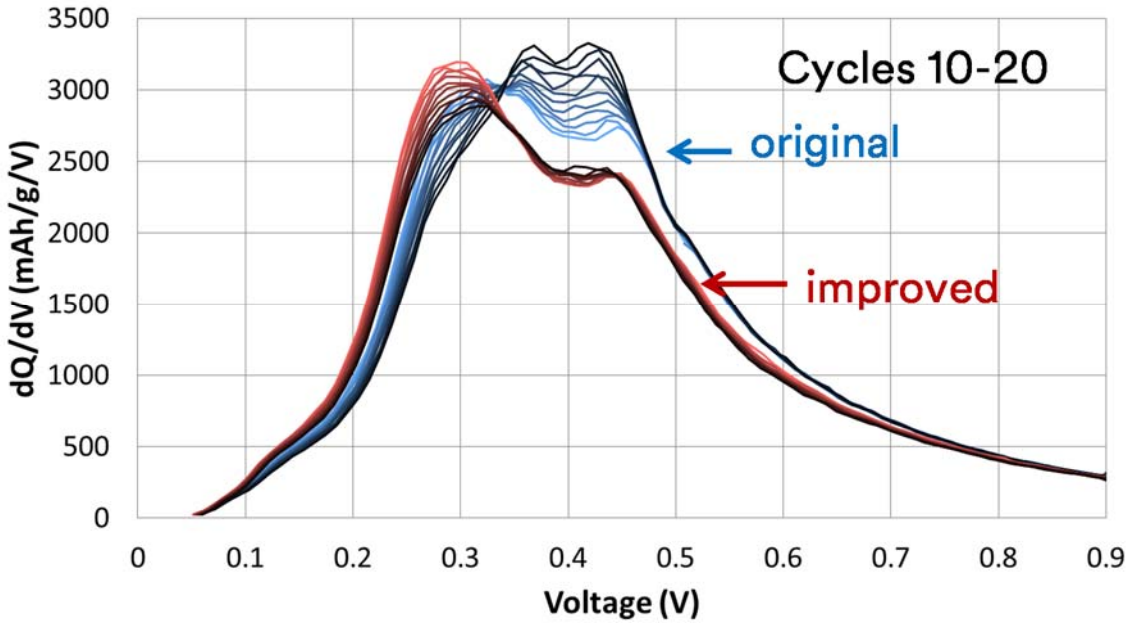

Figure 1. dQ/dV comparison of original Si alloy and the new version of Si alloy with improved microstructure.

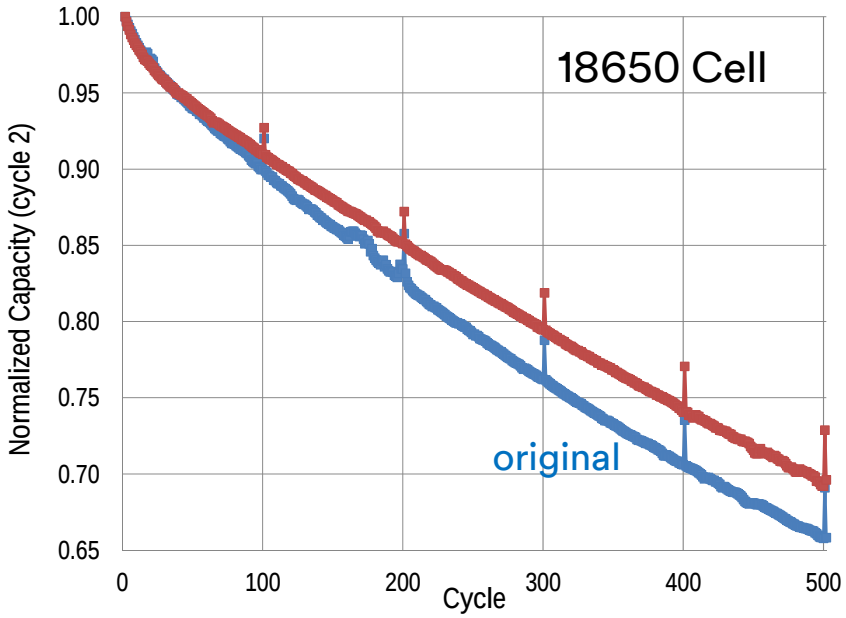

Figure 2. Cycle life comparison (accelerated testing) of original Si alloy and the new version of Si alloy with improved microstructure.

18650 cells with improved microstructures show lower fade than the 18650 cells with the original Si alloy. Various techniques to study particle coating was also studied. Figure 3 shows the effect of pitch coating on the Si alloy anode particle.

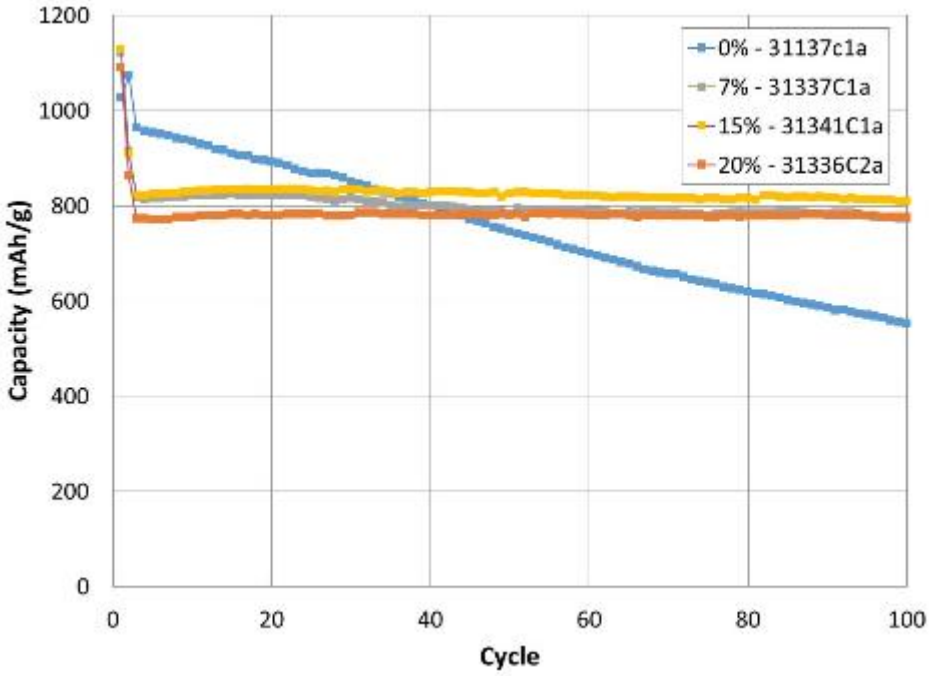

Figure 3. Half-cell cycling of pitch coated V11 annealed at 500 °C, pitch amounts are listed in the legend.

The final advanced Si anode chemistry was decided by appropriately selecting the material formulation, surface treatment and manufacturing scalability. The material formulation for reversible capacity and 1st cycle efficiency. Surface treatment was optimized for lower reactivity and better electrical network during life testing. Table 1 compares the properties of baseline and advanced anode material.

Table 1. Advanced and baseline anode material properties comparison

Si Alloy	BET (m^2/g)	1st Lithiation (mAh/g)	1st Delithiation (mAh/g)	1st Delithiation (mAh/cc)	First Cycle Efficiency (%)	Manufacturability
Advanced Material	--	1170	1060	3370	90.4	✓
Baseline Material	3.5	1050	900	3280	85.7	✓

Two concepts were investigated for developing advanced high voltage (>4.5V) NMC based cathode material. Concept 1 employed a core shell structure and concept two employed a particle coating structure. Concept two was selected for the advanced cathode material selection. Figure 4 shows the different cathode candidates. Finally New_C622 was selected. Table 2 compares the properties of baseline and advanced cathode material.

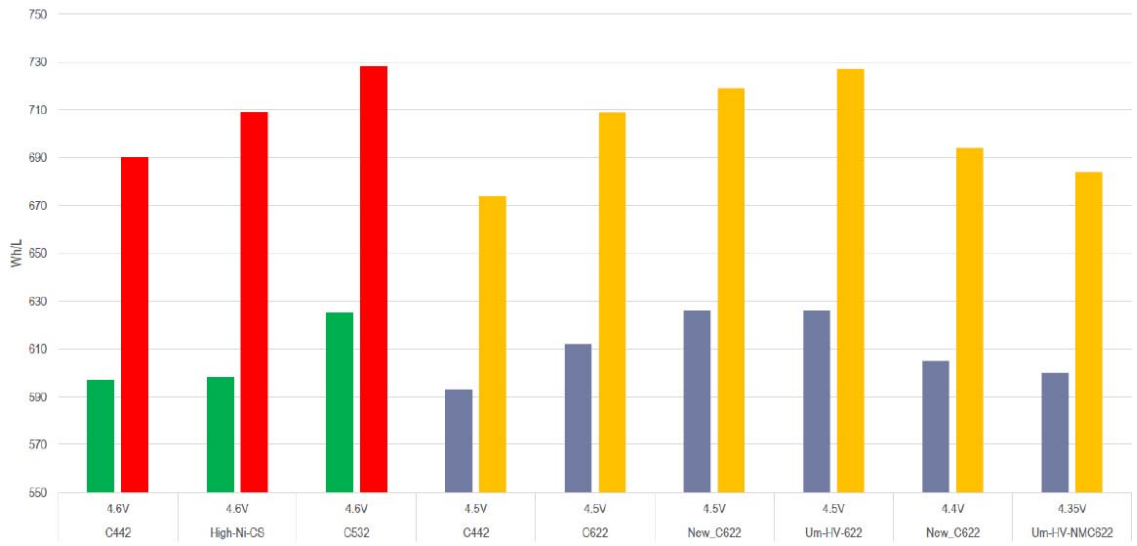

Figure 4. Compares the 18650 energy with different cathode candidates. The taller bar are with Si/graphite anode and the shorter bar is with graphite only anodes.

Table 2. Advanced and baseline cathode material properties comparison

Cathode	BET (m^2/g)	1st Lithiation (mAh/g)	1st Delithiation (mAh/g)	First Cycle Efficiency (%)	Manufacturability
Advanced Material	0.31	230	211	91.9	✓
Baseline Material		273	227	83.3	✓

The above selected anode and cathode material was scaled up in 10's to 100's of kg and then roll to roll coatings were made. The anode and cathode used coating runs are shown in Figure 5 (a & b). Over 40 of 18650 format cells were assembled for sampling to GM and the DOE designated facility. The cells shipped to GM are summarized in Table 3.

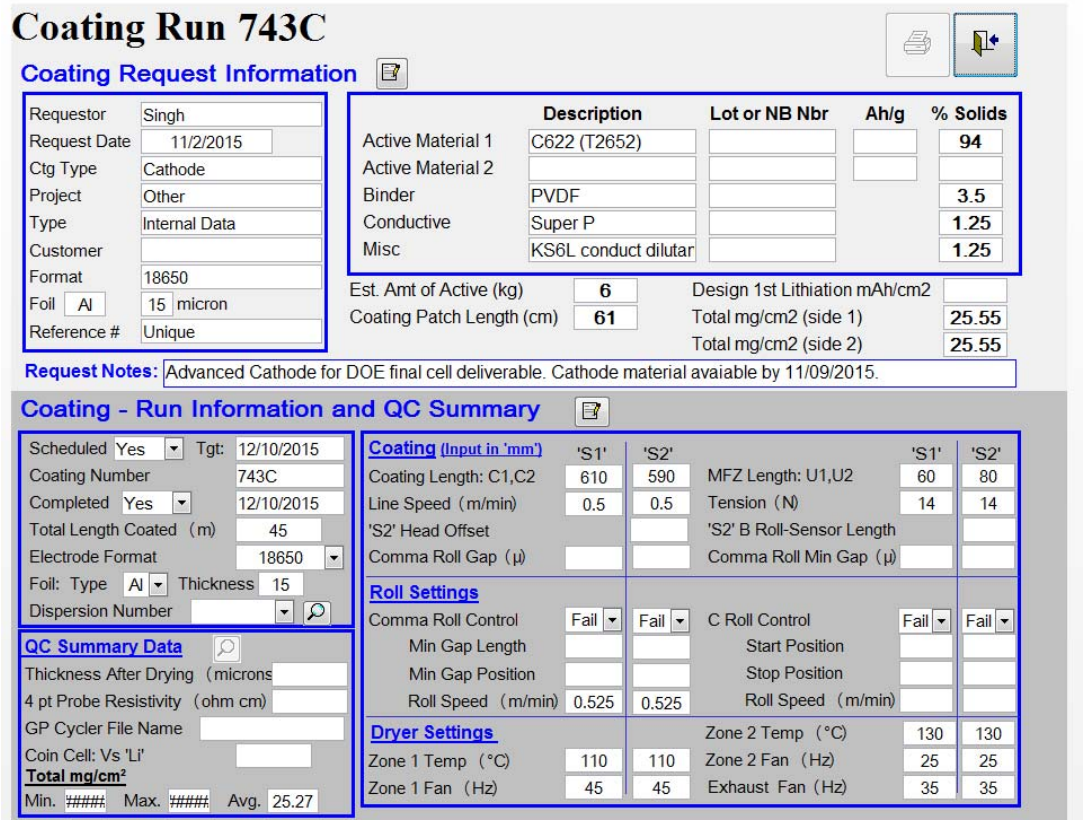

Coating Run 743C

Coating Request Information

Requestor	Singh
Request Date	11/2/2015
Ctg Type	Cathode
Project	Other
Type	Internal Data
Customer	
Format	18650
Foil	Al 15 micron
Reference #	Unique

	Description	Lot or NB Nbr	Ah/g	% Solids
Active Material 1	C622 (T2652)			94
Active Material 2				
Binder	PVDF			3.5
Conductive	Super P			1.25
Misc	KS6L conduct dilutar			1.25

Est. Amt of Active (kg)	6	Design 1st Lithiation mAh/cm2	
Coating Patch Length (cm)	61	Total mg/cm2 (side 1)	25.55
		Total mg/cm2 (side 2)	25.55

Request Notes: Advanced Cathode for DOE final cell deliverable. Cathode material avaiable by 11/09/2015.

Coating - Run Information and QC Summary

Scheduled	Yes
Tgt:	12/10/2015
Coating Number	743C
Completed	Yes 12/10/2015
Total Length Coated (m)	45
Electrode Format	18650
Foil: Type	Al Thickness 15
Dispersion Number	

QC Summary Data

Thickness After Drying (microns	
4 pt Probe Resistivity (ohm cm)	
GP Cycler File Name	
Coin Cell: Vs 'Li'	
Total mg/cm²	
Min. #### Max. #### Avg.	25.27

Coating (Input in 'mm')	'S1'	'S2'		'S1'	'S2'
Coating Length: C1,C2	610	590	MFZ Length: U1,U2	60	80
Line Speed (m/min)	0.5	0.5	Tension (N)	14	14
'S2' Head Offset			'S2' B Roll-Sensor Length		
Comma Roll Gap (µ)			Comma Roll Min Gap (µ)		
Roll Settings					
Comma Roll Control	Fail	Fail	C Roll Control	Fail	Fail
Min Gap Length			Start Position		
Min Gap Position			Stop Position		
Roll Speed (m/min)	0.525	0.525	Roll Speed (m/min)		
Dryer Settings			Zone 2 Temp (°C)	130	130
Zone 1 Temp (°C)	110	110	Zone 2 Fan (Hz)	25	25
Zone 1 Fan (Hz)	45	45	Exhaust Fan (Hz)	35	35

Figure 5(a). Advanced cathode roll to roll coating details for final deliverable cells.

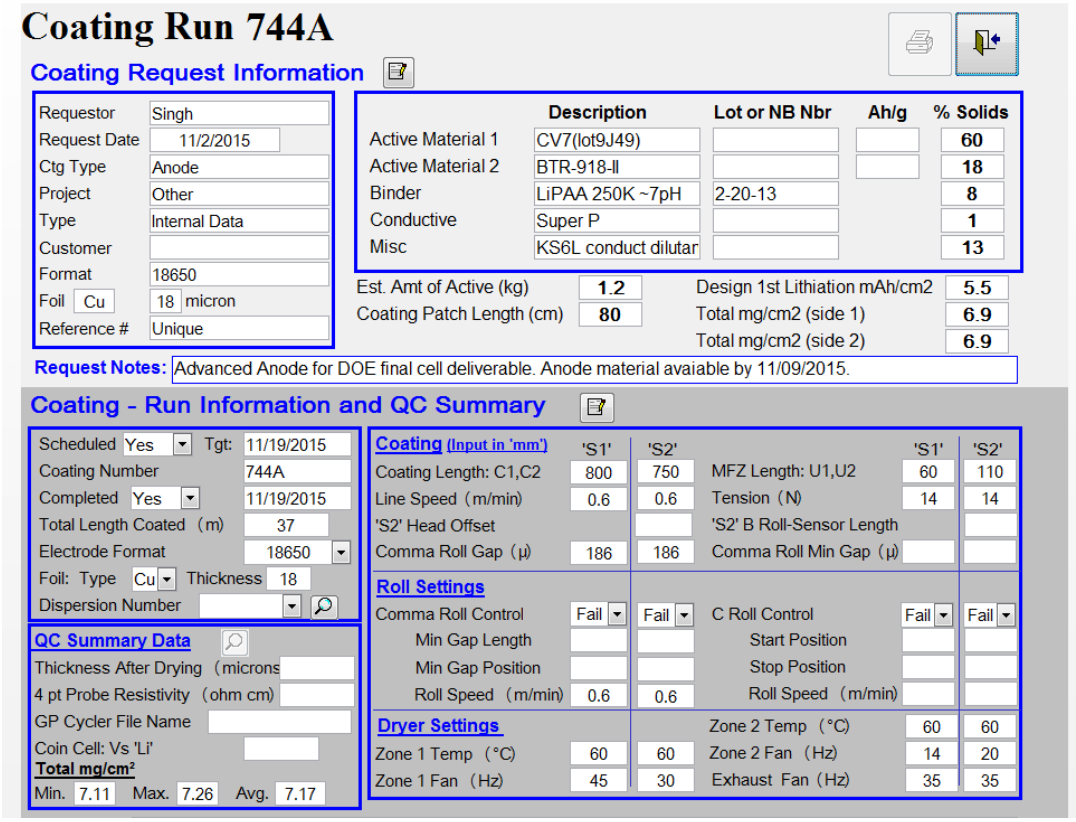

Figure 5(b). Advanced anode roll to roll coating details for final deliverable cells.

Table 3. Average and standard deviation values of final deliverable cells

Rate	C/15	C/15	Irreversible % (After 1st cycle)	C/10	C/10	Irreversible % (after 3 cycles)	C/5	C/5	C/2	C/2	1C	1C
Cycle #	0	0		1	2		3	4	5	6	7	8
Avg	3390	2782	17.9%	2865	2881	15.0%	2864	2864	2823	2818	2759	2751
St Dev	52	57	0.5%	56	54	0.5%	53	53	53	52	56	56
Relative St Dev	1.5%	2.0%	3.0%	2.0%	1.9%	3.0%	1.9%	1.8%	1.9%	1.9%	2.0%	2.0%

Figure 6 shows the Wh/kg (wet laminate) performance of the cell. The gravimetric energy was increased by approximately 24% by further cell design optimization. The key drivers for this energy improvement are thinner separator, wider cathode and anode electrodes, smaller number for N/P ratio, tighter winding, etc. Figure 7 shows the rate capability on energy basis.

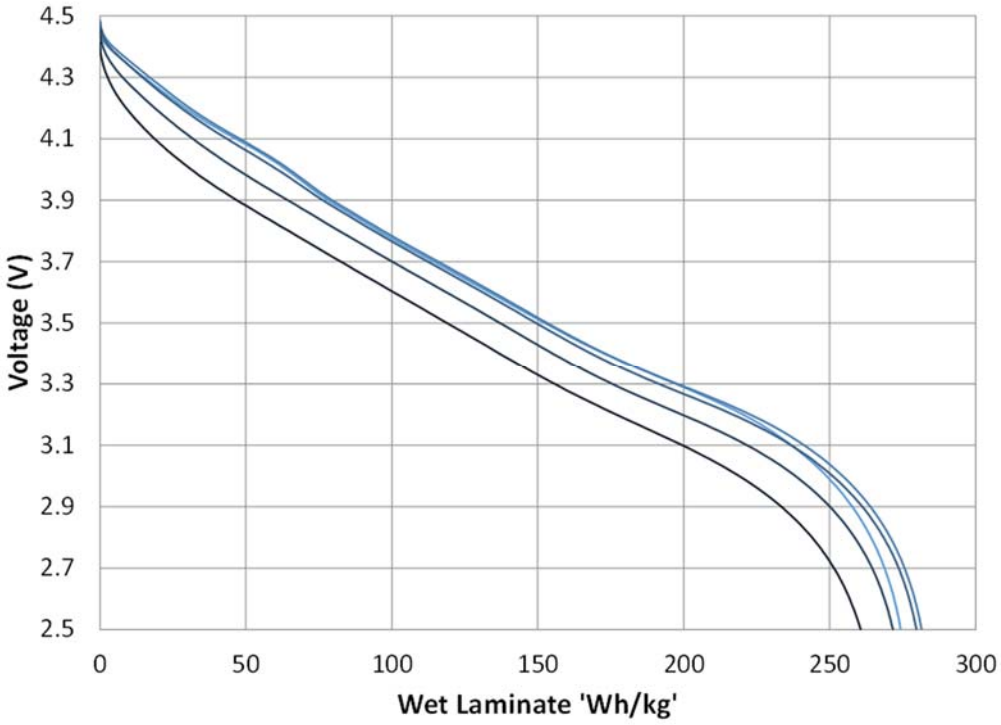

Figure 6. Gravimetric energy at different rates (C/15, C/10, C/5, C/2, 1C)

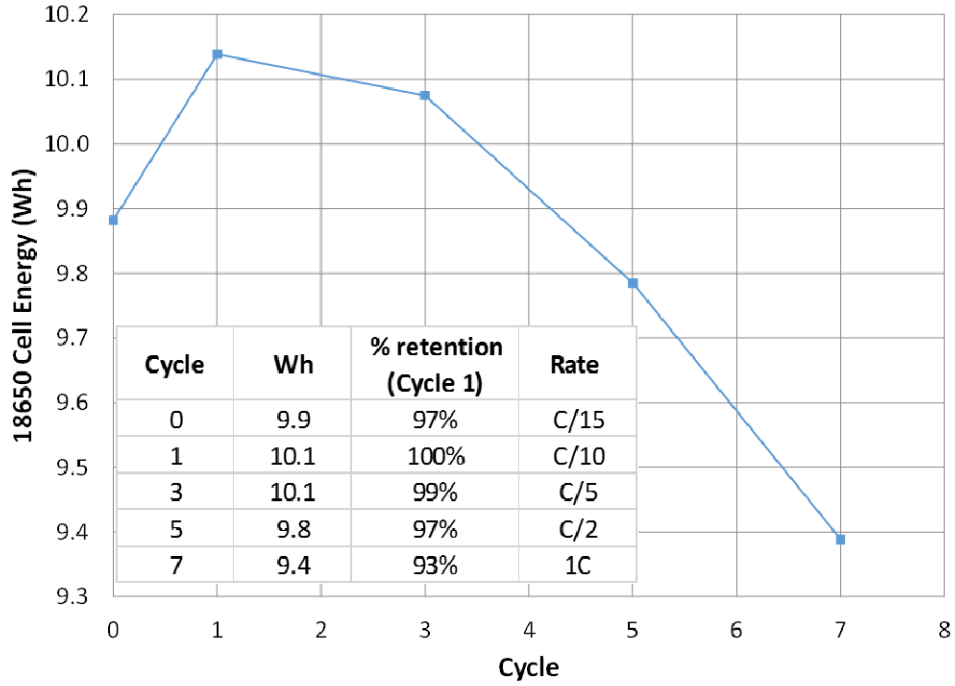

Cycle	Wh	% retention (Cycle 1)	Rate
0	9.9	97%	C/15
1	10.1	100%	C/10
3	10.1	99%	C/5
5	9.8	97%	C/2
7	9.4	93%	1C

Figure 7. 18650 cell Wh and rate capability.

Work Summary and Accomplishments by General Motors

In this project, GM's role was to perform testing of the 3M-fabricated 18650 cells using the protocols shown in Table 4, conduct gap analysis of the cell performance versus the performance targets which were based on USABC vehicle requirements, to carry out post-mortem analysis of the cells to understand the failure mechanisms, and finally to recommend material and cell design improvements to the project team. Three batches of 3M cells (using different cell chemistries) were delivered to GM. The detailed cell chemistry information is listed in Table 5. All of the cells showed 2.4-2.8 Ah capacity at C/3 depending on the upper cut-off voltage (4.4 vs. 4.6 V). The test results of the cells were compared to the battery requirements for electrical vehicles (EV) from the US Advanced Battery Consortium LLC (USABC) to determine the gap between the project cell technology and EV target for. Several cells from each batch were selected for post-mortem analysis. The cells were torn down in an argon-filled glove box, and the electrodes were unwound and washed in preparation for various chemical and electrochemical analyses. The prepared electrodes were punched into small pellets and made into half cells to check the capacities of the individual cathode and anode. They were then studied by Scanning Electron Microscopy (SEM), X-ray Diffraction (XRD), and Electron Probe Micro-analysis (EPMA) to determine the chemical / structural changes in the electrode materials. The test results, gap analyses and post-mortem studies are discussed below.

Table 4: Test protocols for 18650 cells.

Test	No. of Cells	Temperature (°C)	DOD	Test Details
Cycle life	2	30	5-95%	C/3 (RPT at every 50 cycles)
Rate Capability	2	35, 25, 10, 0, -10, -20	100-0%	C/10, C/3, C/2, 1C, 2C, 3C, C/3 for 2 cycles at each rate
HPPC	2	35, 25, 10, 0, -10, -20	100-0%	C/3 CC/CV charge, 100% -C/3 discharge, 5% SOC -1C& 2.5C x20s pulse at 100% SOC, -1C&2.5Cx20s pulses every 5% SOC (C/3), Capacity check at 25°C, CCCV discharge to C/50

Table 5: Cell chemistry of each cell batch

Batch No.	Cell Chemistry
1	Core-shell structure HE-NMC vs. CV6/Graphite
2	Coated NMC (synthesized by 3M) vs. CV7/Graphite
3	Coated NMC (synthesized by Umicore) vs. CV7/Graphite

The Batch 1 cells used the core-shell structured HE-NMC cathode material and Si alloy/graphite mixture anode material and served as the baseline cell for performance in this project. Fourteen cells were delivered to GM in February 2014. They had been through a formation cycle followed by 2C, 1C, 0.3C, 0.2C and 0.1C rate tests at 3M. The same pre-conditioning protocols were used for Batches 2 and 3. The average C/3 capacity of the Batch 1 cells was 2.4 Ah, with 1.3% deviation. Six cells were arbitrarily chosen for cycle life, rate capability and HPPC tests, which followed the protocols listed in Table 4. The test results are compared to the USABC EV targets and are shown in Table 6. Because the weight of the 18650 cell casing is a large fraction of the whole cell weight, the data for cell level and wet laminate level are presented. The wet laminate energy content was the basis for the original project deliverable, which is 415 Wh/kg as proposed in the original funding application by 3M. The baseline (Batch 1) cell performance has large gaps relative to the project targets; especially the cell capacity, which decreased to 65% within 45 cycles. The failure mechanisms were studied by post-mortem analysis and will be discussed later. Another result to note is the poor low temperature performance of the baseline cells; no capacity was obtained when the temperature was below 0ºC.

The Batch 2 cells used surface-coated NMC as the cathode and Si-alloy (CV7)/graphite mixture as the anode. The core-shell HE-NMC material in batch 1 cell was set aside since it is unlikely to meet the project deliverables after initial gap analysis and post-mortem study which will be discussed later. There is 10-20% energy density increase from the Batch 1 to the Batch 2 cells, however there are still large gaps between the Batch 2 cells and the project target.

Three sets of cells were designed for different cutoff voltage windows: 4.4-2.0 V, 4.5-2.0 V and 4.6-2.0 V. The intention of using three voltage windows was to study the stability of the cathode material at different upper cut-off voltage. The cells showed average capacities of 2.46 Ah, 2.61 Ah, and 2.81 Ah for the 4.4-2.0 V, 4.5-2.0 V, and 4.6-2.0 V voltage windows, respectively. As shown in Table 6, the energy density increased with increased upper cutoff voltage, and the gain is from the extra capacity of cathode at higher voltage. There is no difference between the cycle lives of the cells tested in the 4.4-2.0 V and 4.5-2.0 V voltage windows, but the cycle life at 4.6-2.0 V is much lower than both, indicating that the cathode and/or electrolyte material may have experienced significant damage at 4.6V. However, compared to Batch 1 cells, the cycle life of Batch 2 cells was greatly improved, and the cells could be operated at much lower temperature.

Table 6: Gap analysis of the Batch 1 and 2 cells vs. EV targets. (1) End of life requirement for EV application from USABC; (2) Data for beginning of life; (3) Including the weight of electrode, separator, and electrolyte; (4) Data from C/3; (5) Data based on 40% SOC at 25°C using voltage limit for calculation; (6) 35% capacity loss at C/3 with 90% DOD range.

..

	Unit	Target[1]	Batch 1[2](4.55-2.0V)		Batch 2 (4.4-2.5 V)		Batch 2 (4.5-2.5 V)		Batch 2(4.6-2.5 V)	
			Cell Level	Wet Laminate Level[3]	Cell Level	Wet Laminate Level[3]	Cell Level	Wet Laminate Level[3]	Cell Level	Wet Laminate Level[3]
Gravimetric Energy Density	Wh/kg	400	192[4]	247[4]	206	260	218	274	234	295
Volumetric Energy Density	Wh/L	600	490[4]	490[4]	556	556	596	596	633	633
Gravimetric Discharge Power Density	W/Kg	800	366[5]	471[5]	676	853	691	870	NA	NA
Volumetric Discharge Power Density	W/L	1200	933[5]	933[5]	1818	1818	1873	1873	NA	NA
Gravimetric Regen Power Density	W/Kg	400	690[5]	888[5]	1396	1761	1528	1926	NA	NA
Volumetric Regen Power Density	W/L	600	1757[5]	1757[5]	3756	3756	4146	4146	NA	NA
Cycle life	cycles[6]	1000	45	45	194	194	189	189	158	158
Operating Temperature Range	°C	-30~65	0~35	0~35	-20~35	-20~35	-20~35	-20~35	30	30

Whereas the Batches 2 cells cathode materials were synthesized by 3M, Umicore scaled up the cathode material for the Batch 3 cells. Otherwise the cells were identical to the Batch 2 cells; same cell design, anode formulation and electrolyte. The testing was done following the same protocols as listed in Table 4 except that the rate capability and HPPC tests were conducted only at room temperature. As plotted in Figure 8, the Batch 3 cells tested at 4.5-2.0V showed slightly better cycle life performance compared the Batch 2 cells cycled using the same voltage window. The rate capability and HPPC results were similar performance to those of the Batch 2 cells.

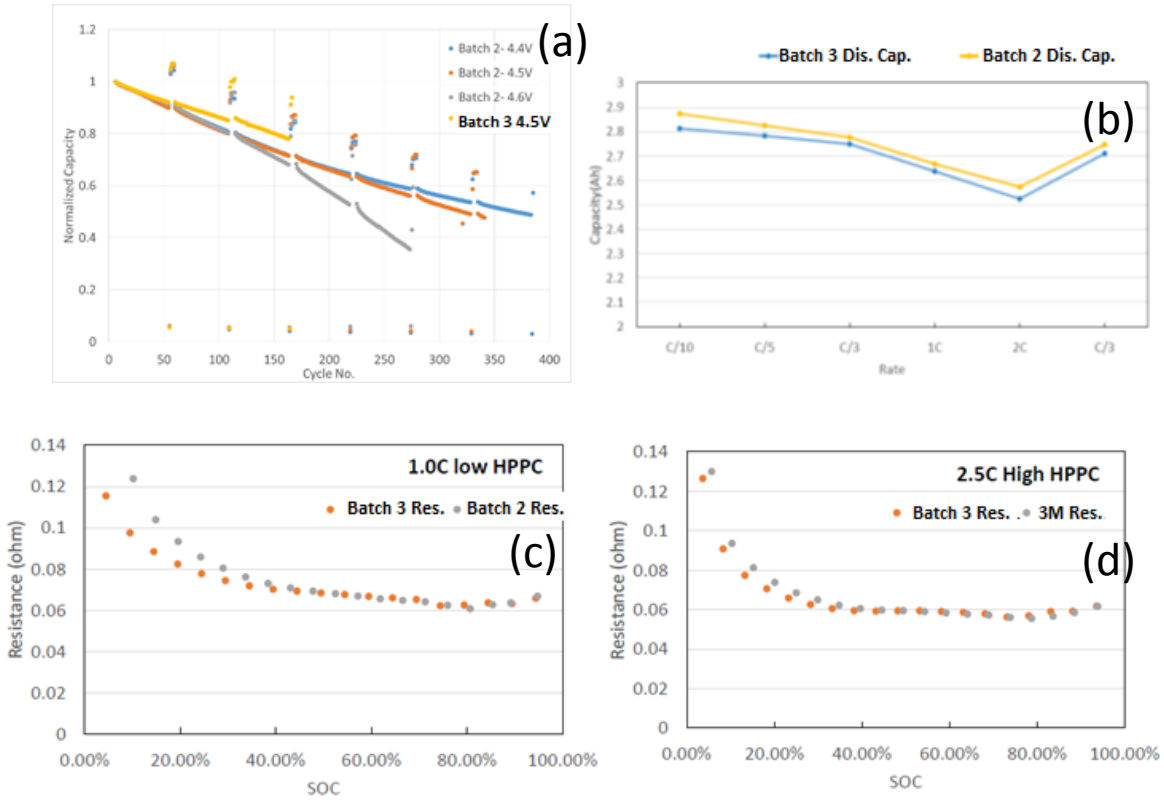

Figure 8: The electrochemical performance comparison between the Batch 2 & 3 cells, (a) cycle life test at C/3 at 30ºC, (b) rate capability test at 25ºC, (c) low HPPC test with 1C pulses at 25ºC under the same voltage window (4.5-2.5V), and (d) high HPPC test at 2.5C at 25ºC.

Post mortem analysis results

Two cells were selected from the Batch 1 cells for post-mortem analysis: one cell went only through the formation cycle followed by rate testing as mentioned above and was labeled as the "fresh" sample; the other cell was cycled to failure (no capacity left) and was labeled as the "cycled" sample. We drew two conclusions about the poor cycle life of the electrode materials. These are summarized in Figure 9. First, elemental mapping showed a large variation in the transition metal distribution, and no core-shell structure was observed in the cathode particles, as shown if Figure 9a. Second, the SEM pictures (Figure 9b) showed very different morphologies for the samples. The pristine sample (as-prepared cathode) and the powder showed clean surfaces. But, a thick passivation layer was observed on the cycle-aged cathode compared to the pristine and fresh samples, which could be due to electrolyte decomposition. The passivation layer could contribute to the internal resistance increase of the cycled cell as observed in the cycle life testing. Third, the fresh anode had a relatively homogeneous oxygen distribution which came from the oxygen in the binder material (LiPAA), but a concentrated oxygen layer was observed on the surface of the cycled anode with little oxygen signal inside the electrode in Figure 9c, indicating the binder decomposed during cycling, which may be the cause of the anode delamination. The oxygen signal on the surface came from the SEI layer as observed in

the SEM image (Figure 9b). Fourth, as shown in Figure 9(d), the fluorine signals representing the solid electrolyte interphase (SEI) were found on the surface of the anode to a thickness of ~5µm. A thin layer of Mn signal was also observed on the surface of the anode, which is due to the Mn dissolution from cathode material. In summary, we conclude that the core-shell structured HE-NMC wasn't made well and that a thick passivation layer was formed on the surfaces of both the cathodes and anodes during cycling leading to resistance increase in the cells, which caused quick capacity failure of the cells.

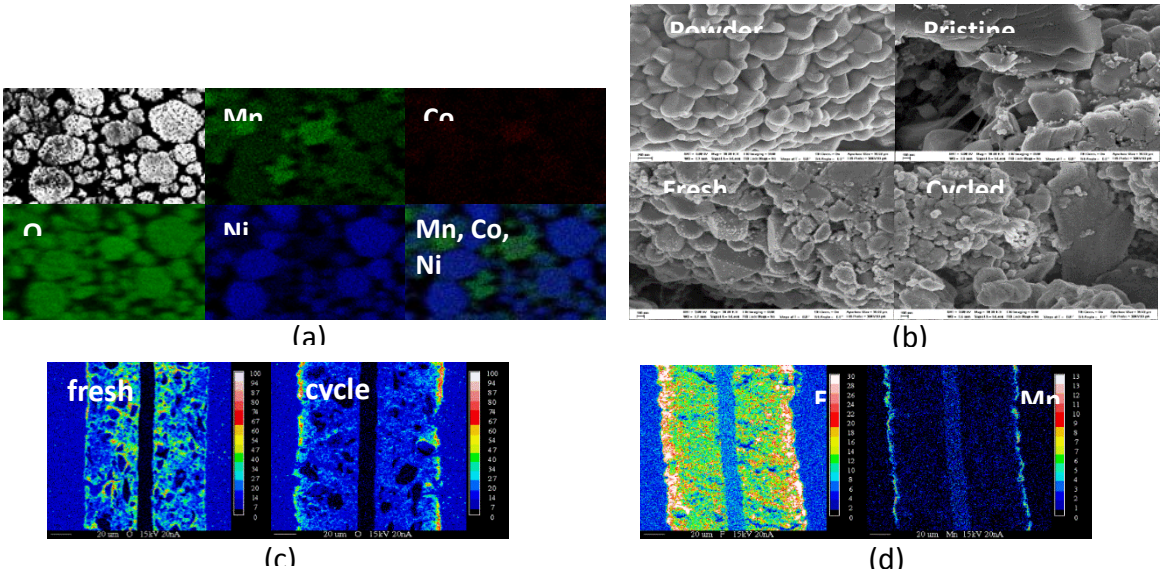

Figure 9: Post-mortem analysis results of batch 1 cells. (a) SEM-EDS analysis of pristine cathode powder material, (b) SEM pictures of cathode materials, (c) EPMA oxygen maps of fresh and cycled *anodes, and (d) EPMA fluorine and manganese maps of cycled anodes.*

Table 7: Half-cell capacity test results of post-mortem electrodes from Batch 2 cells

Sample Type	Voltage Window	Cathode Specific capacity (mAh/g)	Anode Specific capacity (mAh/g)
Fresh	4.4-2.5V	175.16	1210.46
	4.5-2.5V	172.87	1131.93
Rate Tested	4.4-2.5V	178.45	811.21
	4.5-2.5V	170.59	686.44
Cycled	4.4-2.5V	165.64	416.02
	4.5-2.5V	168.26	405

.

Based on the testing results and learnings from the post-mortem analysis, the team decided that the core-shell structure HE-NMC would not be a promising candidate to meet the project targets. Based on calculation of possible cell energy density, the surface coated NMC is proposed as the cathode for the final delivered cells.

Three cells from two voltage windows (4.4-2.5V and 4.5-2.5V) were dissembled for post-mortem analysis. The cells labeled as the "fresh" sample went only through the formation cycle followed by rate testing at room temperature, the "rate tested" cells were tested at different rates and temperatures following the protocols listed in Table 4, and the "cycled" cells were cycled to 40% of initial capacity at 30ºC. All the cells were fully discharged to 2.5 V before disassembling in a glove box. The extracted electrodes were washed by DMC and punched into pellets for half-cell fabrication and chemical/structural analysis. As listed in Table 7, the cathodes from all the cells showed similar specific capacities. Although the cathodes from the cycled cells showed slightly less capacity (~6% decrease) than the fresh samples, the total capacity loss of the cycled cell was about 60%, indicating that the failure of the cell wasn't from the cathode. This is consistent with our interpretation of the XRD patterns for these materials; no structural changes were observed. On the other hand, the specific anode capacity gradually decreased from that of the fresh to those of the rate tested and cycled samples, indicating that the capacity loss observed in the full cells was due to anode degradation.

Further analysis of the anodes was done to identify the failure mechanisms. Figure 10 shows the phosphorous intensity profile across the anodes and their current collector; tested using 4.4-2.5 V and 4.5-2.5 V voltage windows. The reason for the cycled samples showing only one electrode was because one side of the active material coating delaminated from the current collector during cell disassembly. By comparing the edges of the profiles, one notes that the thickness of the cycled sample increased ~10 μm from that of the fresh sample which is likely due to SEI formation and electrode swelling during cycling. The integrated phosphorous intensity of the cycled sample is 2.72 times of that in the fresh sample, in the case of 4.4-2.5 V, which is additional evidence of SEI growth during cycling since phosphorus is one of the main components of the SEI.

The Batch 3 (final) cells were considerably improved compared with the baseline cells; e.g., energy density, cycle life and low temperature performance. Nevertheless, the performance was far from the EV targets. To meet the EV's energy density target, a cathode with much higher capacity will have to be used. Post-mortem analysis results indicate that the anode stability is the biggest road block to meet the cycle life performance, and that a more stable anode material with a better binder will be required to achieve the cycle life. SEI formation is still an on-going problem for Si-enhanced anode materials. To reduce SEI formation and continuous electrolyte decomposition due to the volume change of Si particle, effective electrolyte additives need to be designed to stabilize the SEI layer, therefore, to improve cycle life and diminish cell internal resistance increase.

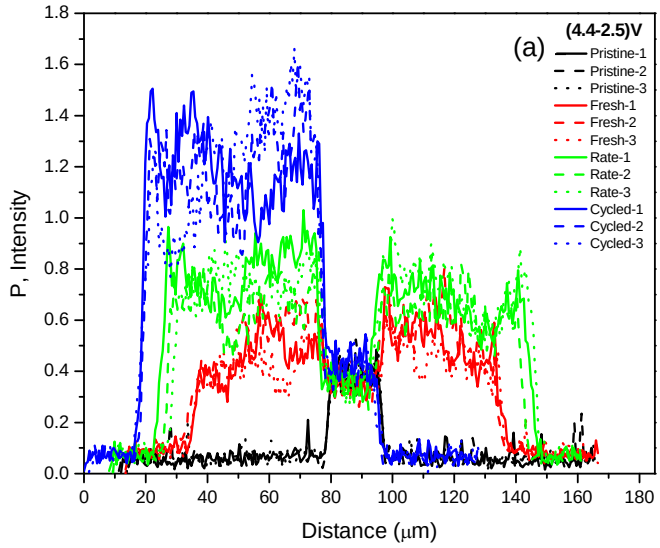

(b)

Phosphorous Intensity in coating	Average
(I_O Rate)/(I_O Fresh)	1.50
(I_O Cycled)/(I_O Fresh)	2.72
(I_O Cycled)/(I_O Rate)	1.82

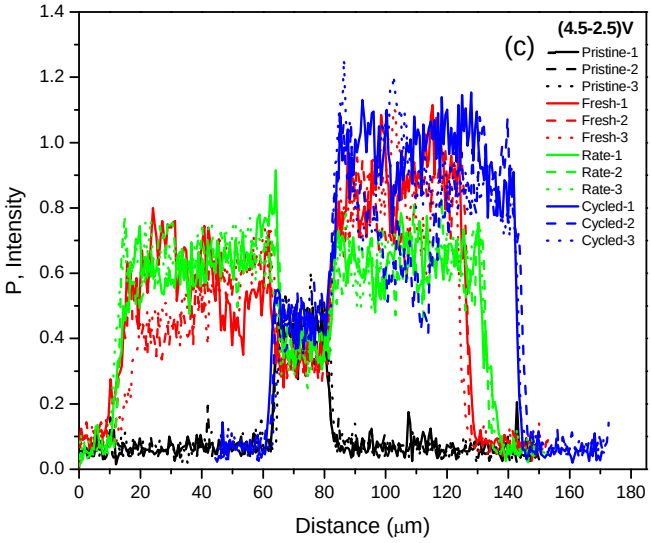

(d)

Phosphorous Intensity in coating	Average
(I_O Rate)/(I_O Fresh)	0.92
(I_O Cycled)/(I_O Fresh)	1.31
(I_O Cycled)/(I_O Rate)	1.43

Figure 10. The phosphorous intensity profiles across the current collectors of anodes tested between (a) 4.4-2.5 V and (c) 4.5-2.5 V, and the integrated oxygen intensity ratios of different samples tested between (b) 4.4-2.5 V and (d) 4.5-2.5 V.

Activity Summary and Accomplishments by Umicore

Scale-up process development for core-shell structured high energy density NMC materials

To increase driving distance of electrical vehicle, lithium ion batteries has an important role to play when a vehicle company designs new vehicle model or when customer decides to purchase electrical vehicle. The design of high energy and power of LIB is mainly dependent on cathode materials' performance. Therefore, it is very important to develop cathode materials with high capacity and energy, long cycle life and low cost. In our project, Umicore will introduce scalable

process for cathode materials with capacity around 250mAh/g by using core-shell structured NMC materials designed by 3M and Umicore will deliver the cathode materials on-time to our project partners.

Previous 3M recipe for core-shell high energy NMC (HE-NMC) has potential issues to scale-up to pilot-scale due to long processing time (double firing), complicated process and difficult handling of lithium source (Lithium Hydroxide, LiOH). To overcome those problems of piloting, Umicore decided to introduce scalable process using single firing and using a different lithium source as lithium carbonate (LiC) instead of LiOH.

Figure 11 shows scale-up steps for core-shell NMC materials. First, Umicore prepared cathode materials by double firing in furnace using precursor (P0332) which is prepared by Umicore group R&D based on 3M recommended process (Step 1). Then, Umicore modified scalable process using single firing (Step 2). Finally, Umicore introduced scalable process and prepared 50kg of product to deliver project partners (Step 3)

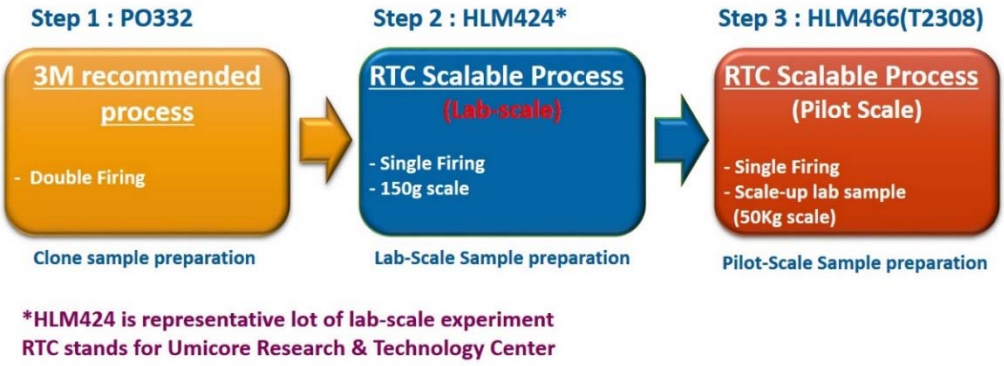

Figure 11. Scale-up steps for core-shell NMC materials at Umicore.

Materials properties of prepared samples were fully analyzed by BET, PSD, XRD, TAP, Moisture, ICP and SEM. In addition, electrochemical properties were measured using CR2032 coin cell for capacity, cycle, and rate performance.

Results and Discussion

Table 8 shows physical properties of final products prepared by each step. There were some differences of products but physical properties are almost the same.

Lithium to metal ratio were analyzed by ICP method and the result (calculated value) showed 1.157 mol% (Step 1), 1.142 mol% (Step 2) and 1.164 mol% (Step 3). Different Li/M ratio were mainly came from using different lithium sources and scale-up factor. (Not shown in Figure) Figure 12 shows SEM images of final products. As seen in Figure, all sample showed similar morphology and crystallite shape. Additionally, XRD patterns of final samples showed the same results. (Not shown in Figure)

Table 8. Physical properties of final products

Sample ID	Sample Information	Comment	BET (m2/g)	TD (g/cm3)	Moisture (ppm)
P0332	Umicore Lithiation (3M recipe)	UmGRD016-20	0.489	-	411
HLM424	Umicore Lithiation (Umicore Recipe, Lab scale)	Repeat of P0332	0.592	-	345
HLM466 (T2308)	Umicore Lithiation (Umicore recipe, Pilot scale)	Scale-up of P0332	0.493	2.12	155

Sample ID	< 1um (%)	< 3um (%)	Dmin (um)	D10 (um)	D50 (um)	D90 (um)	D95 (um)	D99 (um)	Dmax (um)
P0332	0	0	3.476	5.33	8.43	13.2	14.8	17.8	22.73
HLM424	0	0.04	2.908	5.04	8	12.54	14.06	16.91	20.99
HLM466	0	0.17	2.908	4.79	7.92	12.89	14.54	17.58	21.17

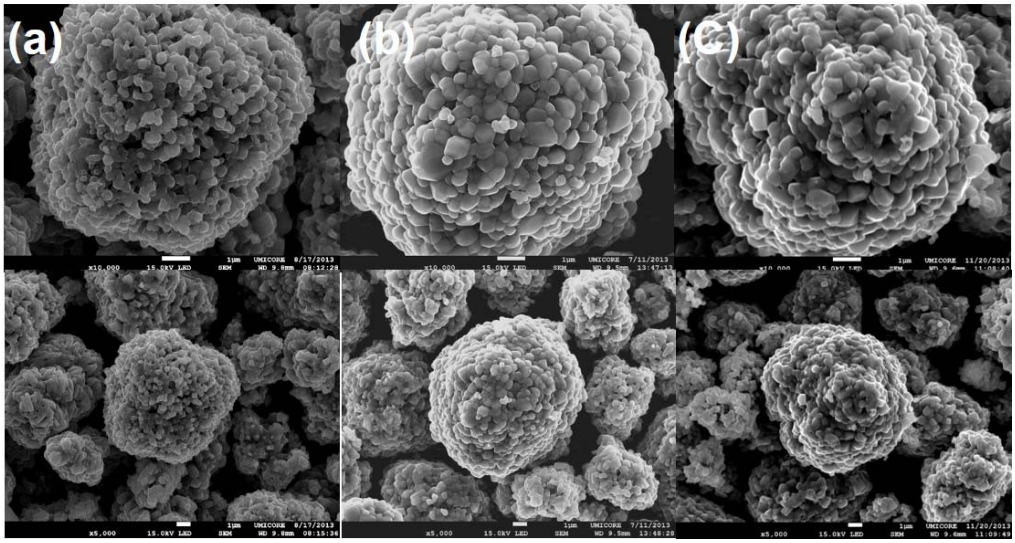

Figure 12. SEM images for final products as (a) Step 1, (b) Step 2, and (C) Step 3.

Figure 13 and Table 9 show electrochemical properties of final products. 3M designed sample (Lab scale) shows high electrochemical properties than other products, which are prepared for scalable process. However, if we consider it as a first scale-up sample, then this result also represents successful scale-up.

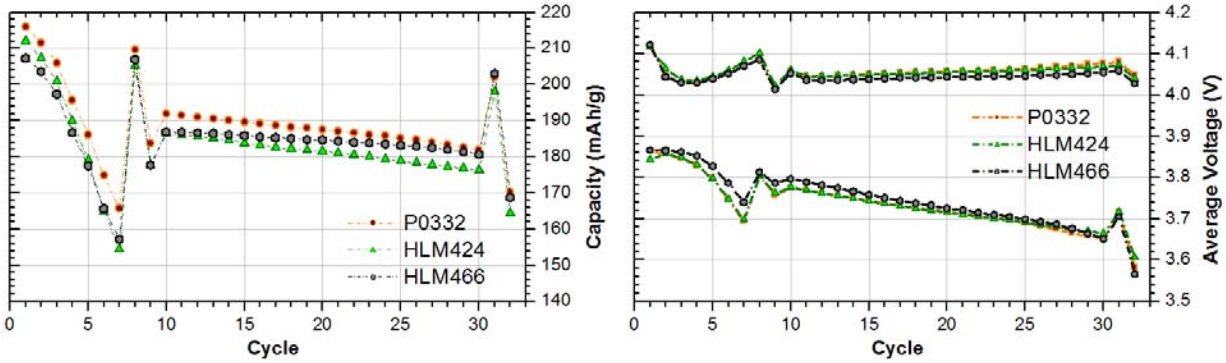

Figure 13. Cell performance of final products prepared by different steps. (PO332: Step1, HLM424: Step2, HLM466: Step 3). Rate performance were measured in C/20, C/10, C/5, 1/2C, 1, 2, and 3C at 4.6V. Cycle was measured at 1C.

Table 9. Electrochemical properties of final products

Sample ID	QD1 (4.6V) (C/20)	Qirr	Q 0.1C	1C	Rate (1C/0.1C)	Rate (2C/0.1C)	Rate (3C/0.1C)	Fade (0.1C)	Fade (1C)
	mAh/g	%	(mAh/g)	(%)	%	%	%	%/100	%/100
P0332	215.98	14.77%	209.6	87.63%	87.99%	82.60%	78.30%	16.32%	33.38%
HLM424	211.16	15.38%	204.98	86.73%	86.68%	80.09%	75.16%	15.99%	34.01%
HLM466	207.25	17.15%	206.84	85.92%	87.19%	81.37%	77.20%	8.16%	22.90%

Umicore introduced simple and scalable process to prepare core-shell structured high capacity NMC materials by single firing. The scale-up sample showed very similar physical and electrochemical properties compared to 3M designed process. Therefore, the first scale-up process was successful. In addition, we already delivered 35Kg of scale-up core-shell NMC to 3M.

Scalable process development for $LaPO_4$ coated high Ni NMC materials

Surface modification by coating is an important method to achieve improved electrochemical properties and the coating layer prevents the direct contact with the electrolyte solution and as a result cycle stability could increase compared to bare cathode materials. Also, preliminary studies done by 3M to compare full cell (18650) properties of Umicore provided HV622 (High

voltage NMC 622, without coating) and La-622 (LaPO4 coated NMC 622) showed similar capacity and energy density. However, with 3M electrolyte formula, $LaPO_4$ coated NMC 622 showed better cycle ability at 30℃ and 45℃.

From the preliminary results, 3M and Umicore agreed to prepare scale-up sample of $LaPO_4$ coated NMC 622 based on 3M provided coating recipe and Umicore did optimization of coating process. Therefore, in this report, we would like to provide scalable process based on wet-coating method and results for their physical and electrochemical tests.

For the preparation of coating solution, different wt% of Phosphoric acid (H_3PO_4) and Lanthanum Nitrate ($La(NO_3)_3$) were mixed together in deionized water and stirred it until white precipitates were created. Then, prepared coating solution were slowly dropped into NMC 622 powders with stirring. After physical mixing, slurries were dried in dry oven at 120℃ for overnight in air. Finally, dried powders were fired at 500℃ in dry air atmosphere muffle furnace. Detailed experiment conditions are shown in Figure 14.

After coating, samples were fully analyzed their physical and electrochemical properties by SEM, EDS, BET, PSD, coin cell, full cell and so on.

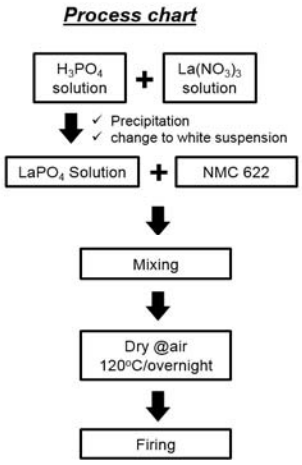

Sample ID	NMC 622	Amount of HX12 (g)	Water (g)	Slurry (g) (2M $LaPO_4$)	Amount of solution	Dry	Post treatment
HX2432	HX1704	200		13.89	7 %	120C/ overnight	Mortar, SM270
HX2433		101	7	5.8	13 %		
HX2434		102	15	7	22 %		

❖ FE-SEM images

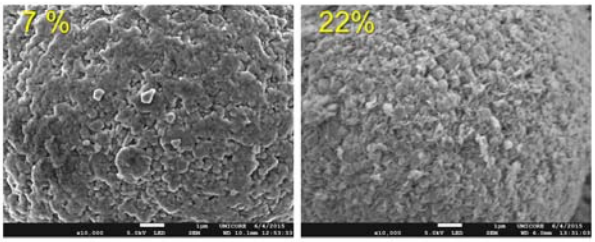

Figure 14. Experiments conditions and FE-SEM images of LaPO4 coated NMC 622 (Lab-scale).

For the optimization of firing temperature after coating, 0.5 mol% $LaPO_4$ coating NMC 622 with various heating temperature were considered and XRD patterns did not show secondary phase until 800℃ as shown in Figure 15 (a). However, coin cell results showed slightly better performance of powders fired at 500℃ compared to others (Figure 15 (b)).

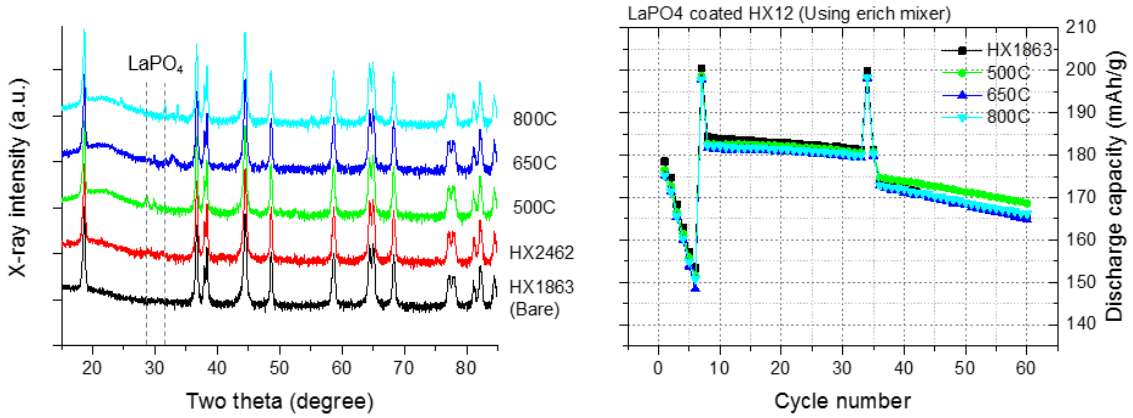

Figure 15(a) Figure 15(b)

Figure 15. Firing temperature optimization results for 0.5mol% LaPO4 coating NMC 622.

Also, it is important to adjust appropriate coating solution amount for the process point of view. To decide optimal solution amount to the powder mass, we prepared different solution concentration as 5%, 10% and 20%, respectively, and investigated their coat ability. For solution concentration as 5%, inhomogeneous coating on powders were observed and also this amount of coating solution was not enough to coat $LaPO_4$ on the powders (Figure 16).

Figure 17 shows the EDS mapping images of powders coated by 10% and 20% of coating solution amount to the sample mass. Still partial aggregation of $LaPO_4$ observed in both case of 10% and 20% of solution amount but with increasing coating solution amount, $LaPO_4$ was homogeneously coated on the powder surface than 10% coating solution. However, if we using more than 10% of solution amount, blend making was too difficult due to sticking of powder. Therefore, Umicore optimized coating solution amount as 10%.

Figure 18 shows the coin cell results of bare NMC 622 (HX1863), samples coated by 3M (P0357) and Umicore scale-up sample (HX2493). Compared to 3M coated sample, Umicore scale-up sample showed better electrochemical properties in capacity, cycle, and rate and this results was similar as bare HX materials. (Full cell test is on-going and data will be available in next report)

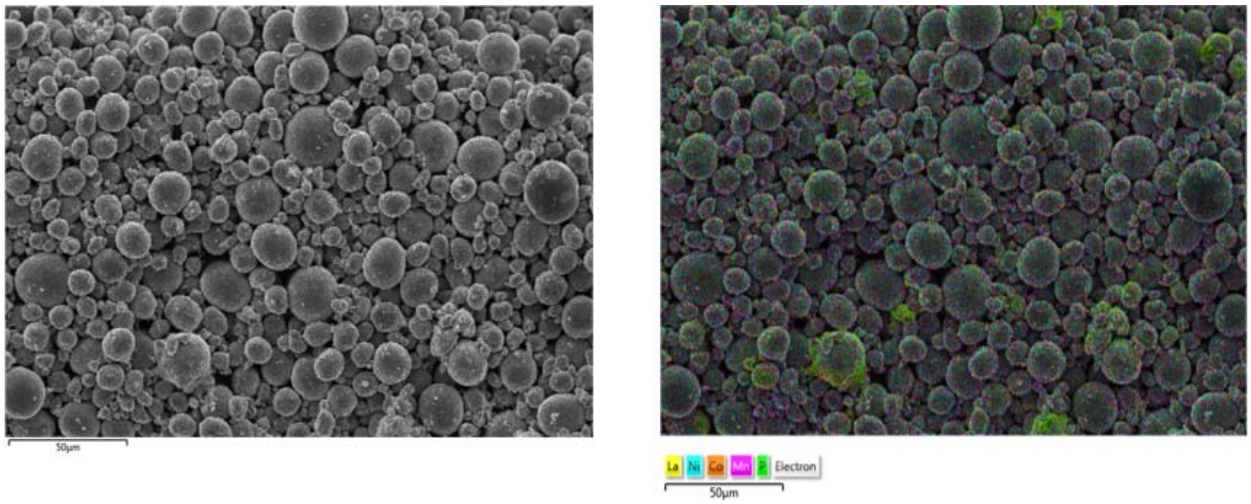

Figure 16. SEM and EDS mapping images of LaPO4 coated NMC 622 with 5% coating solution amount to the sample mass.

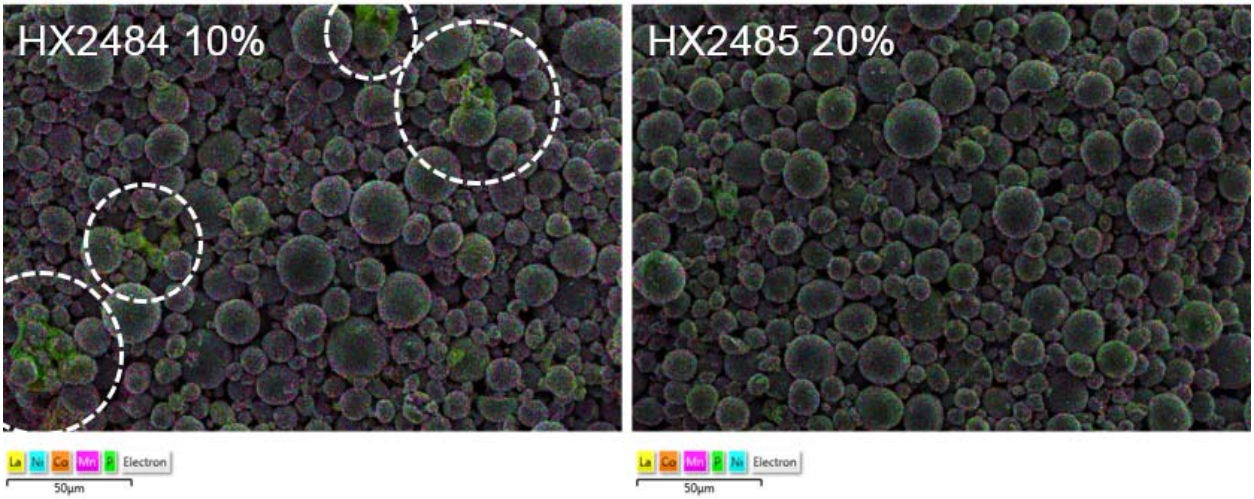

Figure 17. SEM and EDS mapping images of powders coated by 10% and 20% of coating solution amount to the sample mass

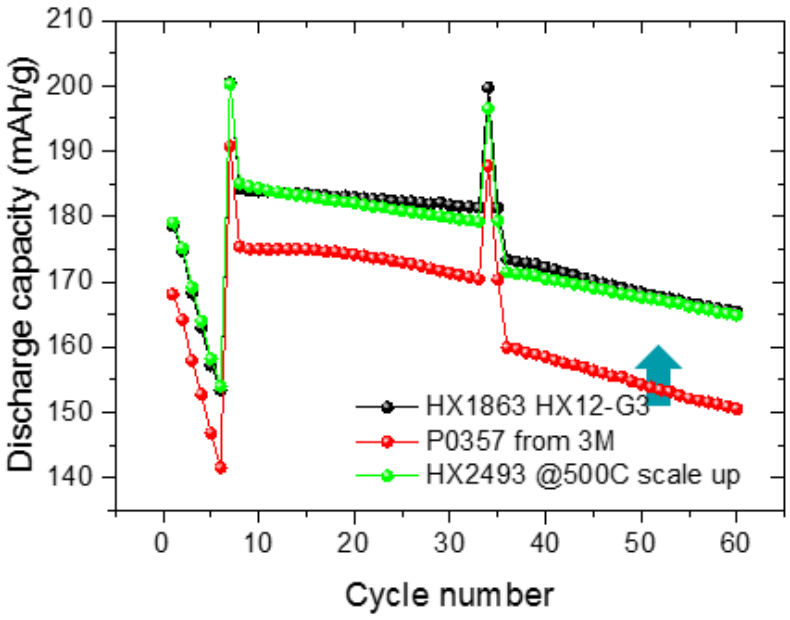

Figure 18. Coin cell comparison results for bare NMC 622 (HX1863), 3M coating NMC 622 (P0357) and Umicore scale-up sample (HX2493).

To optimize $LaPO_4$ coating conditions, Umicore developed scalable coating process based on 3M recipe and 0.5 mol% $LaPO_4$ in 10% of coating solution to the sample mass and 500℃ firing temperature were selected. With those conditions, Umicore $LaPO_4$ coated NMC622 sample showed better electrochemical properties than 3M coating sample.

Optimization of scalable process for $LaPO_4$ coated high Ni NMC materials

To optimize $LaPO_4$ coating conditions, Umicore developed scalable coating process based on 3M recipe and 0.25 mol% $LaPO_4$ coating solution to the sample mass and 700℃ firing temperature were selected. With those conditions, Umicore prepared 20Kg of $LaPO_4$ coated NMC622 sample to achieve final targets.

For the preparation of 0.25M $LaPO_4$ coating solution, phosphoric acid (H_3PO_4) and lanthanum nitrate ($La(NO_3)_3$) were mixed together in 3000ml of deionized water and stirred it until white precipitates were created. Then, prepared coating solution were slowly injected by syringe pump into NMC 622 powders using pilot scale blender which was heated at 80℃. After physical mixing, slurries were dried in dry oven at 120℃ for overnight in N_2 atmosphere to prevent CO_2 uptake. Finally, dried powders were fired at 700℃ in dry air atmosphere muffle furnace and sieved using ASTM #270 screen. After coating, samples were fully analyzed their physical and electrochemical properties by SEM, EDS, BET, PSD, coin cell, and so on.

Table 10 shows the physical properties results of $LaPO_4$ coated NMC 622 (HX2652) powder. BET value shows 0.395m^2/g and total base value was measured as 209.33 μmol. PSD results of prepared sample shows Figure 19. Compared to that with bare NMC 622 powder (HX1863), peak intensity decreased but no size changing was observed.

Coin cell results of 3M sample, lab scale sample (3Kg scale), and pilot scale sample (20Kg scale) are showed in Figure 20. Umicore scale-up sample showed better electrochemical properties in rate, cycle stability compared to 3M sample. Also, coin cell results of lab scale and pilot scale sample showed no big difference.

From the upscaling study on $LaPO_4$ coated NMC 622 powder, pilot scale wet coating method showed the exactly same properties in physical and electrochemical test. Therefore, successful scale-up process was developed by together with 3M and Umicore and it will be applicable for mass production scale.

Table 10. Physical properties of LaPO4 coated NMC 622 (HX2652) sample

Sample ID	BET	Carbon	pH titration 2.5g				
	SSA (m2/g)	C (ppm)	LiOH(%)	Li_2CO_3(%)	Ratio CO_3/Total Base	Total Base (umol/g)	Cal.Carbon
HX2652	0.3095	174.36	0.2749	0.3493	0.4516	209.33	582

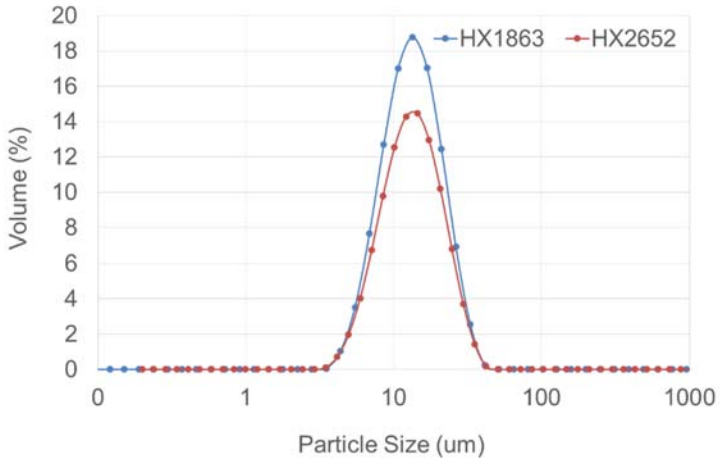

Figure 19. PSD results of bare NMC 622 (HX1863) and LaPO4 coated NMC 622 (HX2652)

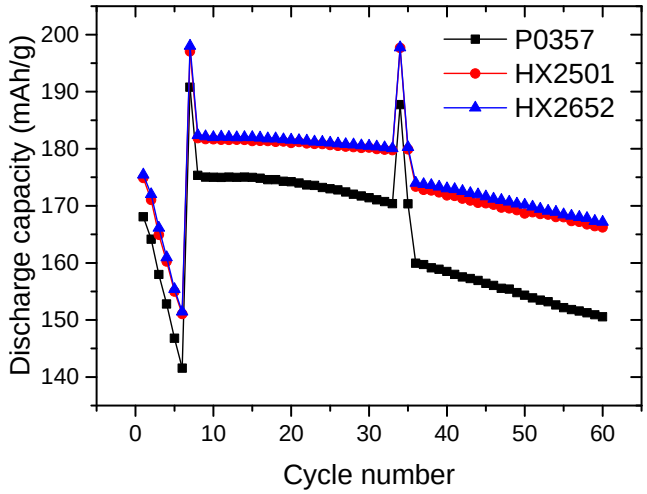

Figure 20. Coin cell test results of 3M sample (P0357), lab scale sample (HX 2501) and pilot scale sample (HX2652).

Work Summary and Accomplishments by Iontensity

In addition to assembling dry and filled Li-ion pouch cells for this program for testing by others in the consortium, Iontensity ran several test matrices to determine the "mechanical" effect on different current collectors using varying percentage Si alloy/graphite formulations.

First Matrix: 20% to 60% Si Alloy

Cells with a 42 x 61 mm footprint and 0.5Ah capacity were assembled and tested. A range of CV-7 formulations from 20% to 60% were tested against 3M's NMC 622C formulated with 96.5% active material. Three current collectors were tested: (1) 10 µm Cu foil, (2) 18 µm Cu foil and (3) 15 µm Ni foil. The high loadings of the Si alloy anode formulations made it difficult to process the thin 10 µm Cu foil on our roll-to-roll coater. The 15 µm Ni foil is lighter than the 18 µm Cu foil providing higher gravimetric energy density in addition to higher volumetric energy density based on thickness. Ni foil also has a higher tensile strength than either of the Cu foils. The energy densities and cell expansion were quantified. Cells were cycled between 2.5 to 4.4V and 4.5V at a C/3 rate.

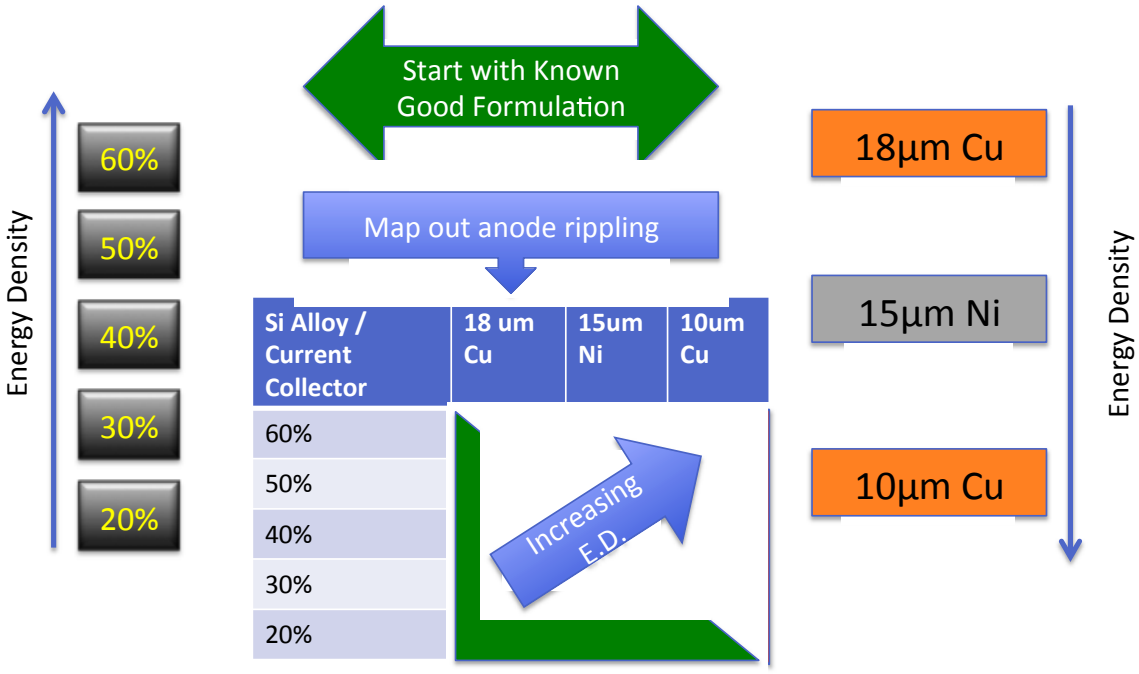

Figure 21. Si Alloy % / Current Collector Matrix

For a given Si anode there are two competing forces:

1. Si particle expansion / contraction within anode matrix; and
2. Tensile strength of current collector.

A great deal of the industry's R&D effort is going into Si particle expansion / contraction. In addition to studying the nature and structure of the Si particle or alloy, extensive work is in progress to better understand the role of binders and conductive additive components. Our focus in this test matrix was on the second force: the tensile strength of the current collector.

A major observation from this study was the occurrence of "rippling" seen on the surface of some of the pouch cells. We have previously found that the tensile strength of current collector is important as thinner Cu foil provides higher energy density but with lower tensile strength, expansion and contraction of the Si anode coating leads to rippling which results in a thicker cell and ultimately lower volumetric energy density. Substitution of Cu foil with Ni or alternate foil increases tensile strength but also cost. Obviously this rippling is not observed with 18650 cells and can go undetected. Autopsies revealed that the rippling originated at the anode current collector. Three factors were identified: (1) use of a stiff PAA binder, (2) the % Si alloy in the formulation and (3) the tensile strength of the current collector.

The cells with the 10 µm Cu foil rippled even at the low 20% Si alloy formulation. The cells with the 18 µm Cu foil showed minor rippling with 40% Si alloy and major rippling at 50% and 60%. In the 18 µm copper cells, excessive rippling seen in the higher Si alloy formulations resulted in lower volumetric energy densities even though the capacities were higher. Maximum

energy density in the 18 µm Cu foil cells was seen at 30% Si alloy. The cells with the Ni foil did not ripple and their energy densities were not as affected.

Table 11. Rippling of Li-ion pouch cell anodes (Green = no rippling; Red = rippling)

Si Alloy / Current Collector	10µm Cu	18µm Cu	15µm Ni
60%			
50%			
40%			
30%			
20%			

Energy density measurements at 2.5V to 4.4, 4.5 and 4.6V are shown in Table 12 and Figures 11 and 23. The gravimetric energy densities at each temperature are shown in Figure 22 with 50% Si having the highest gravimetric energy density at 282 Wh/kg at 4.5V. Figure 23 shows the energy density for the full 2mm x 42mm x 61mm cell. At 4.5V, the 30% Si alloy cell reached 604 Wh/L (625 Wh/L at 4.6V). Note that assembling a larger Li-ion pouch cell, 58mm x 145mm for example, will have a higher energy density than the 42mm x 61mm test vehicles we used, due to the volumetric efficiencies gained primarily by a smaller top seal area; thickness is also an important factor.

Table 12. Si % Energy Data for 2.5V to 4.4V, 4.5V, 4.6V in 42mm x 61mm Pouch Cells

204261			Mass and Dimensions					Discharge Energy to 2.5V					
Lot-				Stack only	4.35V,4.5V	Volume	Expansion	(Wh/kg)			(Wh/L)		
Cell ID	Si%	Foil	Mass(g)	Thick(mm)	Thick(mm)	(cc)	(%)	4.4V	4.5V	4.6V	4.4V	4.5V	4.6V
131-B04	20	18um Cu	11.902	1.40	2.04	5.2	30	234	251	256	533	571	583
142-A01	20	10um Cu	9.5110	1.21	1.78	4.6	28	219	230	243	479	502	517
142-B01	20	18um Cu	10.0072	1.23	1.76	4.5	25	207	222	227	477	492	518
142-E02	20	15um Ni	9.8174	1.19	1.71	4.4	25	217	228	237	490	515	534
132-B03	30	18um Cu	12.079	1.44	2.04	5.2	26	242	258	267	558	596	618
132-C03	30	15um Ni	11.703	1.40	2.01	5.1	27	249	266	275	567	604	625
133-B04	40	18um Cu	11.911	1.40	2.11	5.4	35	227	240	229	500	528	505
133-C04	40	15um Ni	11.591	1.38	1.98	5.1	27	250	263	266	571	601	609
142-C02	40	18um Cu	12.5845	1.56	2.44	6.3	42	259	273		519	547	
142-D03	40	15um Ni	12.2093	1.56	2.23	5.7	28	261	274	286	565	594	
134-B05	50	18um Cu	11.709	1.32	1.95	5.0	31	236	253	246	554	593	576
134-C03	50	15um Ni	12.019	1.49	2.22	5.7	34	271	282	293	533	556	577
135-B03	60	18um Cu	11.517	1.31	2.20	5.6	51	245	258	263	501	527	537
135-C03	60	15um Ni	11.309	1.33	1.96	5.0	30	222	239	239	500	538	537

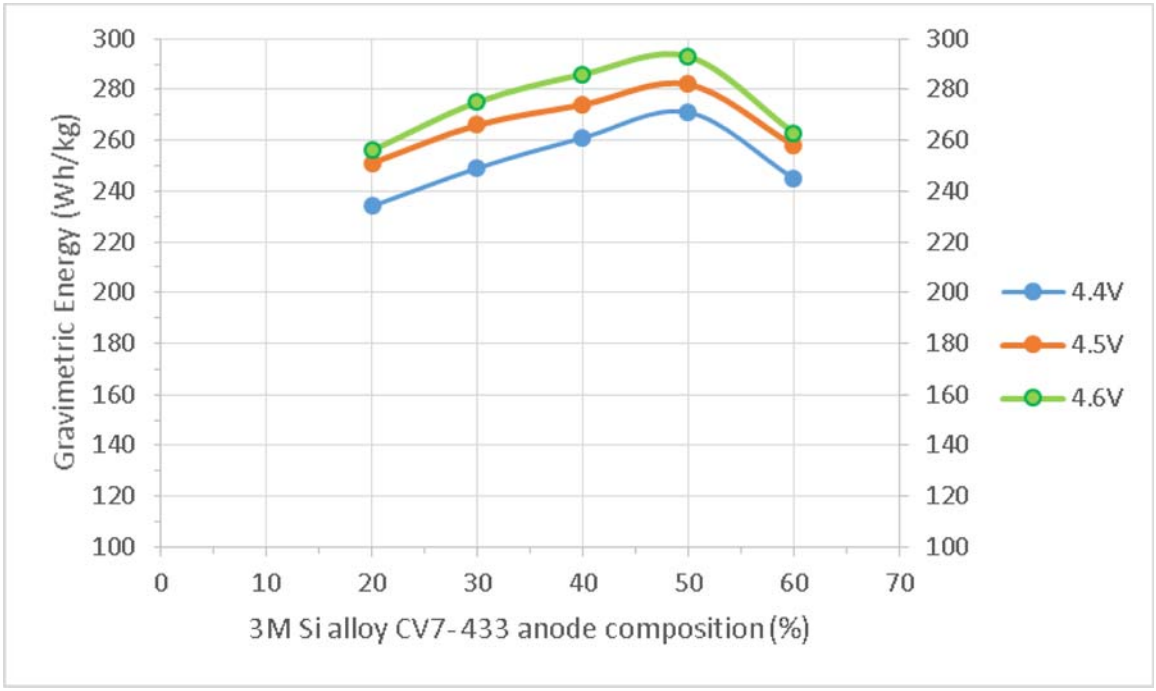

Figure 22. Gravimetric Energy Density in Pouch Cells

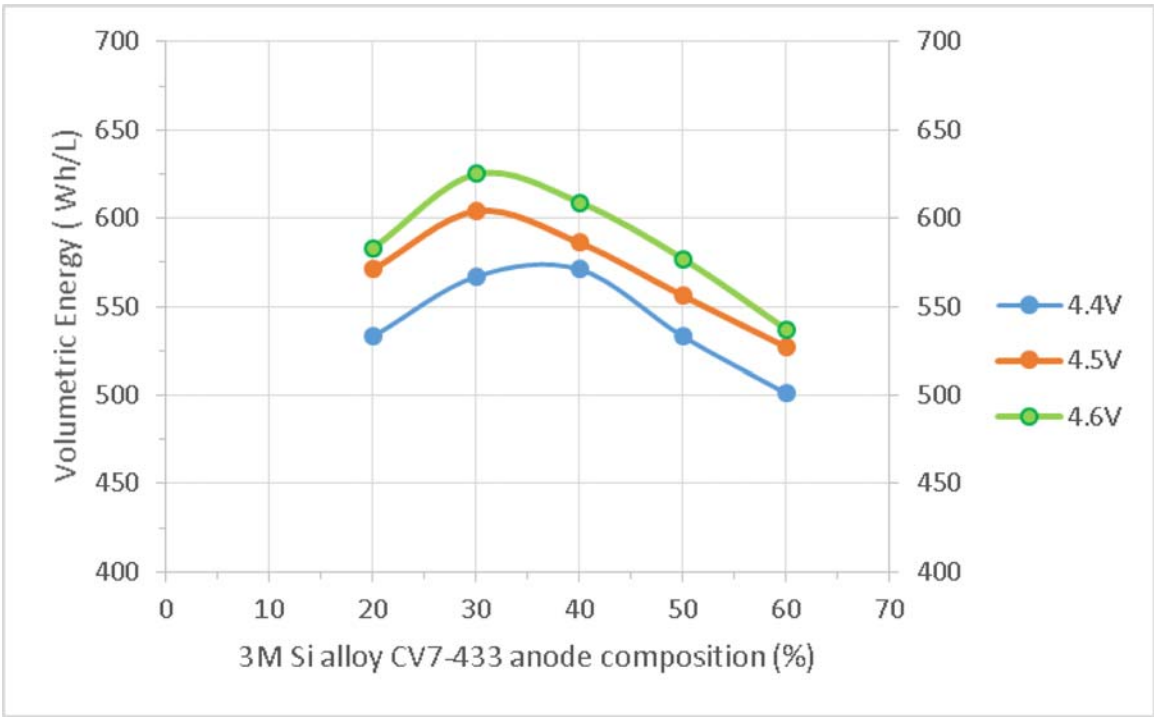

Figure 23. Volumetric Energy Density in Pouch Cells

Cycle life of the lithium-ion pouch cells was higher for (1) lower % Si alloy content and (2) lower charge voltage of 4.35V versus 4.4V or 4.5V. A greater amount of Si expansion and particle isolation in the higher % Si alloy and higher upper charge voltages is believed to lower the cycle life. Higher charge voltage is also known for increased electrolyte degradation also leading to lower cycle life. Note that optimizing the electrolyte formulation for high voltages was not part of this program.

Table 13. Legend for Cell Numbering for % Si Alloy / Current Collector Matrix

Cell Lot #	% Si Alloy		Sub Lot	Current Collector
131	20%		A	10 µm Cu foil
132	30%		B	18 µm Cu foil
133	40%		C	15 µm Cu foil
134	50%			
135	60%			

Cycling to 4.35V provided good cycle life albeit at low energy as shown in Figure 24. Best cycling was with 20% Si alloy (131). All of the other cells were cycled to 4.5V @ C/4 as shown in Figure 25. The 18 µm Cu foil series is shown in Figure 26. The 20% Si alloy (131) outperformed the higher concentration cells. In Figure 27 the 15 µm Ni foil cells were cycled. The 30% Si alloy (132) had the best cycle life but note that there were no 20% cells available in the testing.

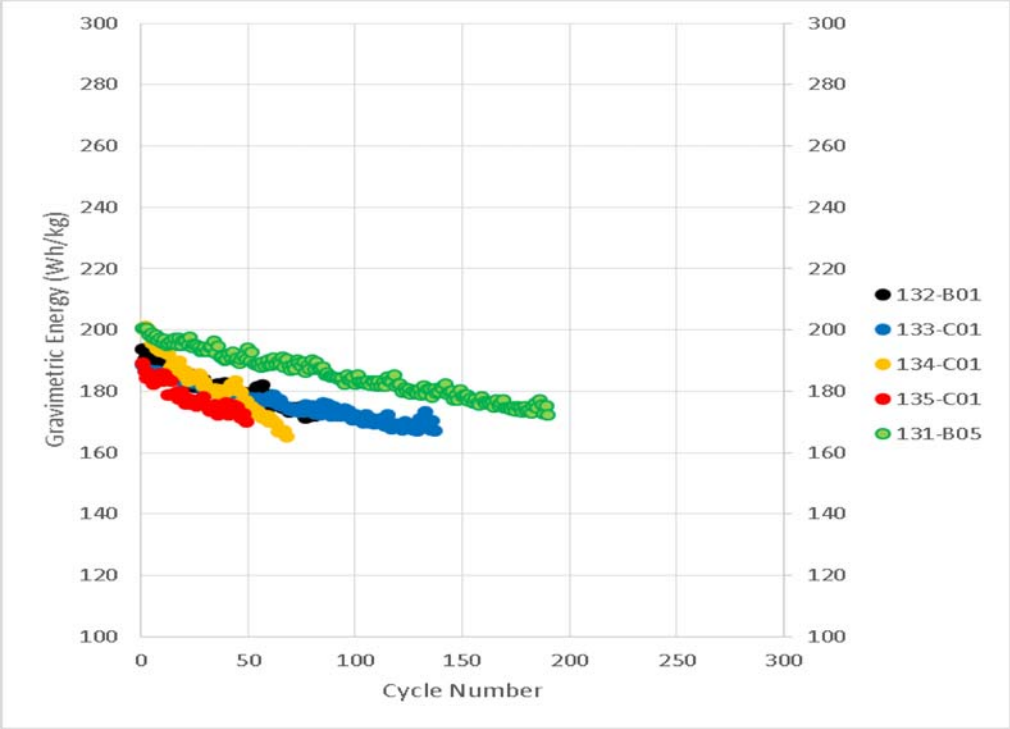

Figure 24. Cycle Life: 20% to 60% Si Alloy; 3 to 4.35V @ C/4

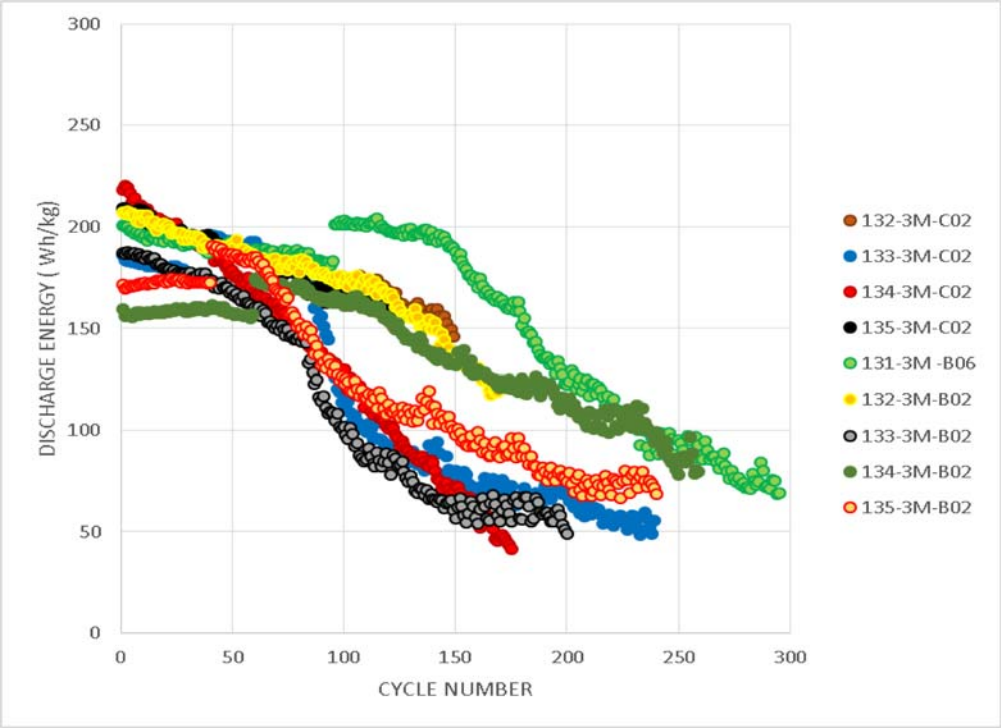

Figure 25. Cycle Life: 20% to 60% Si Alloy; 3 Current Collectors; 3 to 4.5V @ C/4

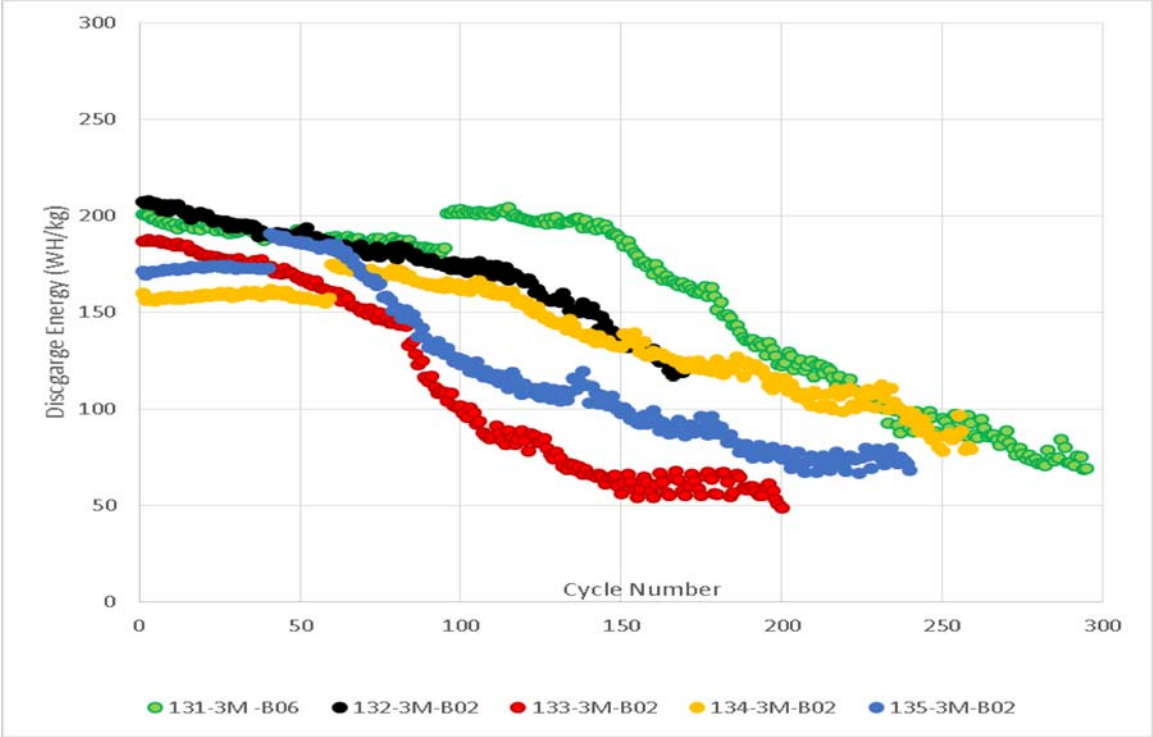

Figure 26. Cycle Life: 20% to 60% Si Alloy; 18um Cu Foil; 3 to 4.5V @ C/4

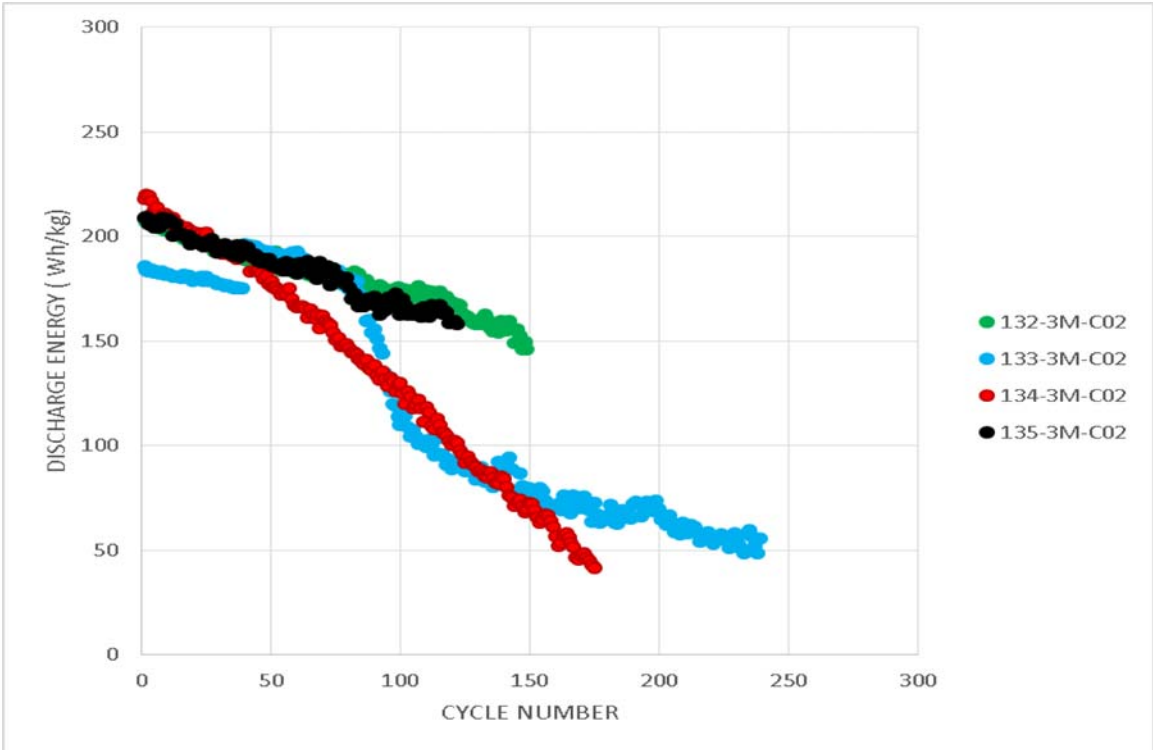

Figure 27. Cycle Life: 20% to 60% Si Alloy; 15um Ni Foil 3 to 4.5V @ C/4

Our measurements for the increase in thickness from a fresh (as assembled) cell, to a fully charged cell during the formation process are shown in Figure 28. It is clear that the percentage in cell thickness increase is a function of the percentage of Si alloy in the formulation for the 18 µm Cu foil to a greater extent than the higher tensile strength 15 µm Ni foil.

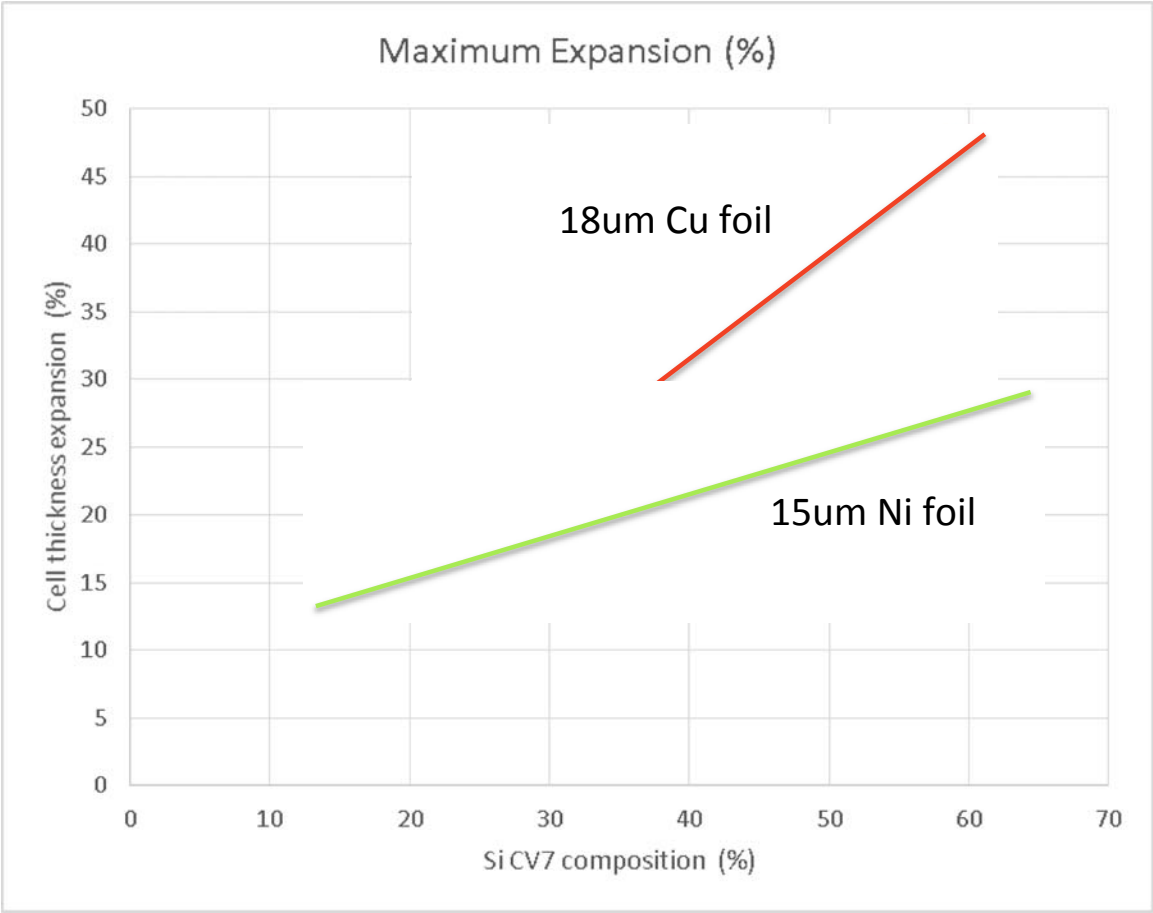

Figure 28. Cell Thickness Expansion vs.% CV7 Si Alloy in Anode

Second Matrix: 20% to 40% Si Alloy

Following the complete Si alloy % / current collector matrix, five new cell lots were assembled. A 20% Si alloy formulation was coated onto 10 µm and 18 µm Cu foil and 15 µm Ni foil. A 40% Si alloy formulation was coated onto 18 µm Cu foil and 15 µm Ni foil. Energy density, cell thickness expansion and cycle life were measured.

Energy density measurements at 2.5V to 4.4, 4.5 and 4.6V are shown in Table 14 and Figures 29, 30 and 31. In Figure 29 the gravimetric energy densities follow the mass of the current collectors with the 10 µm Cu foil, providing the highest energy and the 18 µm Cu foil the lowest with the 20% Si alloy. At 40% Si alloy the cells reached 275 Wh/kg at 4.5V.

Figure 30 shows the energy density for the full 2mm x 42mm x 61mm cell. At 4.5V, the 40% Si alloy cell reached 600 Wh/L and exceeded 600 Wh/L at 4.6V. Figure 31 was calculated for

"chemistry only" by extracting all volume outside of the cell stack. Note that by assembling a larger Li-ion pouch cell, EV size: 225mm x 225mm for example, will have a higher energy density than the 42mm x 61mm test vehicles we used, due to the volumetric efficiencies gained primarily by a smaller top seal area; thickness is also an important factor. At 4.5V, the 40% Si alloy chemistry achieved over 1000 Wh/L.

Table 14. Energy Density for 20% and 40% Si Alloy (42x61mm) Li-ion Pouch Cells

LOT			Cell	Max.	Vol.	Grav. Energy(Wh/kg)			Vol. Energy(Wh/L)		
142-3M	Si%	Foil	Mass(g)	Thick(mm)	(cc)	4.4V	4.5V	4.6V	4.4V	4.5V	4.6V
CELL Series											
A	20%	10um Cu	9.5104	1.70	4.36	219	230	243	479	502	517
B	20%	18um Cu	10.3523	1.75	4.48	207	218	227	477	502	518
E	20%	15um Ni	9.8215	1.70	4.36	217	228	237	490	515	534
C	40%	18um Cu	12.5845	2.44	6.25	259	273	284	519	547	569
D	40%	15um Ni	12.4819	2.21	5.66	261	274	285	565	594	614

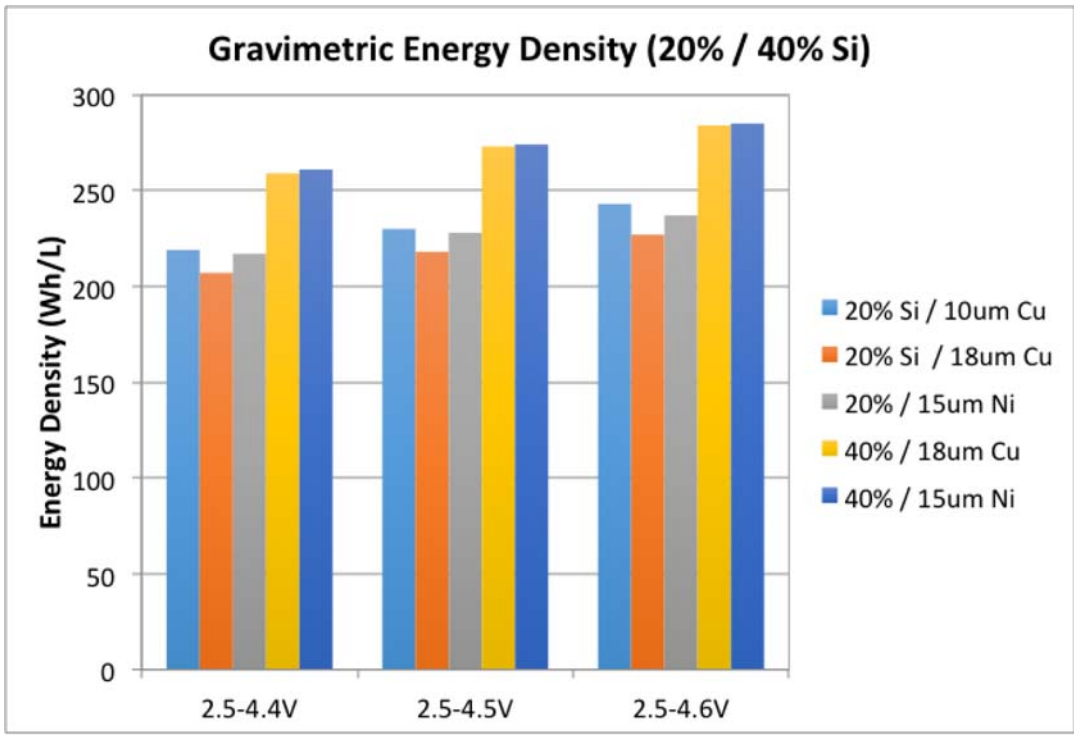

Figure 29. Gravimetric Energy Density for 20% and 40% Si Alloy

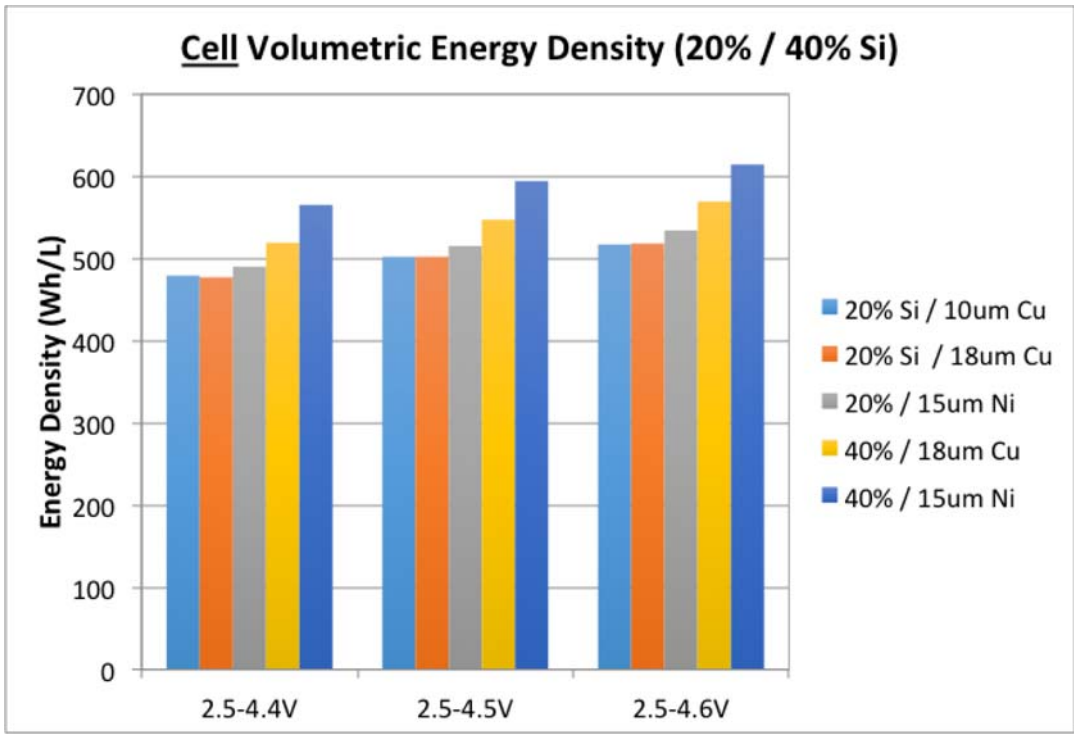

Figure 30. Volumetric Energy Density for 20% and 40% Si Alloy (Cell Level)

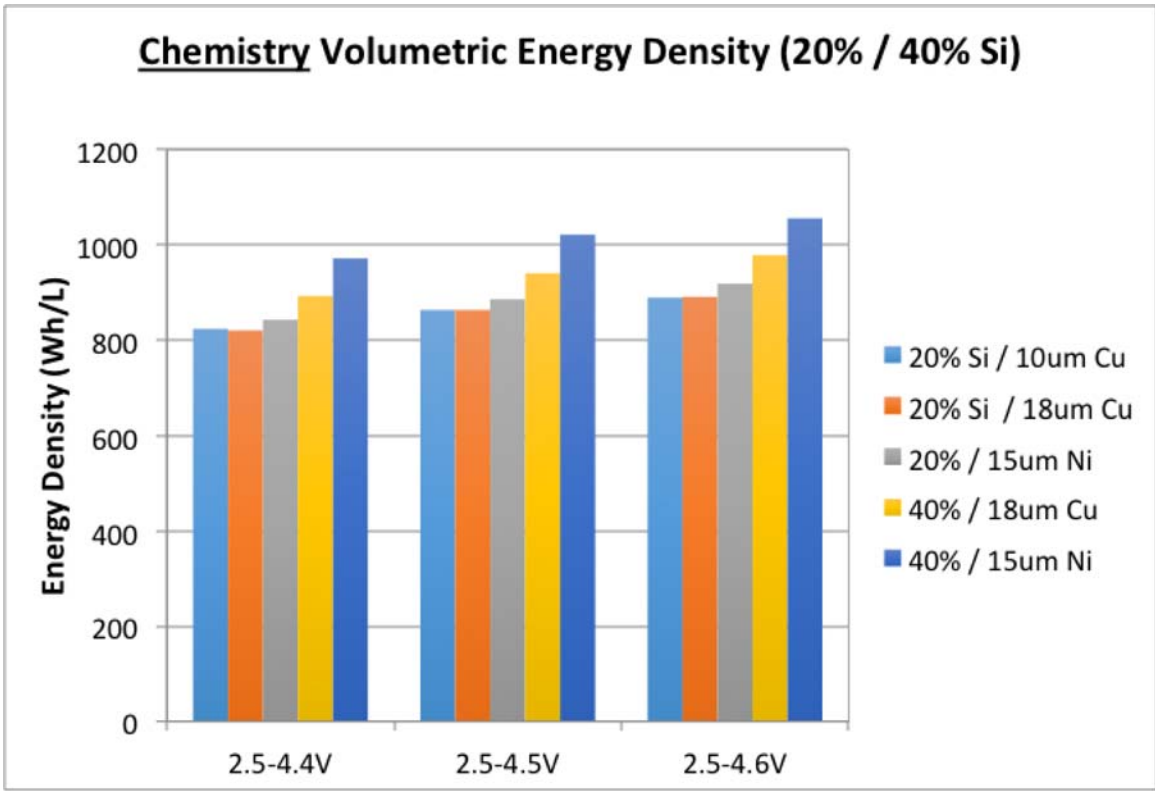

Figure 31. Volumetric Energy Density for 20% and 40% Si Alloy (Chemistry Level)

Our measurements for the increase in thickness from a fresh (as assembled) cell, to a fully charged cell during the formation process were similar to the previous test matrix. It is clear that the percentage in cell thickness increase is a function of the percentage of Si alloy in the formulation for the 18 µm Cu foil to a greater extent than the higher tensile strength 15 µm Ni foil.

The cells were cycled from 2.5V to 4.4V @ C/3 at room temperature as shown in Figure 32 and 2.5V to 4.5V @C/3 in Figure 33. During cycling the higher energy 40% Si alloy cell capacity dropped off at a lower cycle number than the lower energy 20% Si alloy. Overall the cycle life was poor.

One of the first cells assembled in this program in August 2014 is shown for comparison in purple. This cell used an LCO cathode. The cell had higher energy density and cycled well before dropping precipitously.

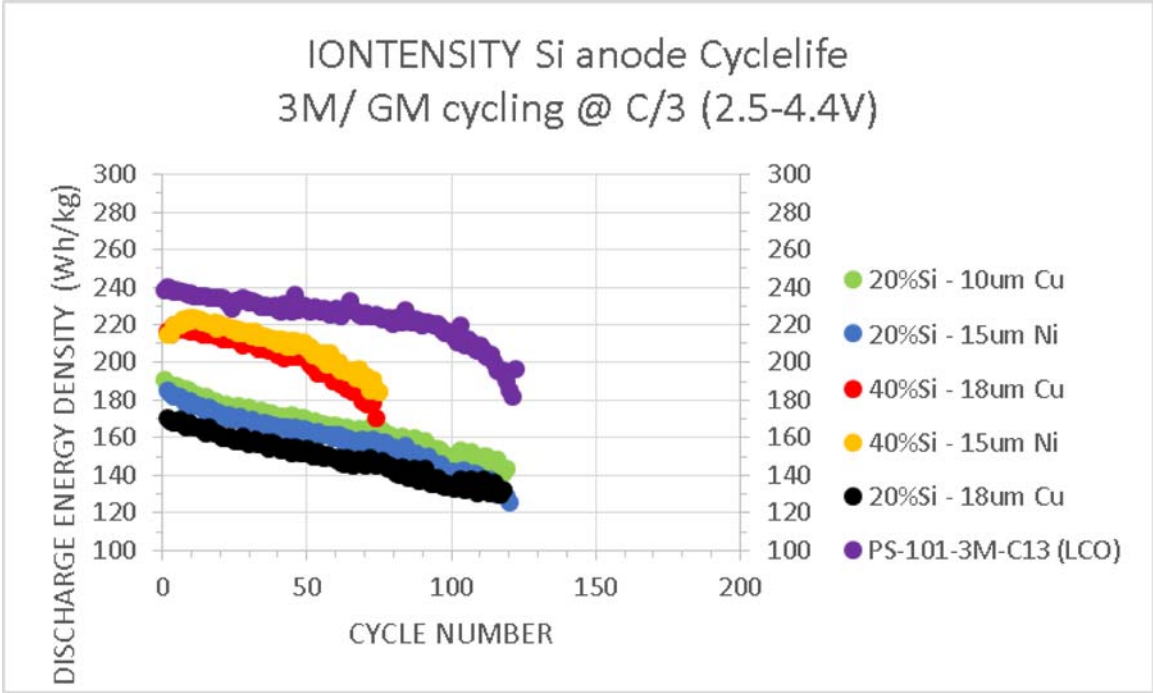

Figure 329. Cycle Life for 20% and 40% Si Alloy vs. 3M NCM622C (2.5V to 4.4V)

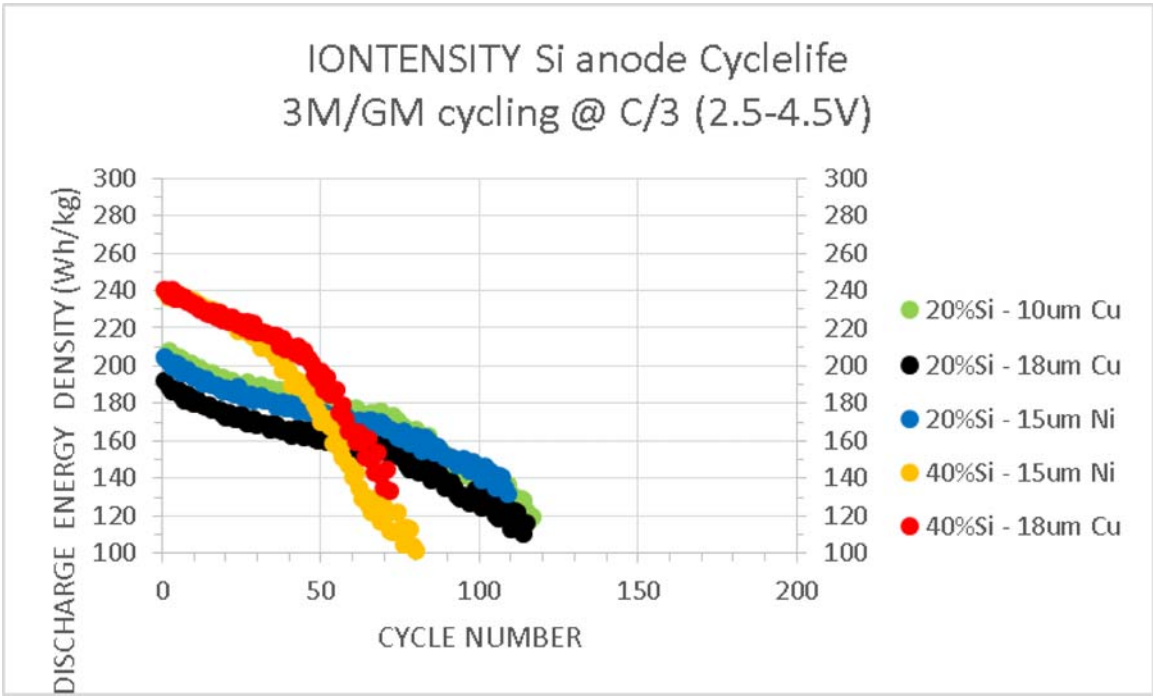

Figure 3310. Cycle Life for 20% and 40% Si Alloy vs. 3M NCM622C (2.5V to 4.5V)

The new cells were inspected visually to determine if rippling occurred and reported in Table 15. As expected the Cu foils all rippled to an extent but no rippling was seen with the Ni foil cells.

Table 15. Visual Inspection of Li-ion Pouch Cells Following Cycle Life

Si Alloy Content	Current Collector	Visual Inspection
20%	10 μm Cu	Minor rippling
20%	18 μm Cu	Very minor rippling
20%	15 μm Ni	No rippling
40%	18 μm Cu	Rippled
40%	15 μm Ni	No rippling

Test matrices with different Si alloy % and various current collectors were completed. In these matrices we found that the least cell thickness expansion (15%) was with only 20% Si alloy and independent of current collector. Cell thickness expansion was found to be proportional to Si alloy %. Not surprising but the best cycling was also found for the 20% Si Alloy cells. When tested at different voltages, 4.35V cycled better than 4.4V and 4.5V, respectively; also not surprising with greater Li insertion at higher voltages and increased electrolyte degradation at higher voltages. To achieve high energy density, cycling to ≥ 4.5V is critical as opposed to 4.35V or 4.4V. At 4.5V the 20% Si alloy cells cycled better than the higher % Si alloys. The highest gravimetric energy density at 4.5V was achieved with 50% Si alloy at 280 Wh/kg. The highest volumetric energy density at 4.5V was achieved with 30% Si alloy at 600 Wh/L. This is presumably due to the greater thickness increase in the higher Si alloy content.
In some test cells we observed rippling of the surface of the cells. This rippling leads to increased cell thickness and lower energy density. After disassembly it was clear that the anode was rippling and the ripples on the anode could be seen through the outer package. In our study we found that Ni foil, even when thinner than Cu foil will not ripple due to its higher tensile strength. 10 μm Cu foil easily ripples with any Si content. 18 μm Cu foil ripples at 40% and higher Si alloy content. Although not seen due to the metal 18650 cans, we believe the anode current collector, if rippled, could have detrimental effects on the performance of the cells.

Work Summary AND Accomplishments by Army Research Laboratory

The baseline electrolyte contained 1M $LiPF_6$ in a solution of 3:7 wt% ratio of ethylene carbonate:ethyl methyl carbonate. Electrolyte additives were initially investigated in coin cells in full cell configuration using core-shell NCM cathode material and CV6 Si-carbon alloy. Of the various different additives tested, six additives showed potential in the initial cycles for improving the fade rate of the cells. However, these tests were carried out in electrolyte flooded coin cells such that the amount of electrolyte additive per unit active electrode materials might be too high. In pouch or 18650 prototype cells, the amount of electrolyte per cell is limited. The

results obtained in flooded coin cells may not translate well into real cells with limited amount of electrolyte. The electrolyte additives were then tested using a limited amount of electrolyte in the coin cells. To compare to the pouch cells formulated by Iontensity, 2.2g electrolyte per Ah, resulting in 12 µg electrolyte for 6.4 mAh coin cells, was tested. However, the results were not reproducible and displayed erratic cycling behavior. It was concluded that the limited electrolyte introduced wettability issues due to the spread of electrolyte to the void space in the coin cells. When the electrolyte amount was increased to 25 µg, the coin cells showed reproducible cycling with excellent efficiency (as high as 99.95%).
Next, the upper and lower voltage cutoff potentials were examined using the same electrode materials. Two lower voltage cutoffs (2.5 and 3.0V) and 5 upper voltage cutoffs (4.35, 4.40, 4.45, 4.50 and 4.55V) were examined (Figure 34). Raising the lower cutoff voltage has a much more dramatic effect on the cell performance than lowering the upper cutoff voltage. While the cells cycled to 2.5V have a higher initial capacity, the fade rate begins to increase dramatically after around 60 cycles. The cells cycled to 4.55V have higher initial capacity than those cycled to 4.50 and 4.45V but the fade rate is higher. We have determined that a voltage range of 3.0-4.45V is ideal for this system for improved cycle life while maintaining a high capacity.

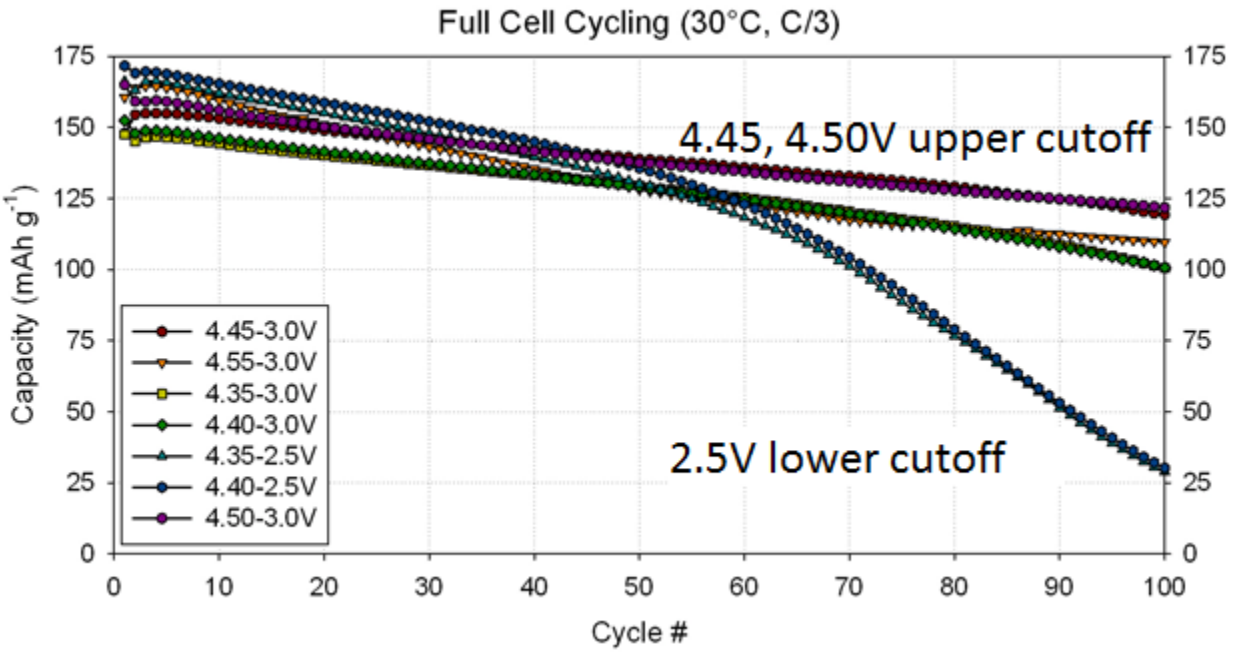

Figure 34. Cycle life performance under different voltage windows

Several different electrolyte formulations were cycled in full coin cells with coated NCM-622 cathode material (683C-2) and CV7 anode material (684A-1). The cells were cycled from 4.45-3V at 30°C at C/3 rate (baseline, baseline + 1% succinic anhydride, baseline + 1% Fluoroethylene carbonate (FEC), baseline + 10% FEC, and 1M $LiPF_6$ in a solution of 1:4 wt% FEC:dimethyl carbonate). The electrolyte containing 10% FEC suffered from gassing in pouch cell testing leading to the formulation of electrolytes without FEC or with decreased FEC. For comparison, an electrolyte containing only FEC and DMC in a 1:4 ratio was also tested to see if more gas was produced (there appeared to be more gas by comparing the amount the pouch cell expanded to the other pouch cells). Decreasing the FEC content to 1% also produced similar cycling results to the 10% FEC electrolyte. An electrolyte containing 1% succinic anhydride

(SAH) was tested and it maintained capacity as well as the FEC containing electrolytes for the first 300 cycles (Figure 35). The concentration of SAH needs to be optimized to determine if the results can be improved.

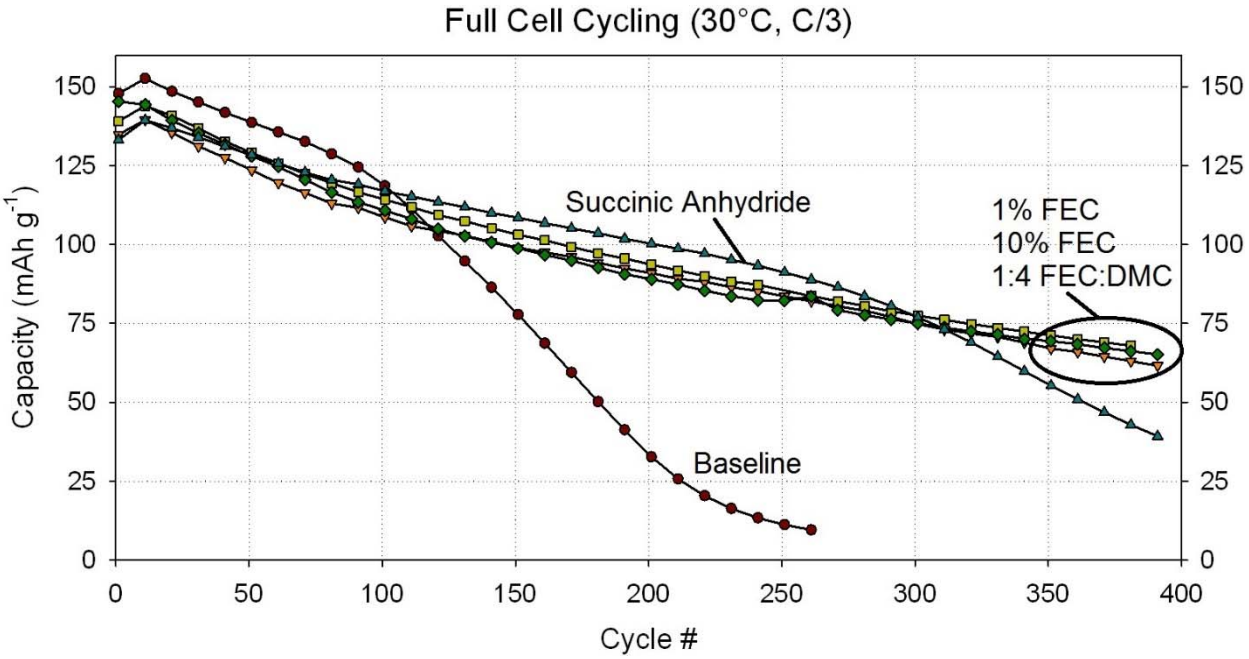

Figure 35. Effect of different electrolyte formulations baseline and advanced chemistry.

Various additives were screened for cycle life using coin cells in a full cell configuration with coated NCM-622 cathode material (683C-2) and CV7 anode material (684A-1). The electrolytes tested were baseline, baseline + 1% tris(trimethylsilyl) phosphate (TMSP), baseline + 1% SAH, baseline + 1% lithium difluoro(oxalate)borate, baseline + 0.5% TMSP + 0.5% SAH, baseline + 10% FEC, baseline + 10% FEC +1% TMSP and baseline + 10% FEC +1% SAH. The use of the additives TMSP, SAH or LiDFOB increased the cycle life compared to the baseline. The addition of 10% FEC also increased the cycle life over that of the baseline. However, the addition of other additives such as TMSP or SAH to the 10% FEC electrolyte did not increase the cycle life. The use of two additives (TMSP + SAH) in the baseline provided the longest cycle life (Figure 36).

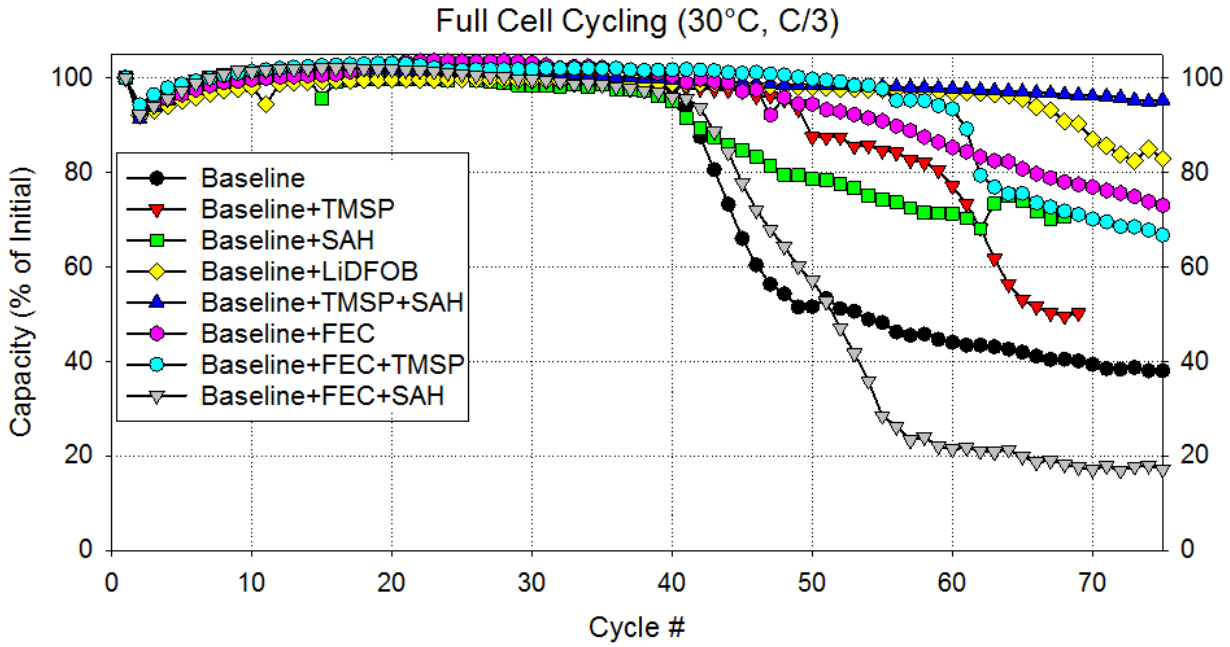

Figure 36. Cycle life of different electrolyte formulations with advanced chemistry.

Work Summary and Accomplishments by Lawrence Berkeley National Laboratory

The lithium-ion battery (LIB) has enabled the development of portable computers, cell phones, and digital cameras, long-driving-range electric vehicles and the storage of renewable nergy in the utility grids are also experiencing revolutionary changes by LIB. High-capacity active materials and components are key to the next generation of high-power LIB. The most popular graphite anode only has a gravimetric specific capacity of 372 mAh/g, while the alternative alloy anode materials such as tin (Sn, 994 mAh/g) or Si (Si, 4200 mAh/g) have much higher gravimetric specific capacities.[1] However, almost 300% volume expansion occurs as the material transitions from Si to its fully lithiated phase.[2] Because of this large volume change, the electronic integrity of the composite electrode is disrupted, and high and continuous surface side reactions are induced, leading to a drastic capacity decay.[3] Polymeric binders have shown their unique role in addressing this problem. Incorporating the hydrogen bonding structure to a low T_g polymer, the binder with a self-healing property was shown to heal the electrode crack and enabled a satisfactory cycling performance of a Si micro-particles.[4] Cross-linking systems using dual binder with carboxylic acid and hydroxyl groups was shown to effectively accommodate the large volume change during cycling, resulting good cycling stability.[5,6] An intrinsically-conductive polymer eliminates the use of brittle acetylene black conductive additives, electronic conductive channel of the electrode rely on the ductile polymer binder and the integrity is perfectly maintained during cycling. These previous work demonstrate the modification of binder as a viable path to drive the application of high-capacity Si-based anodes.[7,8]

In spite of different novel concepts toward a better polymer binder,[9] the imperative property still lies on its original function and also suggested by its name, binding. The electrode laminate adheres onto the current collector as a whole, active materials particles need good cohesion to ensure the flow of ions and electrons. A perfect adhesion property by the binder is a prerequisite to endure the drastic volume changes in the Si-based system. Numerous material developments

are inspired by the observation and investigation of phenomena in the natural world.[10] Mussels rely on byssal threads to attach to a firm substrate for essential activities. The long-lasting adhesion in the wet environment comes from 3,4-dihydroxy-L-phenylalanine (DOPA) in the specialized adhesive proteins.[11,12] Inspection of mussel adhesive protein gave insight into the rational design of mussel-mimetic polymeric binders for Si-based lithium-ion batteries.[13] This work systematically studied the catechol content in a conductive polymer binder for a Si-alloy anode. Perfect stable cycling performance is achieved by the dual strategy of mussel-inspired adhesion and conductive polymer, with this strong adhesion supported by comparing the AFM unbinding force measurements of pulling single catechol-containing conductive polymer chain on a silica substrate to single chain of other conventional polymer binders on the same surfaces. To ensure the real single molecule event, a screen protocol was applied here as well to filter the force data based on several criteria (see supporting information) established to reject curves that exhibit the stretching of multiple chains in parallel or from bundles.

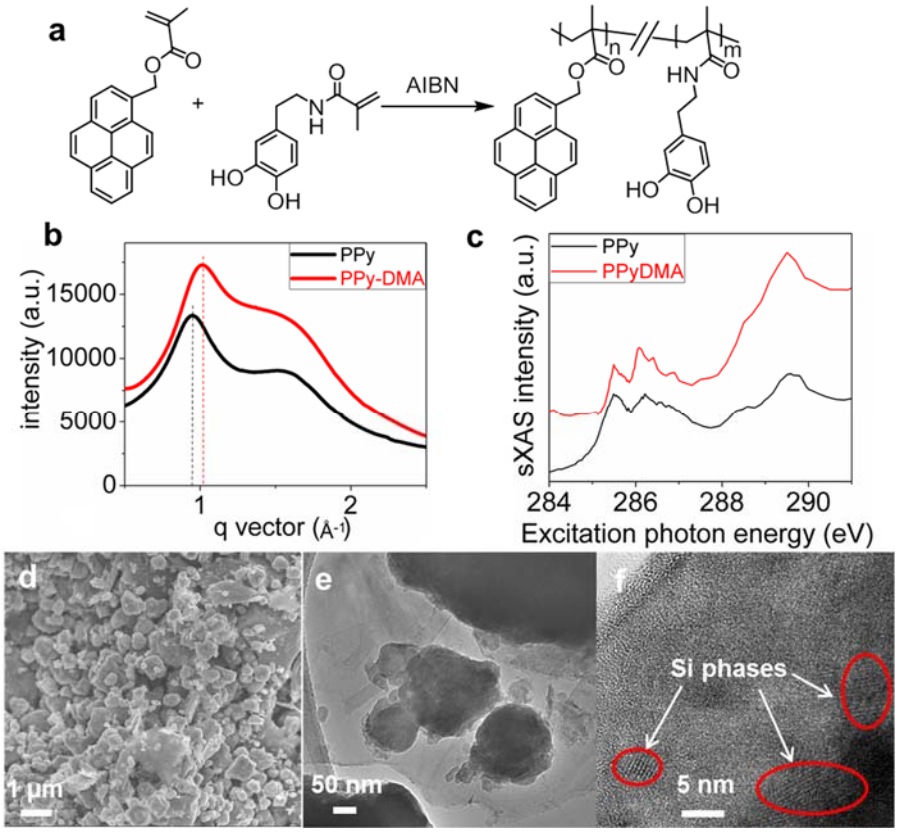

Figure 37. (a) Generic synthesis of Poly(1-pyrenemethyl methacrylate-co-dopamine methacrylamide) (PPyDMA). (b) Wide angle X-ray scattering (WAXS) of PPy and PPyDMA polymers. (c) Carbon K-edge sXAS of PPy and PPyDMA shows that the LUMO energy is intact in PPyDMA, although non-conductive DMA groups are introduced. (d) SEM and (e) (f) High resolution TEM (HRTEM) of the CV7 Si alloy pristine particle.

Pyrene-based polymers, poly(1-pyrenemethyl methacrylate) (PPy), were established as an excellent electric-conducting polymers. Pyrene molecules are connected to the flexible backbone along the chain, they are close in position to be easily self-assembled into ordered structures,

realizing electron conductivity via the side chain π-π stacking force of the aromatic moieties.[14,15] A versatile radical-based polymerization is used to synthesize this type of polymer, which facilitate the incorporation of different functional groups. Dopamine methacrylamide (DMA) was synthesized based on a literature procedure,[13] Poly(1-pyrenemethyl methacrylate-*co*-dopamine methacrylamide) (PPyDMA) was synthesized through free-radical polymerization where the adhesive monomer, DMA, accounts for 36% of this copolymer by mole (^{1}H- nuclear magnetic resonance spectroscopy). PPyDMA has a high number-average molecular weight of 28,672 Dalton and a polydispersity index of 1.9, typical value for a free-radical process, while being soluble in solvents such as tetrahydrofuran (THF) and N-Methylpyrrolidone (NMP). Wide-angle X-ray scattering (WAXS) results show the ordered phase characteristic of the pyrene in both PPy and PPyDMA (Figure 37b). Diffraction peaks are located at ~0.95 $Å^{-1}$ and ~1.02 $Å^{-1}$, respectively. This corresponds to a lattice spacing of ~0.6 nanometers (nm). The broadening of the diffraction peak for the PPyDMA sample indicates that the crystal grain size is smaller when copolymerized with DMA moieties (Figure 37b).

To ensure that the newly-designed PPyDMA binder still maintains the electronic conductivity, the study looked at the electronic structure of both the PPy and PPyDMA polymers using synchrotron-based x-ray absorption spectroscopy (sXAS). sXAS is a direct probe of the excitations of core level electrons to the unoccupied valence states. Previous results of this work demonstrated that sXAS could be employed to study the electric properties of polymer materials efficiently.[7,16] The methodology is based on the fact that the lowest-energy sXAS feature directly corresponds to the state of the lowest unoccupied molecular orbital (LUMO), which is very sensitive to the electric properties of the polymers.[17] Figure 37c shows the sXAS spectra of PPy and PPyDMA. The splitting peaks around 285-286 eV correspond to the $\pi^*_{C=C}$ bonds with conjugation, and the features around 288 eV are from $\pi^*_{C=O}$.[17] The study focused on the low-energy sXAS features corresponding to the LUMO states. It is obvious that incorporating the DMA group does not change the lowest-energy features in sXAS, indicating the LUMO of the PPy polymer is intact in PPyDMA. The consistency of the overall lineshape also implies that the electron states close to the Fermi level are dominated by the pyrene-based PPy states. This comparison is thus reliable without core-hole potential concerns.[7]

A CV7 Si-alloy is used as an anode to evaluate the electrochemical performance of the PPyDMA polymer as a binder (Figure 37 c, d). The pristine particles have a diameter of typically less than 1 μm. Alloying the active Si elements with inactive elements can reduce volume expansion, an improved cycle life is obtained while still maintaining a specific capacity much higher than the graphite anode.[18] Si is present in nano-size domains (Figure 37e) within a matrix of other elements, such as Al and Fe. Not only the volume expansion of the active Si phase is buffered by the matrix, the existence of the nano-Si domain could also suppress the formation of the crystalline $Li_{15}Si_4$.[19] A typical specific capacity of 800~1000 mAh/g is expected for this anode, resulting only 100% volume change during cycling.

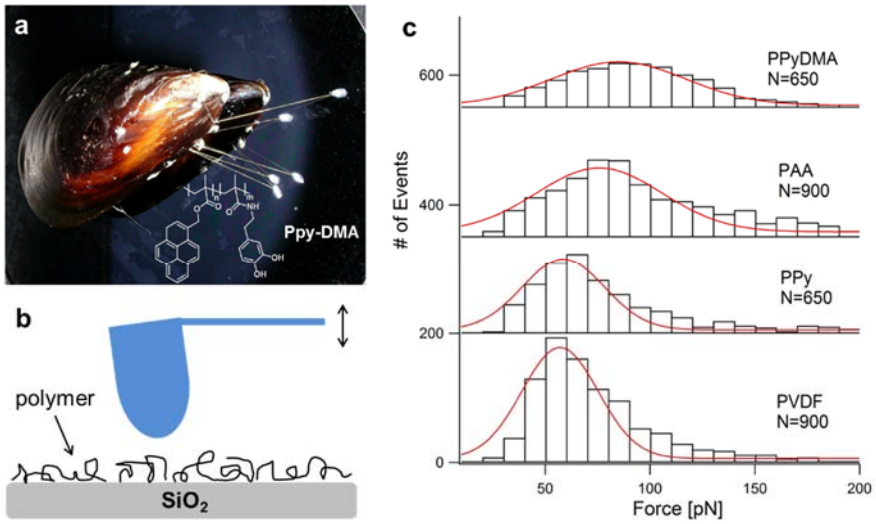

Figure 38. AFM tapping mode on the adhesion test of PPy-DMA polymer binder. (b) A schematic illustration of how the characterization of adhesion force is performed. (c) Histograms of AFM rupture force distribution corresponding to pulling a single polymer chain from a silica substrate. N=900 for PVDF, N=650 for PPy, N=900 for PAA, and N=650 for PPyDMA. N is number of observations.

The high volume changes of the Si-based anode during cell cycling may cause particle isolate from the polymer during delithiation/shrinkage of the active material particles, which is one of the major electrode failure mechanisms for these high-capacity anodes.[9] To characterize the binding affinity between polymer binders and the Si-alloy anode particles, we have investigated the unbinding forces originated from pulling a single polymer chain of different binders from silica substrate, with the consideration of that the higher unbinding force of a single attached polymer chain, the stronger its affinity to substrate. To enable a strict comparison of the unbinding force resulting from different polymers, it is important to isolate and detect a single molecular rupture force.[11] Otherwise, it would be meaningless if the comparison of unbinding force is no single molecular event since the strong unbinding force may come from multiple chains involved at the same time, which is not due to the intrinsic adhesion. To ensure that the observed force was originated from single molecular event, a novel and complete screening protocol was employed. Figure 38c thus shows the histogram of unbinding event of pulling a single PPyDMA, PPy, and PVDF binders on silica substrate at a constant speed. As shown, a single PPyDMA was strongly attached to the silica substrate with the averaged unbinding force value on this surface being higher than that of a single PPy and PVDF chain on the same surface while the averaged unbinding forces involved were actually very similar between the last two binders, thus suggesting the strongest binding affinity between polymer binders containing DOPA moiety and the Si-alloy anode particles. Taking into consideration that the improved adhesion of binders on silica surface could stabilize the cycling performance toward the Si-alloy anode, it is apparent that rom AFM unbinding force measurements the PPyDMA is an ideal binder for Si-alloy anode in lithium ion batteries, as expected.

The dual functionality of intrinsic electronic conductivity and strong adhesion property of the PPyDMA polymer makes it a promising binder in the use of Si-based high-capacity anode. The electrode was fabricated by dissolvent PPyDMA polymer into *N*-methylpyrrolidone (NMP) solvent, active material particles are then dispersed into the polymer solution by high-speed homogenizer for 1 hour before coating the slurry onto Cu current collector using doctor blade.

PPyDMA is determined to be a good binder for either graphite or pure Si nanoparticles, without any need of the conductive additives. The good cycling performance indicate that by randomly incorporating catechol structure into the polymer backbone, pyrene moieties still form good π-π stacking, enabling a good electric conductivity of the polymer binder and cycling performance of active materials.

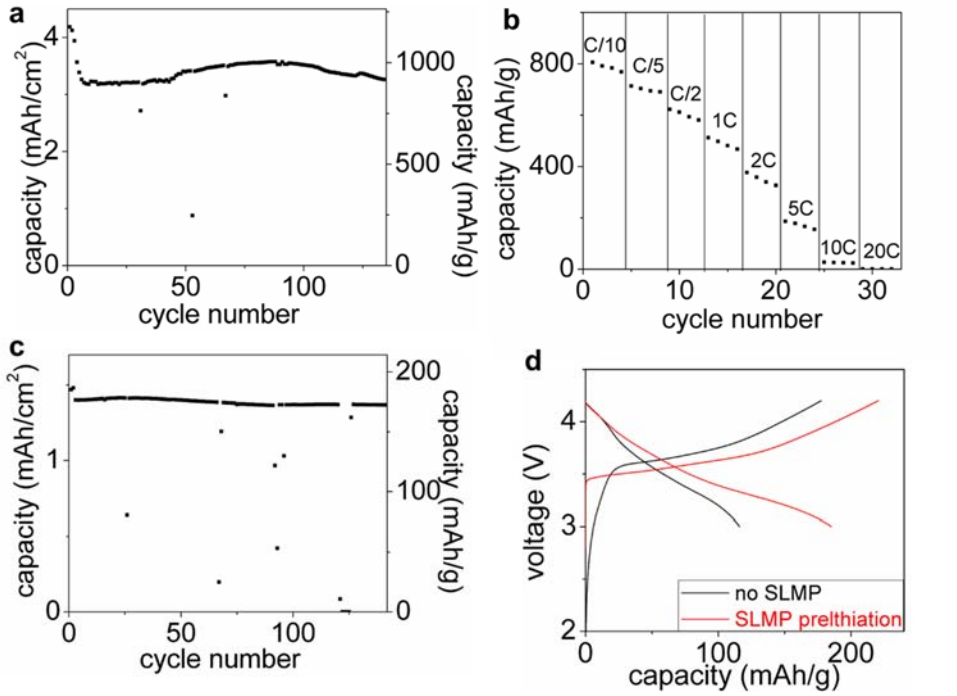

Figure 39. Electrochemical performance of PPy-DMA/CV7 Si alloy anode. (a) Specific capacity vs. cycle number of the PPy-DMA/Si alloy anode with different binder contents at C/10. (b) Specific capacity vs. cycle number of Si alloy anode with different types binders (10 wt% binder content) at C/10. (c) Galvanostatic voltage curves and (d) rate performance of the PPyDMA/Si alloy anode laminate. (e) cycling performance and (f) 1st cycle voltage curves of full cells using PPyDMA/Si alloy anode, with or without SLMP prelithiation.

When used for the Si alloy anode, as shown in Figure 39a, 10 wt% PPyDMA content is determined to be the best composition, which maintains a stable cycling of the CV7 Si alloy anode for more than 100 cycles with a specific capacity of 800 mAh/g. Compared to conventional binders such as polyvinylediene difluoride (PVDF) and carboxymethyl cellulose (CMC), which are intrinsically non-conductive, PPyDMA exhibits an obvious advantage (Figure 39 b). The homo-PPy polymer is also synthesized and used as a binder. However, PPy does not furnish a good adhesion strength between the binder and the Si alloy particles. Although PPy is established as a conductive polymer binder for Si-based anode, PPy/Si-alloy electrode still suffers capacity decay. The minimum capacity fade from PPyDMA binder is also shown in the voltage curves shown in Figure 39d, the voltage curves at 10^{th} and 100^{th} cycles almost overlap with each other. The rate performance of the PPyDMA/Si alloy anode is shown in Figure 3d. Without any conductive additives, the specific capacity enabled by only PPyDMA binder could still retain a specific capacity of above 500 mAh/g at 1C.

Table 16. Electrochemical data of the Si alloy anode based on different binders at C/10.([a] charge (delithiation) capacity [b] Coulombic efficiency)

		10%PPyDMA	5%PPyDMA	10%CMC
1st cycle	Q_c[a](mAh/g)	845.2	1006.9	918.6
	H[b] (%)	64.64	77.95	82.69
10th cycle	Q_c[a] (mAh/g)	780.2	710.1	686.4
	H[b] (%)	99.38	98.27	97.86
70th cycle	Q_c[a] (mAh/g)	741.1	439.7	94.6
	H[b] (%)	99.85	99.20	98.22

Table 16 summarizes the electrochemical results of Si alloy with different binders at a C/10 rate. The excellent capacity retention based on 10 wt% PPyDMA binder is directly correlated to the good coulombic efficiency (CE) of the cell, which has a high value of 99.85% at 70th cycle, compared to 98.22% for the CMC binder. Note that the typical 1st CEs for the Si alloy is in the range of 70%, an prelithiation method should be able to address issue toward a lithium-ion full cell application, which was demonstrated recently in a SiO anode.[20] A nickel-cobalt-manganese (NCM 6/2/2) cathode is used to assemble full cell for the PPyDMA/Si alloy anode. A 48-hour rest period was used to allow the crushed SLMP to fully prelithiate the Si alloy anode before current-driven charging of the cells. Both full cells were put in a formation process consisting of two cycles at C/10 prior to C/3 cycling. Apparent improvement was shown for the SLMP-loaded full cells. The first cycle CE increased from 65.41% to ~84% with the SLMP. Compared to the regular cell without SLMP, the voltage profile at both ends (start of charge and end of discharge) are distinctly different, indicating different lithiation and delithiation of Si alloy anode during these two stages. In the first cycle charge process, SLMP eliminated the needs for SEI formation and activation of the anode, so the curve goes directly to the anode lithiation voltage region. When SLMP is not used, this charging curve shows a long multi-plateau curvature accounting for a capacity of ~30 mAh/g, which is typical for irreversible processes of Si alloy anode activation and SEI formation.

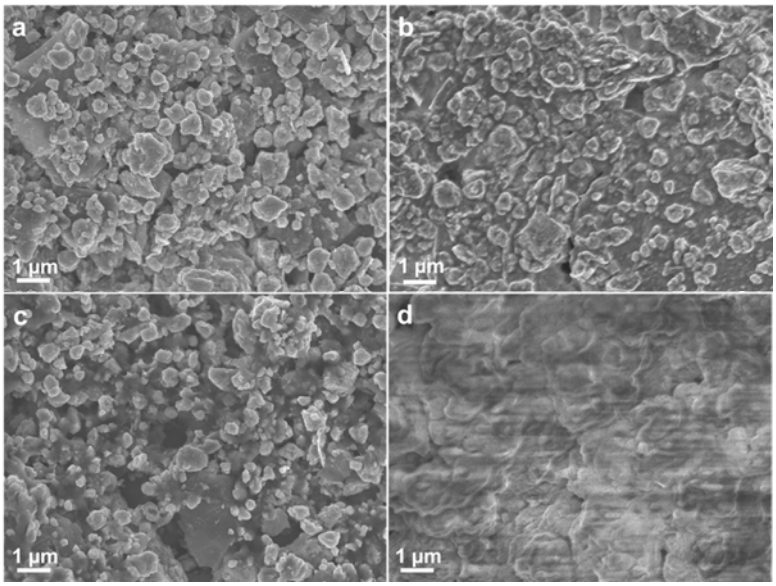

Figure 40. SEM images of the Si-alloy anode-based electrodes. (a) pristine and (b) after 10 cycles at C/10 of the PPy-DMA-based electrode. (c) pristine and (d) after 10 cycles at C/10 of the PVDF-based electrode.

The SEM images of the Si electrodes after long-term cycling are shown in Figure 40. Compared to the conventional electrode with a nonconductive binder (PVDF), the decomposition layer on the PPyDMA-based electrode was much thinner. The Si alloy particles were still individually visible after 10 cycles of deep charge and discharge. In a conventional electrode with PVDF binder, the continuous volume change of active material particles makes the stable SEI formation impossible. The volume expansion of Si alloy during lithiation exposes new surfaces, leading to additional SEI formation and more side reaction products. However during delithiation, the Si particles shrink, and the SEI crumbles from the Si surface. These processes cause the formation of a thick layer of organic species due to the continuous decomposition of the electrolyte (Figure 40d). In contrast, the PPyDMA conductive binder-based electrode has a much thinner SEI layer after repeated cycles, and SEI growth is very minimal. The edges of Si alloy particles are clearly visible with very minimum size changes after 10 cycles (Figure 40b). The PPyDMA-based electrode has 10% binder to entirely cover the Si alloy particle surfaces. Due to the electric conductivity of the pyrene and the strong adhesion force of the catechol moiety, the intimate binding between binder and Si alloy particle is consistently maintained during cell cycling. The strong adhesion between PPyDMA and Si-alloy particles ensures that the particle surface is completely covered by the binder to form an artificial SEI. The real SEI is formed on the surface of the PPyDMA binder instead of on the active material particle surface directly. Since the polymer tends to have higher free volume, the PPyDMA binder provides volume stability during Si volume expansion and contraction. PPyDMA polymers completely cover the particle surface during the volume change, which reduces the contact between the Si alloy particles and the electrolyte, and the continuous consumption of the electrolyte is hindered. Therefore, the SEI on the PPyDMA/Si alloy electrode is much more stable compared to the SEI on the conventional composite. This is also confirmed by the high coulombic efficiency of 99.8% during long-term cycling.

Inspired by the mussel holdfast foot protein, combined with the established side-chain conductive polymer, a DOPA-containing conductive polymer was developed and characterized as an effective binder for a Si-alloy anode in lithium-ion batteries. The facile synthetic route of the side-chain conductive polymer relaxes the requirement for synthesis and allows easy incorporation of the functional adhesion moieties such as DOPA. A quantitative analysis of the adhesion between polymer and silica confirms the strong adhesion force, which contribute significantly to improving the capacities and cycle lives of the Si alloy anode. The commercial Si-alloy anodes reaches a high specific capacity of 800 mAh/g, a much higher value compared to the state-of-the-art graphite anode. Combined with a prelithiation method, the lithium ion full cell based on this novel binder-enabled high capacity anode delivers a high 1st cycle efficiency (84%) and a stable cycling at high material loadings. The mussel-inspired functional conductive polymer binder solves the volume expansion and low first-cycle coulombic efficiency problems, leading to a high-energy lithium-ion chemistry.

Inventions/Patent Applications Created Under this Project

DOE Agreement DE-EE0006448				
IP Summary				
Subject			Date Reported	
Invention #	Title	Inventors	to DOE	DOE S #
1	Formation processes for Li-ion batteries with oxygen loss cathodes	X. Ma	11/4/2014	144,469
2	Silicon based anode material with phosphates as inactive phases	X. Ma	11/4/2014 3/18/2016	144,145
3	Alloy with Lithiated Active Phase	V. Chevrier	11/4/2014 12/11/2015	143,724
4	Electrochemical Cells that inlude Lewis Acid: Lewis Base Complex Electrolyte Additives	A. Xiao, W. Lamanna, J. Dahn, M. Nie, and K. Smith	9/25/2015	142,046
5	Silicon Alloy Anode Materials	X. Ma, D.B.B Le, and L. Li	9/25/2015	142,047
6	Coatings for Silicon Alloy Anode Materials	F. Sun, V. Chevrier, S. Ling, D.B. Le, L. Liu, K. Eberman, X. Ma, and L. Krause	12/20/2016	145,586
7	Electrolyte Solutions and Electrochemical Cells Containing Same	W. Lamanna, K. Smith, and A. Xiao	12/20/2016	145,587

Appendix One: Slide Deck Presented at DOE AMR, June 7, 2016

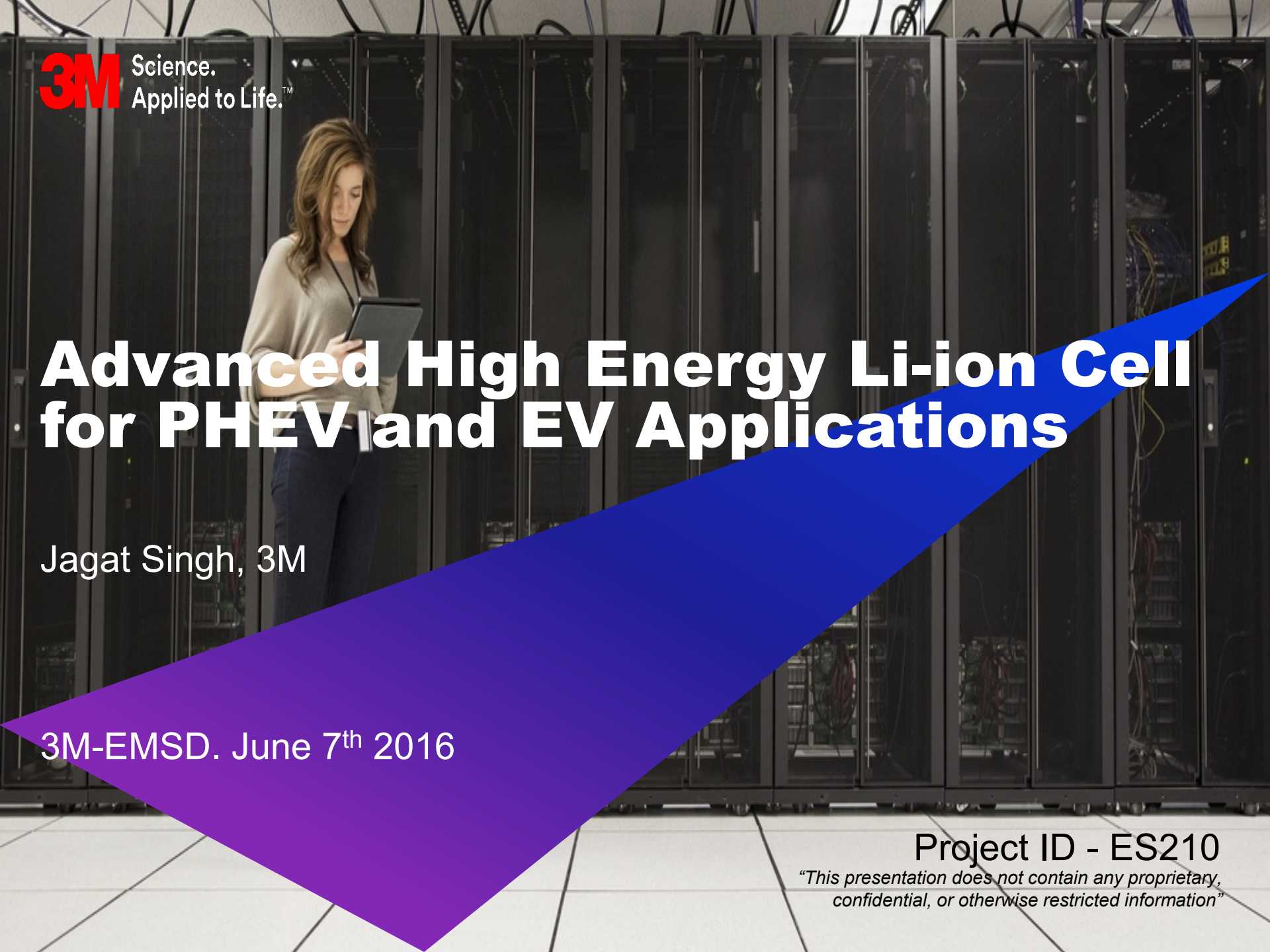

3M Science. Applied to Life.™

Advanced High Energy Li-ion Cell for PHEV and EV Applications

Jagat Singh, 3M

3M-EMSD. June 7th 2016

Project ID - ES210

"This presentation does not contain any proprietary, confidential, or otherwise restricted information"

Overview

Timeline

- Start Date:10/01/2013
- End Date:03/31/2016
- Percent Complete:100%

Barriers

- Cycle Life,
- Specific Energy,
- Cost

Budget

- Total Project Funding
  - $3,145,571
- DOE* Share
  - $2,250,043
- Contractor Share
  - $895,528

3M and the team appreciates the support and funding provided by DOE

Partners

- Collaboration:
  - GM: Dr. Meng Jiang
  - Umicore: Wendy Zhou
  - Iontensity: Marc Juzkow
  - ARL: Dr. Richard Jow
  - LBNL: Dr. Gao Liu
- Interaction
  - Dalhousie University
  - ANL: Deliverable Testing
- Project Lead:3M

Relevance

A collaborative team approach to leverage crucial Li-ion battery technologies and expertise to help enable

- Advanced High Energy Li-Ion Cell
- Superior Performance Envelope
  - Long Cycle Life,
  - High Power Capability,
  - Wide Operating Temperature
- Lower Cost ($/Wh)

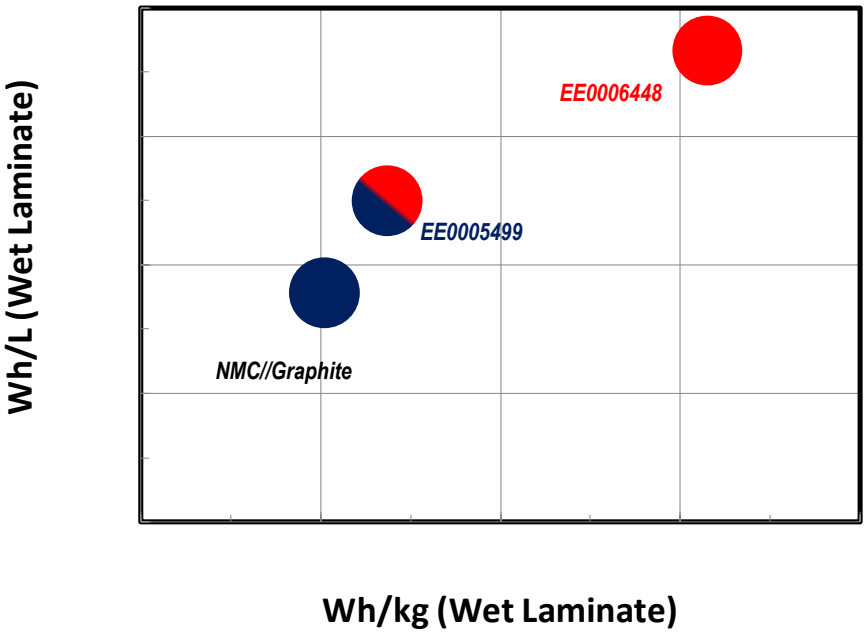

Milestones

Month / Year	Milestone	Status
	Phase I (Oct 1st, 2013 to Sept 30th, 2014)	
Dec / 2013	Scale up baseline anode and cathode material	✓
April / 2014	Baseline cells shipment	✓
	Phase II (Oct 1st, 2014 to March 31st, 2016	
Aug / 2015	Advanced anode and cathode materials selection	✓
Dec / 2015	Advanced anode and cathode materials scale up	✓
March / 2016	Data package – Advanced cells	✓
April / 2016	Advanced cells shipment	✓

Approach

Synergistic Team Approach to Address Vital Components.

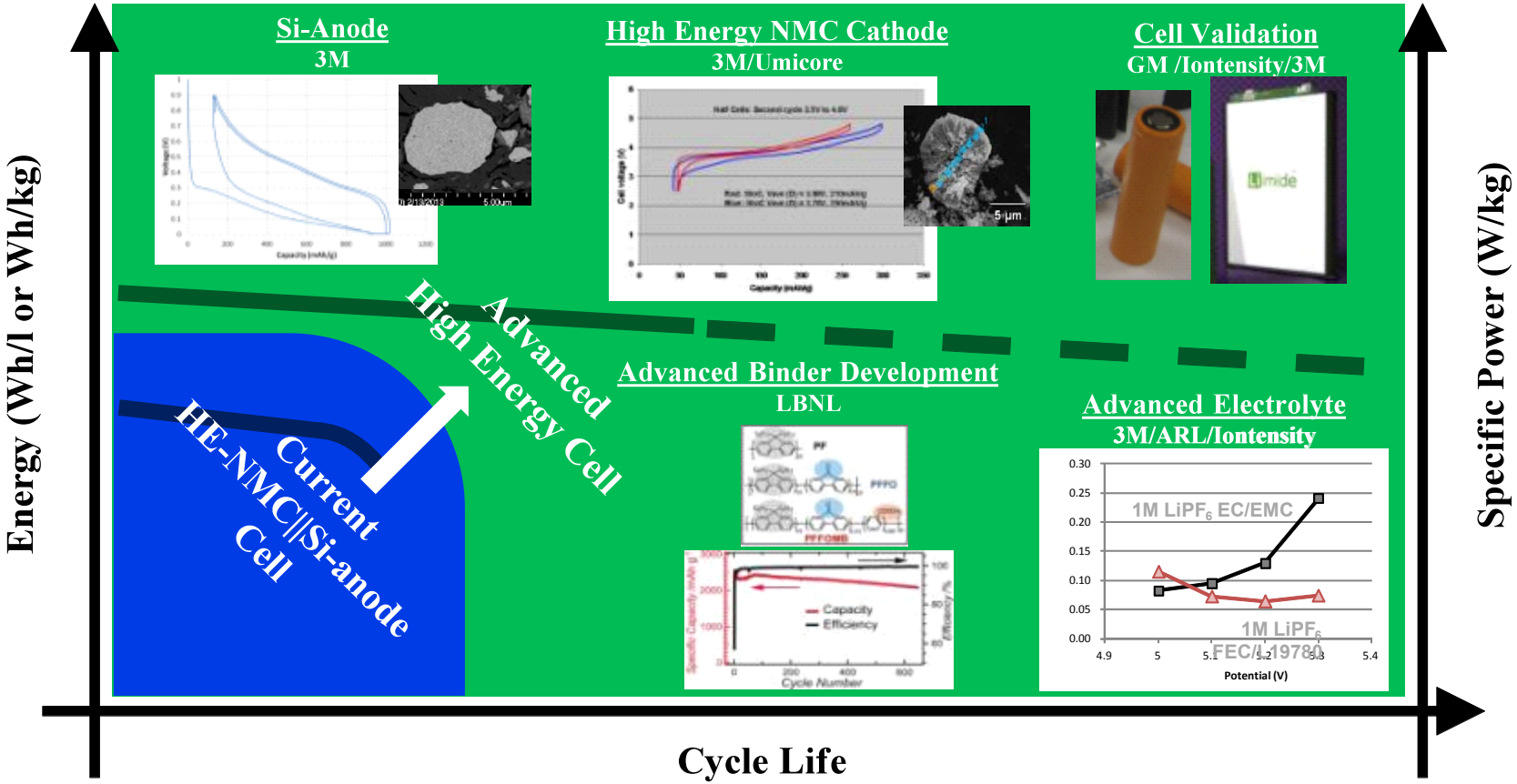

Approach

1 - Develop Advanced Material to meet Energy Targets

Si Alloy Anode

Scalable process to develop high capacity Si alloy with stable microstructure

Binder - Si Anode

Innovative conductive binder for superior Si anode composite

High Energy NMC Cathode

Develop composition with high Wh/kg to increase cell energy

Advanced Electrolyte / Additives

SEI and high voltage stability to enhance performance

2 - Characterize Performance in 18650 / Pouch Cells

Electrode Formulation Study

Tune Formation Protocol

Evaluate Dispersion, Roll to Roll Coating and Drying

Gap Analysis and Diagnostics

Energy and Life Validation

Silicon Alloy Anode Development - 3M

Developed advanced Si alloy anode with better properties

Baseline Material

3M Si Alloy Anode shows excellent cycling and coulombic efficiency compared to Si nano-particles

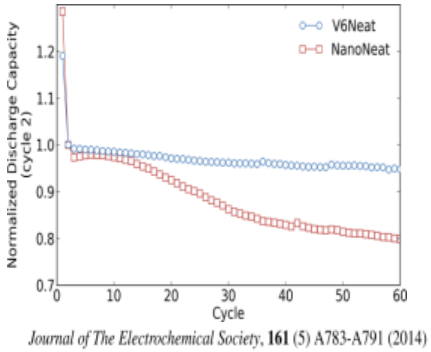

Journal of The Electrochemical Society, **161** (5) A783-A791 (2014)

Advanced Material

Develop Si alloy to target

- 20% ↑ mAh/g
- 10% ↑ mAh/cc
- Higher efficiency

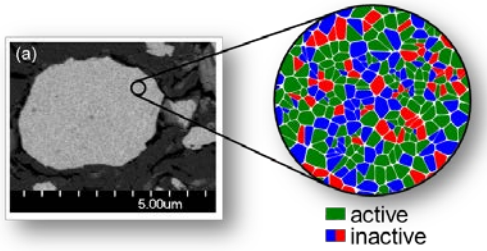

Si Alloy	BET (m^2/g)	1st Lithiation (mAh/g)	1st Delithiation (mAh/g)	1st Delithiation (mAh/cc)	First Cycle Efficiency (%)	Manufacturability
Advanced Material	--	1170	1060	3370	90.4	✓
Baseline Material	3.5	1050	900	3280	85.7	✓

Silicon Alloy Anode Development - 3M

Developed advanced Si alloy anode with better properties

Baseline Material

3M Si Alloy Anode shows excellent cycling and coulombic efficiency compared to Si nano-particles

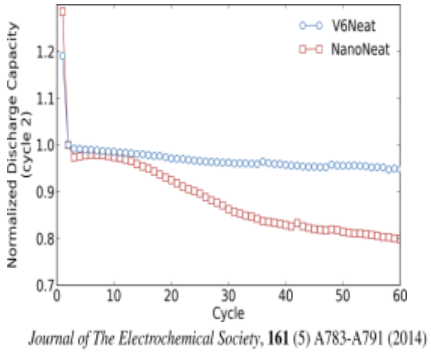

Journal of The Electrochemical Society, **161** (5) A783-A791 (2014)

Advanced Material

Develop Si alloy to target

- 20% ↑ mAh/g
- 10% ↑ mAh/cc
- Higher efficiency

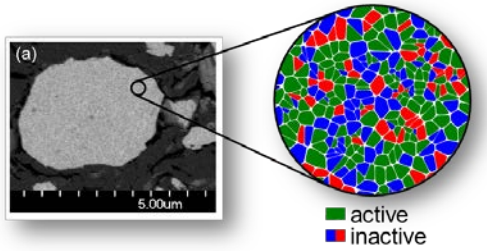

Si Alloy	BET (m^2/g)	1st Lithiation (mAh/g)	1st Delithiation (mAh/g)	1st Delithiation (mAh/cc)	First Cycle Efficiency (%)	Manufacturability
Advanced Material	--	1170	1060	3370	90.4	✓
Baseline Material	3.5	1050	900	3280	85.7	✓

Silicon Alloy Anode Scale Up - 3M

Demonstrated material scale up & commercial manufacturing feasibility

StarTribune | business

News Local Sports Business Politics Opinion Lifestyle Entertainment Obi

Local | Nation | World | Investigators | Weather | Obituaries

Home › Business

Helping to build a better battery

Article by: SUSAN FEYDER , Star Tribune

A 3M pilot project is making longer-lasting lithium ion batteries for consumer electronics. Next up: electric vehicle batteries.

High volume manufacturing feasibility underway.

Scale-up plan to meet the demand forecast.

Binder Development - LBNL

Demonstrated higher areal capacity electrodes with Si Alloy Anode

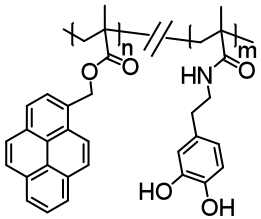

PPyDMA

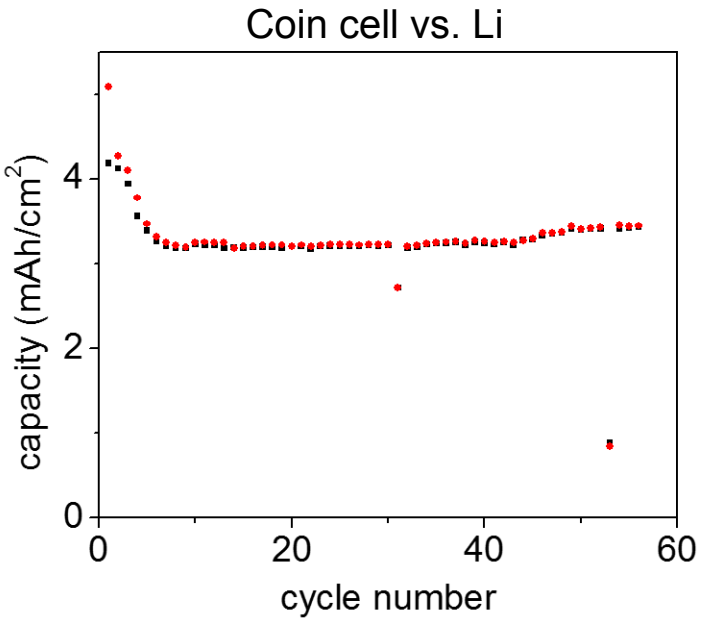

PPyDMA with Advanced Si anode electrode
C/10, 0.005V-1V; constant voltage until 0.02C at the end of lithiation
1st cycle efficiency: 82.35%, 1st cycle delithiation capacity: 1175.9 mAh/g
50th cycle efficiency: 99.83%, 50th cycle delithiation capacity: 955.3 mAh/g

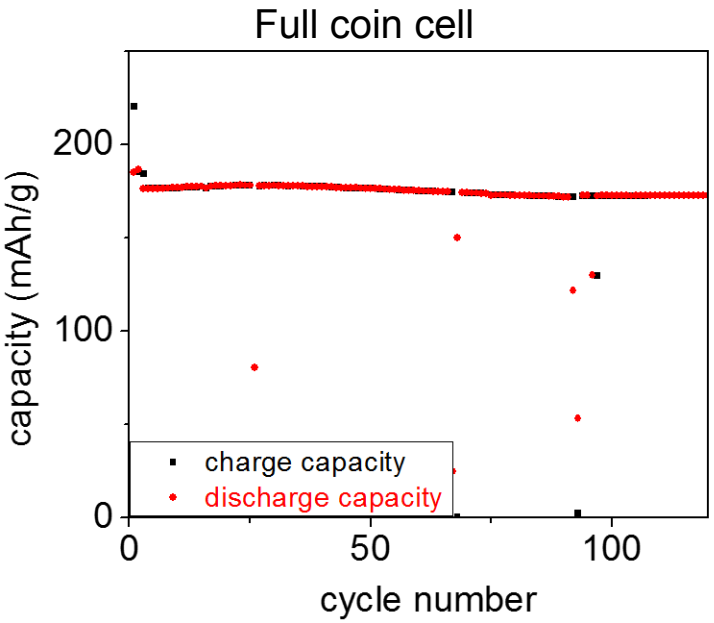

PPyDMA/ Advanced Si anode electrode w/o graphite; C/10 for 2 cycles, then C/3; 1st cycle efficiency: 82.34% (prelithiation with SLMP); Electrolyte: EC/DEC=3/7, 30% FEC, 1.2M LiPF6; Capacity reported based on cathode active materials

H.E. NMC Cathode Development - 3M

Developed advanced cathode material with better properties

Two Concepts: Core-Shell and Coated NMC

Core-Shell NMC

- Small advantage in energy compared to alternatives
- Challenges for cycle life, rate capability and gassing

3M coatings on NMC

- Better cycle life and energy
- Better rate capability

Cathode	BET (m^2/g)	1st Lithiation (mAh/g)	1st Delithiation (mAh/g)	First Cycle Efficiency (%)	Manufacturability
Advanced Material	0.31	230	211	91.9	✓
Baseline Material		273	227	83.3	✓

H.E. NMC Cathode Development - 3M

Developed advanced cathode material with better properties

Two Concepts: Core-Shell and Coated NMC

- Core-Shell NMC
  - Small advantage in energy compared to alternatives
  - Challenges for cycle life, rate capability and gassing
- 3M coatings on NMC
  - Better cycle life and energy
  - Better rate capability

Cathode	BET (m^2/g)	1st Lithiation (mAh/g)	1st Delithiation (mAh/g)	First Cycle Efficiency (%)	Manufacturability
Advanced Material	0.31	230	211	91.9	✓
Baseline Material		273	227	83.3	✓

H.E. NMC Cathode Development - 3M

Developed different candidates and demonstrated energy improvement

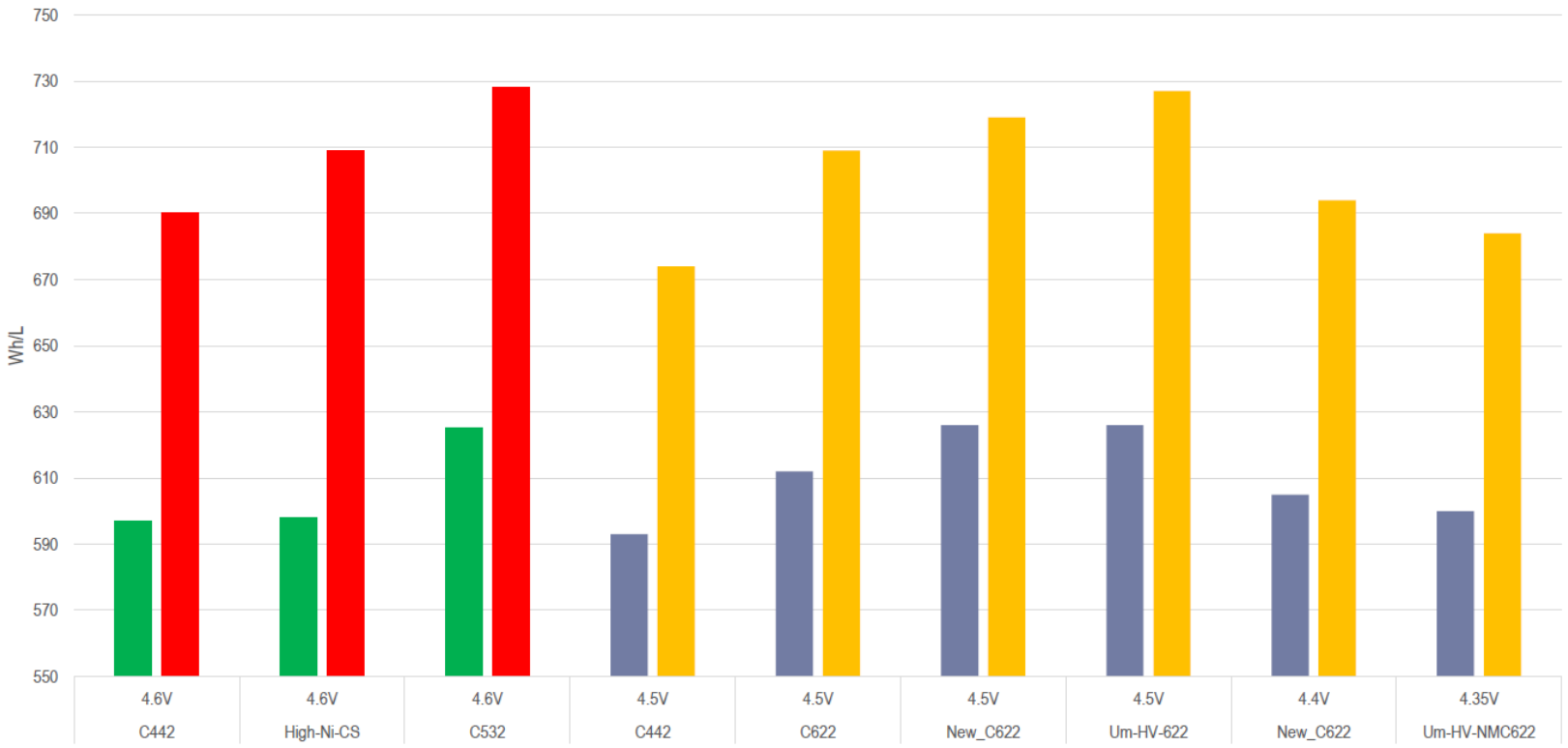

H.E. NMC Cathode Development - 3M

Developed different candidates and demonstrated energy improvement

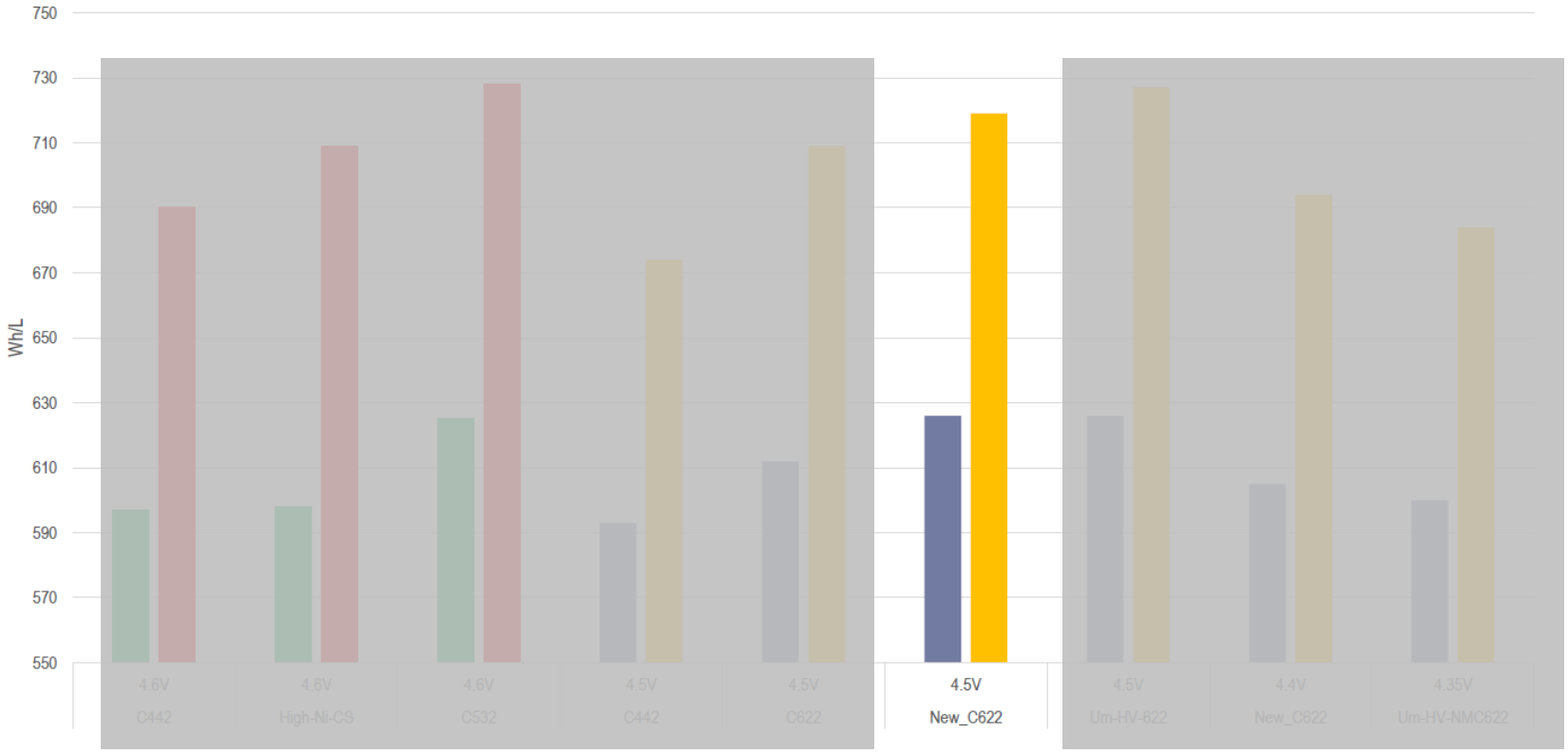

H.E. NMC Cathode Scale Up - Umicore

Demonstrated material scale up & commercial manufacturing feasibility

Process chart

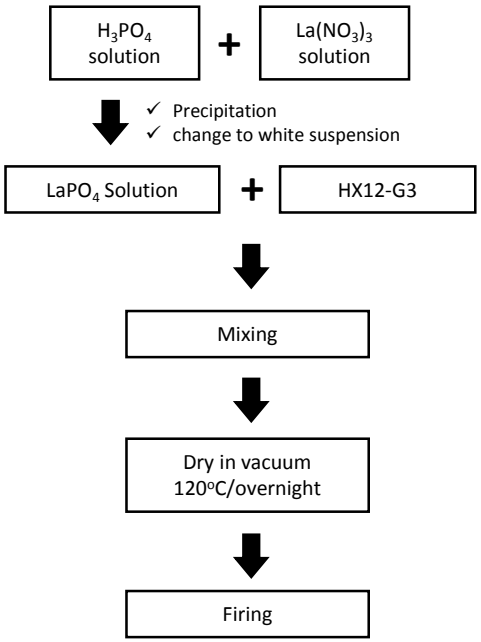

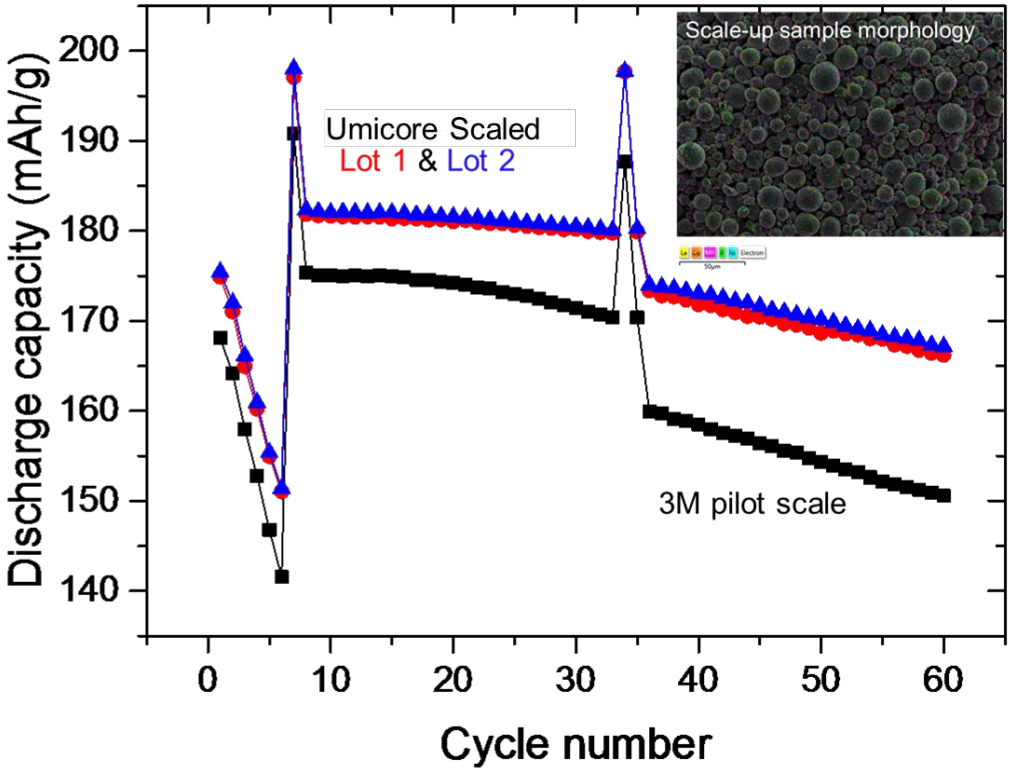

Electrolyte Development - ARL

Identified cycle life enabling electrolyte for advanced chemistry

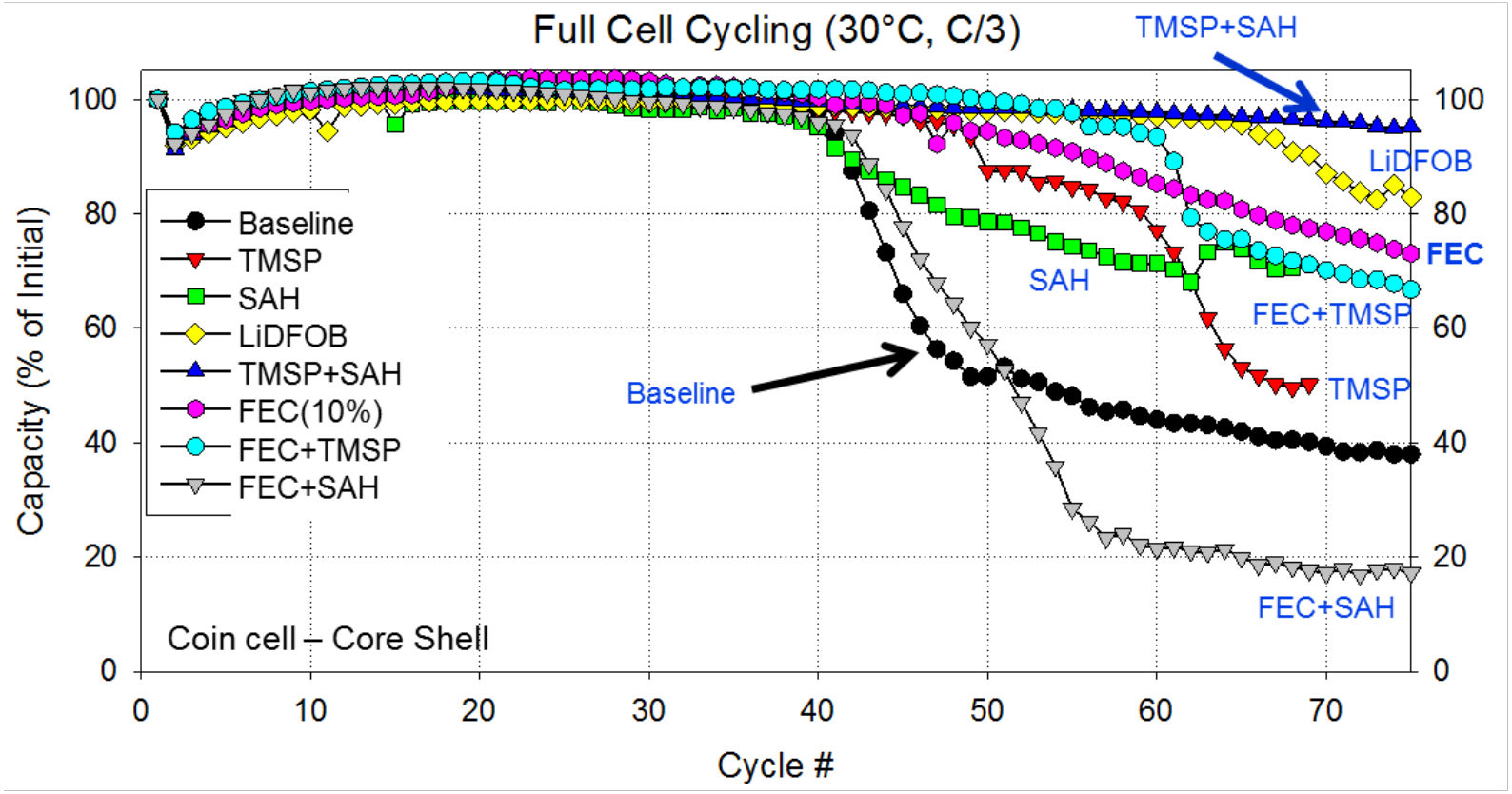

Advanced Chemistry 18650 Evaluation - 3M

≥ 93% energy retention at 1C rate

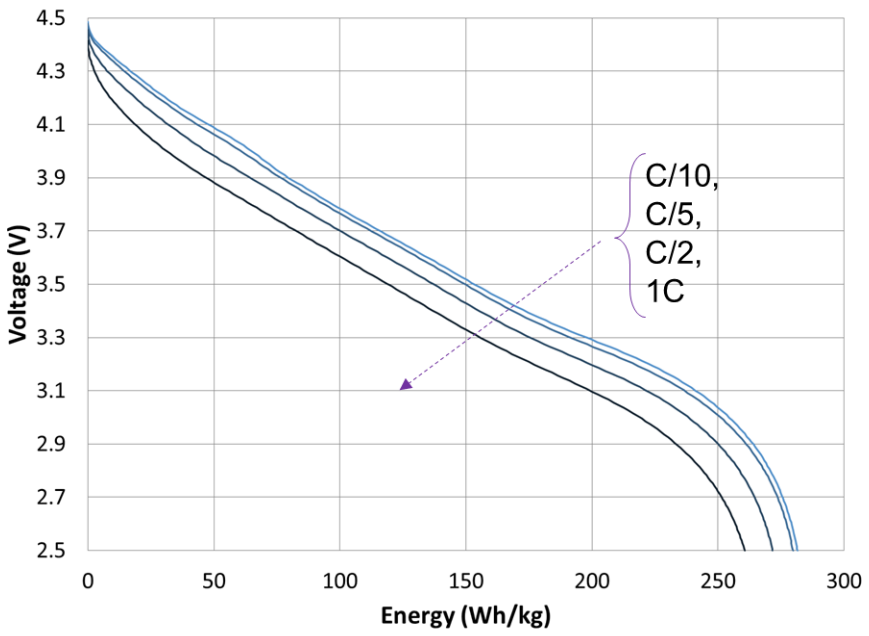

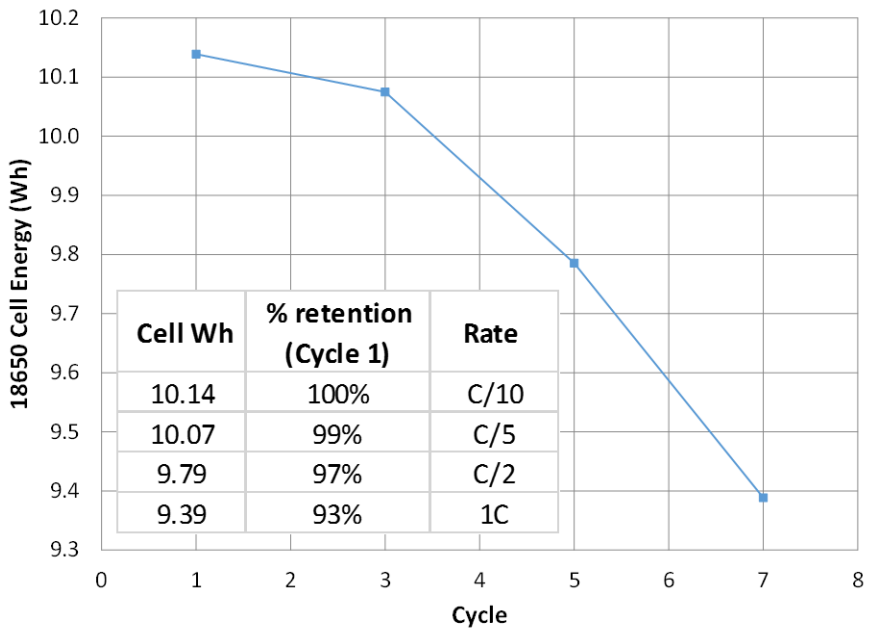

Cell Wh	% retention (Cycle 1)	Rate
10.14	100%	C/10
10.07	99%	C/5
9.79	97%	C/2
9.39	93%	1C

~24% increase in energy by *further* cell design optimization (12um separator, 58 mm wide cathode, N/P=1.05, Tighter winding)
Si alloy anode from 3M production scale facility; High energy NMC cathode from 3M pilot scale facility

Advanced Chemistry 18650 Evaluation - GM

Improved rate capability at low temperatures

Baseline Material

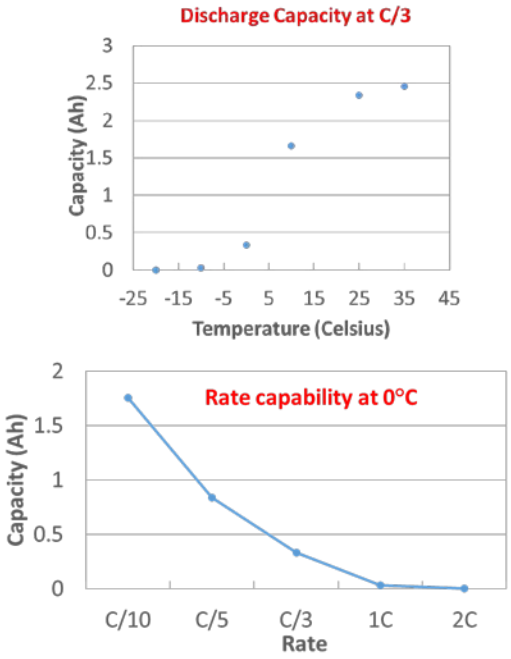

Advanced Material

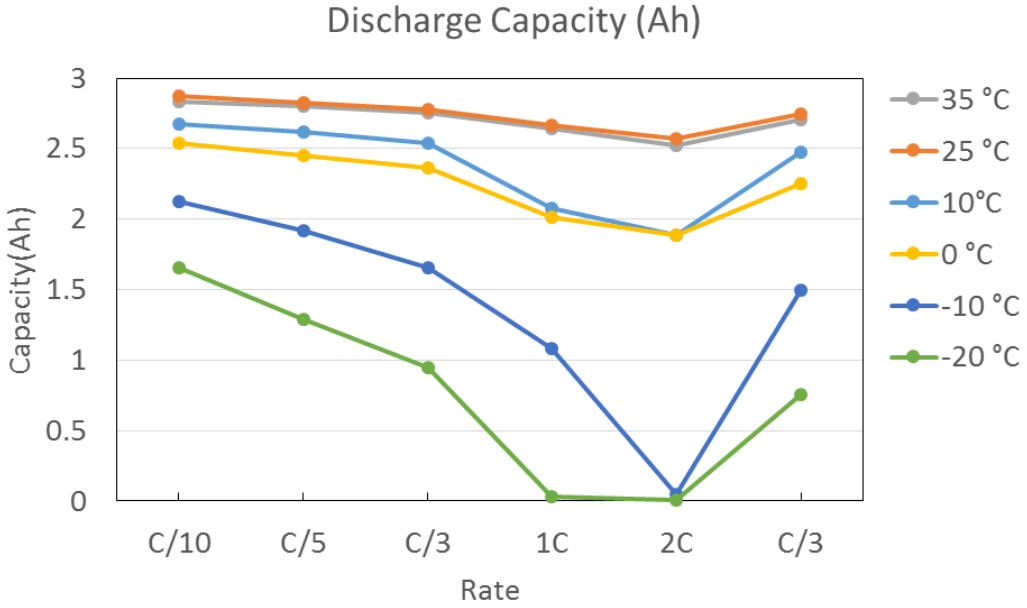

Low capacity at high C-rate at low temperature may be due to resistance built up during previous test.
Si alloy anode from 3M production scale facility
High energy NMC cathode from 3M pilot scale facility

Advanced Chemistry 18650 Evaluation - GM

Effect of UCV on Cycle Life

4.4V

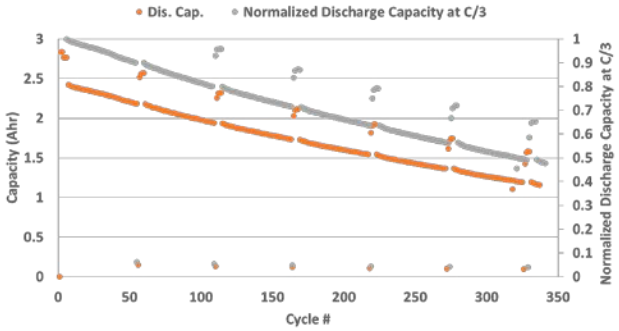

4.5V

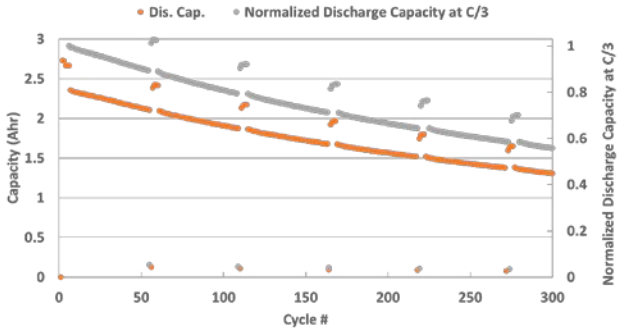

4.6V

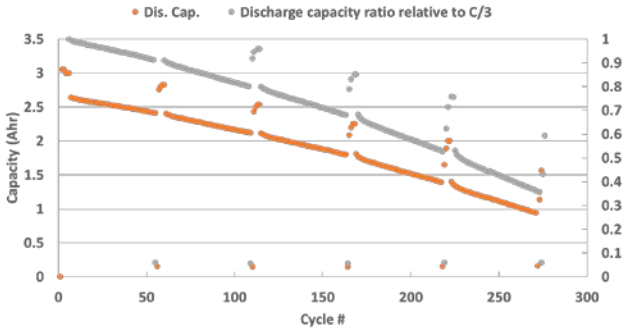

C/3 cycling 5%-95% SOC; After every 50 cycles at C/3, HPPC and C/10 capacity check were carried out

Si alloy anode from 3M production scale facility

High energy NMC cathode from 3M pilot scale facility

Advanced Chemistry 18650 Evaluation - GM

Effect of UCV on Cycle Life

4.6V

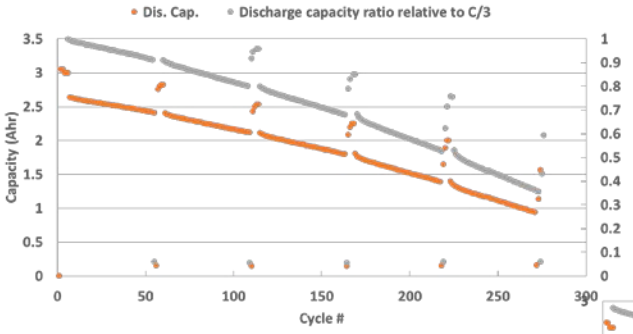

C/3 cycling 5%-95% SOC; After every 50 cycles at C/3, HPPC and C/10 capacity check were carried out

Si alloy anode from 3M production scale facility

High energy NMC cathode from 3M pilot scale facility

4.5V

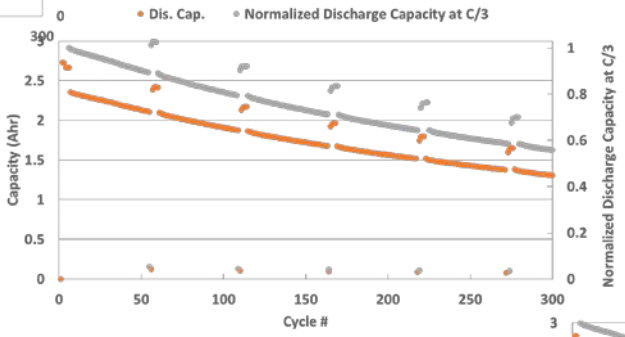

4.4V

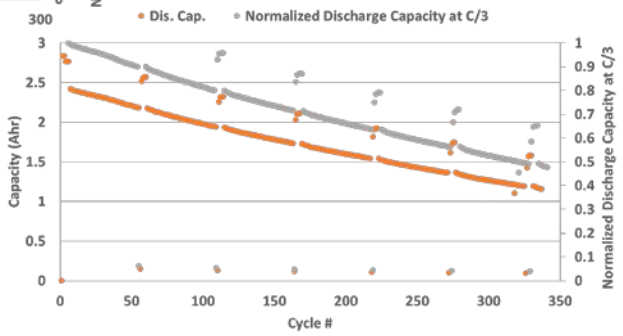

Energy

Cycle Life

Gap Analysis, Advanced vs. Baseline - GM

Improved key cell level properties. Cycle life improvement WIP.

	Unit	Target[1]	Benchmarks[2]		4.4-2.5 V		4.5-2.5 V		4.6-2.5 V	
			Cell Level	Wet Laminate Level[3]	Cell Level	Wet Laminate Level[3]	Cell Level	Wet Laminate Level[3]	Cell Level	Wet Laminate Level[3]
Gravimetric Energy Density	Wh/kg	400	192[4]	247[4]	206	260	218	274	234	295
Volumetric Energy Density	Wh/L	600	490[4]	490[4]	556	556	596	596	633	633
Gravimetric Discharge Power Density	W/Kg	800	366[5]	471[5]	676	853	691	870		
Volumetric Discharge Power Density	W/L	1200	933[5]	933[5]	1818	1818	1873	1873		
Gravimetric Regen Power Density	W/Kg	400	690[5]	888[5]	1396	1761	1528	1926		
Volumetric Regen Power Density	W/L	600	1757[5]	1757[5]	3756	3756	4146	4146		
Cycle life	cycles[6]	1000	45	45	194	194	189	189	158	158
Opt. Temp. Range	°C	-30~65	0~TBD	0~TBD	-20~35	-20~35	-20~35	-20~35	30	30

[1] - End of life requirement from F; [2] - Beginning of life data; [3] - Including electrode, separator, and electrolyte; [4] - Data from C/3; [5] - 40% SOC; Vm, 25°C; [6] - 35% capacity loss at C/3 with 90% DOD range

Advanced Chemistry 18650 Evaluation - GM

Cycle life testing with deliverable cells in progress

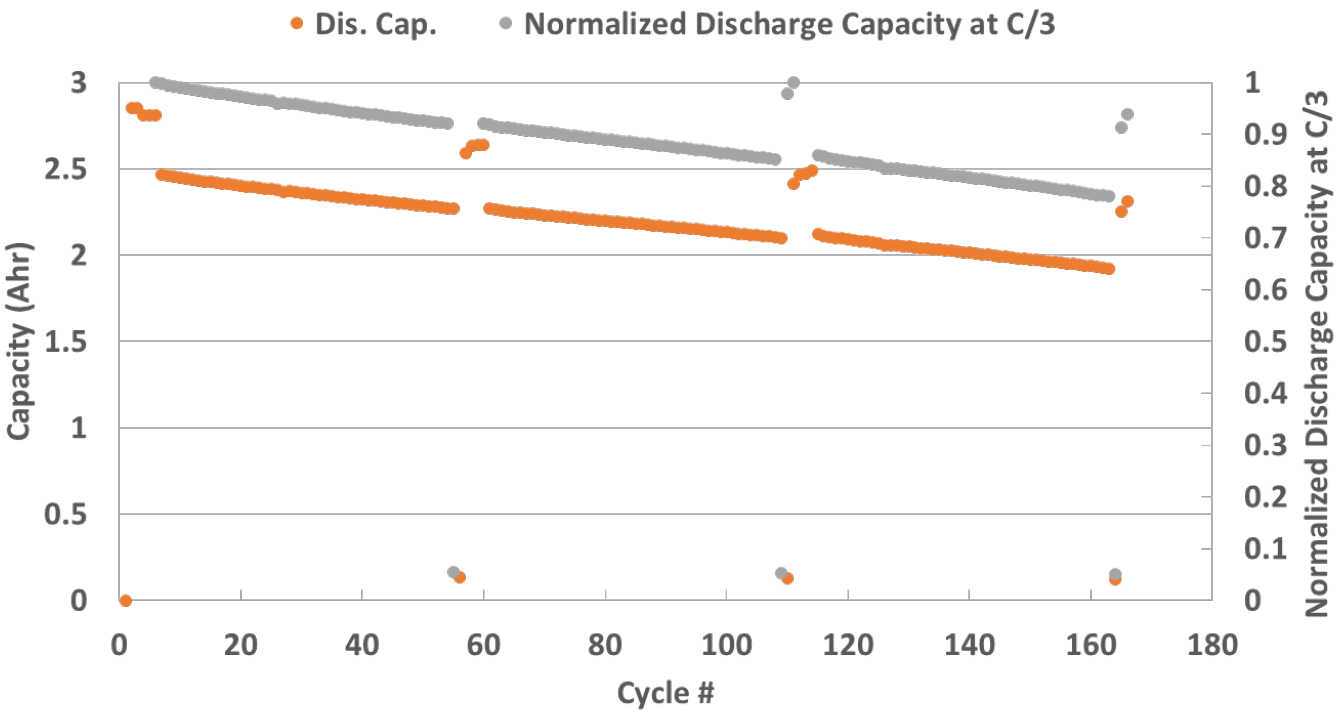

Si alloy anode from 3M production scale facility

High energy NMC cathode from Umicore production scale facility

C/3 cycling 5%-95% SOC; 80% capacity retention: 135 cycles; RPT's (C/3, HPPC and C/10 capacity) after every 50 cycles

Pouch Cell Evaluation - Iontensity

Identified pouch cell energy levels with varying wt% content of Si alloy anode

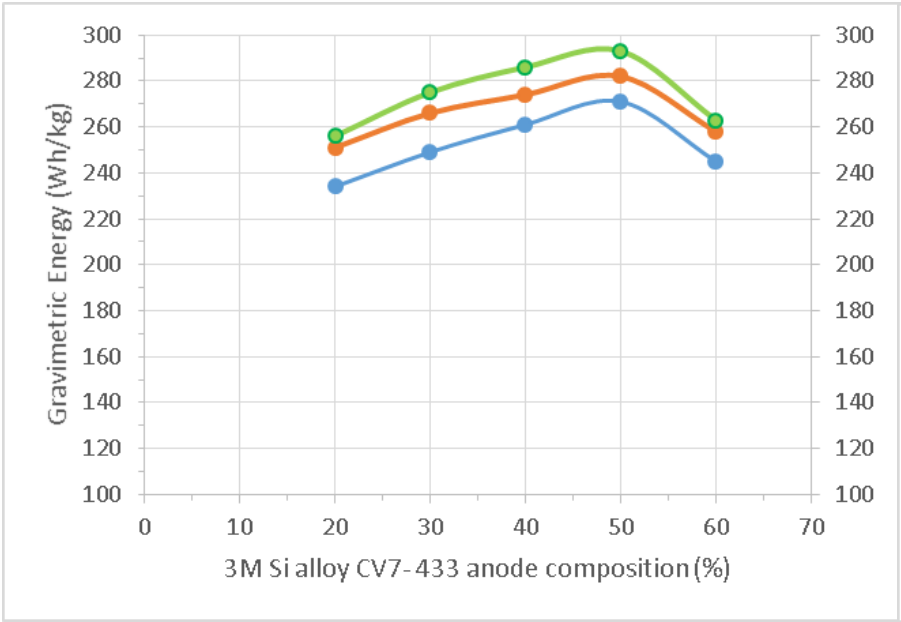

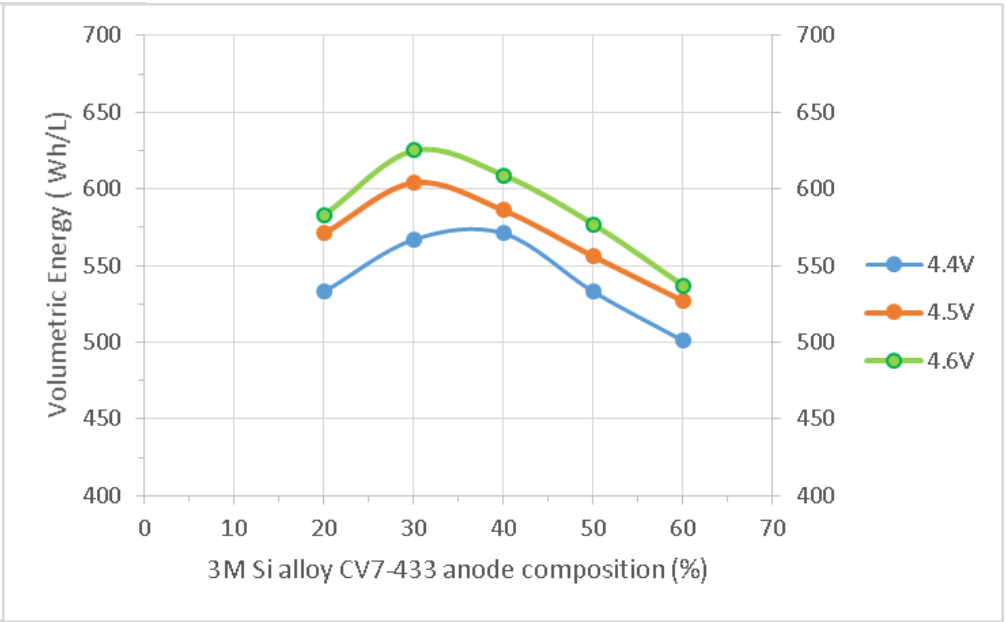

Si alloy anode from 3M production scale facility
High energy NMC cathode from 3M pilot scale facility
Cycle life testing initiated

Cell Sampling to Argonne National Lab - 3M

Sampled 18650 cells with advanced chemistry

Rate	C/15	C/15	Irreversible % (After 1st cycle)	C/10	C/10	Irreversible % (after 3 cycles)	C/5	C/5	C/2	C/2	1C	1C
Cycle #	**0**	**0**		**1**	**2**		**3**	**4**	**5**	**6**	**7**	**8**
Avg	3390	2782	17.9%	2865	2881	15.0%	2864	2864	2823	2818	2759	2751
St Dev	52	57	0.5%	56	54	0.5%	53	53	53	52	56	56
Relative St Dev	1.5%	2.0%	3.0%	2.0%	1.9%	3.0%	1.9%	1.8%	1.9%	1.9%	2.0%	2.0%

Response to Previous Year Reviewers' Comments

- Si Alloy anode and advanced cathode: Cycle life improvements for commercialization
  - Made improvements but achieving long cycle life (>1000 cycles) is still a challenge.
  - Working on key enablers: High voltage electrolyte, anode composite, stable electrochemical couple match

- Si Alloy anode and advanced cathode: Powder production
  - Generated >1000 kg Si alloy anode materials (advanced material).
  - Generated >50 kg of particle coated NMC cathode material.

- Harmonizing test conditions and cycling test
  - Each partner used the same material lot or coated electrode
  - Balanced approach:
    - Cycle life testing in large cells were harmonized for C/3 rate
    - Optional testing via partner's preferred conditions

3M

Collaboration and Coordination

- 3M
  - Sample Electrodes (ARL, Iontensity, GM), Si Alloy Anode Powder (Iontensity, GM, LBNL), High Energy NMC Cathode Powder (Iontensity, GM) and Cells (GM).
- ARL
  - Develop and Sample Electrolyte and Additives (3M, Iontensity).
- GM
  - Evaluate, Analyze and Diagnose Cells (3M,Iontensity).
- LBNL
  - Optimize and Evaluate Binder Chemistry for Si Alloy Anode (3M).
- Iontensity
  - Optimize Composite Electrodes and Pouch Cells. Sample Cells (GM, 3M).
- Umicore
  - Optimize Process and Scale Up Cathode Material. Sample Materials (3M).

Remaining Challenges / Barriers

- Long cycle life
  - Electrolyte formulation for high voltage (4.5V) chemistries
  - Superior Si anode composite
    - Binder evaluation in large format cells such as 18650 or pouch cells
    - More stable SEI formation
    - Further reduced controlled volumetric expansion over life
  - Stable match of high voltage cathode and high voltage electrolyte

Proposed Future Work

- Complete life testing with advanced chemistry
- Analyze life degradation root causes
- Discuss advanced chemistry performance from cells sampled to ANL
- Prepare final project report

Summary

- Successfully leveraged collaborative R&D
  - Anode and Cathode material development at 3M
  - Binder development on 3M Si Alloy Anode at LBNL
  - Cathode material scale up and process optimization at Umicore.
  - Gap analysis, cell evaluation and validation at GM
  - Electrolyte and additive screening for baseline and advanced chemistry at ARL
  - Advanced chemistry's pouch format cell feasibility at Iontensity.
- Successful Scaled up Baseline and Advanced Materials
- Demonstrated performance improvement

Q & A

Reviewer Only Slides

Critical Assumptions and Issues

- Stable high voltage electrolyte can be discovered in project timeline
  - Particle surface treatment may prolong life
- Iterative process of optimizing cell design and testing can be achieved as per the project timeline
- A high energy (Wh/kg & Wh/l) cells with targets close to DOE EV targets may have limited life performance
  - May need to find a suitable balance between cell energy and cell performance over life
- Cost of active and electrolyte materials, which enable superior performance, would be low.
  - Look for cost effective and commercially viable options in material development and testing

3M